

Antagonistic activities of CDC14B and CDK1 on USP9X regulate WT1-dependent mitotic transcription and survival

Michael Dietachmayr

Vollständiger Abdruck der von der Fakultät für Medizin der Technischen Universität München zur Erlangung eines

Doktors der Medizinischen Wissenschaft (Dr. med. sci.)

genehmigten Dissertation.

Vorsitz: apl. Prof. Dr. Klaus-Peter Janssen

Prüfer*innen der Dissertation:

1. Prof. Dr. Florian Bassermann
2. Priv.-Doz. Raquel Mejías-Luque, Ph.D.
3. apl. Prof. Dr. Robert Oostendorp

Die Dissertation wurde am 31.08.2022 bei der Technischen Universität München eingereicht und durch die Fakultät für Medizin am 22.02.2023 angenommen.

Contents

1. Introduction	1
1.1 Mitosis and spindle assembly checkpoint (SAC)	1
1.2 The phosphatase CDC14B	3
1.3 The kinase CDK1-Cyclin B	4
1.4 The Ubiquitin-proteasome system and USP9X	5
1.5 The transcription factor Wilms' tumor protein 1 (WT1)	9
1.6 The chemokine IL-8	10
1.7 Mitotic bookmarking and active mitotic transcription	12
2. Aim of the study	14
3 Results	
3.1 CDC14B interacts with USP9X in mitotic cells	15
3.2 Stable isotope labeling of amino acids in culture (SILAC) under CDC14B overexpression	16
3.3 CDC14B dephosphorylates USP9X on serine 2563 in mitosis	17
3.4 USP9X phosphorylation on serine 2563 is highly regulated during cell cycle	19
3.5 CDK1 phosphorylates USP9X on serine 2563 in mitosis	20
3.6 USP9X phosphorylation on serine 2563 regulates its enzymatic activity	21
3.7 USP9X dependent ubiquitome analysis in mitotic HEK 293T cells	23
3.8 Mass spectrometry yields Wilms' tumor protein 1 (WT1) as possible mitotic substrate of USP9X	25
3.9 USP9X interaction with WT1 is enhanced in mitosis	27
3.10 WT1 binding to USP9X in mitosis is modulated by serine 2563 phosphorylation	28
3.11 USP9X stabilizes WT1 in mitosis by rescuing WT1 from proteasomal degradation	29
3.12 USP9X deubiquitinates mitotic WT1 in a	

phosphorylation dependent manner	30
3.13 USP9X knockdown leads to enhanced ubiquitination of WT1 in mitosis	32
3.14 USP9X inhibition with WP1130 destabilizes WT1 in mitosis	32
3.15 USP9X and WT1 colocalize in mitotic cells	33
3.16 RNA sequencing of mitotic U2-OS cells under WT1 knockdown and in USP9X ^{Mut} U2-OS cells	34
3.17 WT1 and USP9X regulate mRNA levels of IL-8 in mitosis	36
3.18 WT1 binds to the CXCL8 promoter in mitosis	37
3.19 WT1 and USP9X regulate abundance of IL-8 protein in Mitosis	39
3.20 Actinomycin D inhibits active transcription of IL-8 in Mitosis	40
3.21 IL-8 regulates mitotic survival in U2-OS cells	41
3.22 Blocking CXCR1 and CXCR2 receptor using reparixin induces mitotic apoptosis	42
3.23 Mitotic apoptosis induced by CXCL8 knockdown can be rescued by exogenous IL-8	43
3.24 WT1 knockdown induces apoptosis in mitotic U2-OS cells which can be rescued by exogenous IL-8	44
3.25 WT1 and IL-8 act in the same signaling pathway to regulated cell survival in mitosis	45
3.26 Regulation of cell survival in mitosis by IL-8 is not restricted to microtubule-targeting drugs	45
3.27 Effect of WT1 and IL-8 on mitotic cell survival is not restricted to U2-OS cells	46
3.28 USP9X serine 2563 phosphorylation influences mitotic survival	47
3.29 USP9X serine 2563 phosphorylation influences mitotic survival via WT1	48
3.30 Flow cytometry using PI-staining underlines that USP9X serine 2563 phosphorylation regulates mitotic survival via WT1	49
3.31 CDC14B regulates mitotic survival via USP9X	

phosphorylation in U2-OS cells	50
4. Discussion	
4.1 CDC14B and CDK1 regulate mitotic phosphorylation of USP9X on serine 2563 and regulate activity of USP9X	52
4.2 USP9X deubiquitinates WT1 in mitosis in a phosphorylation dependent manner	54
4.3 Active transcription and secretion of IL-8 in mitosis is regulated by WT1 and USP9X	56
4.4 CDK1 and CDC14B mediated phosphorylation of USP9X on serine 2563 regulates survival in mitosis via WT1 and IL-8	57
5. Materials	
5.1 Instruments	60
5.2 Reagents and chemical compounds	61
5.3 Consumables	63
5.4 Enzymes	64
5.5 Cell culture media and supplements	64
5.6 Primary antibodies (dilution and company)	65
5.7 Primary antibodies costume-made	65
5.8 Secondary antibodies	66
5.9 Kits	66
5.10 Primers	66
5.10.1 Primers used for quantitative RT-PCR	66
5.10.2 Primers used for ChIP	67
5.10.3 Primers used for luciferase reporter assay	67
5.10.4 Primers used for cloning of CDC14B	67
5.10.5 Primers used for GST-USP9X constructs	67
5.10.6 Primers used for USP9X S2563A mutagenesis PCR	67
5.10.7 Primers used for cloning WT1 constructs	68
5.10.8 Primers used for cloning 6xHis-Ubiquitin construct	68
5.10.9 Primers for short hairpin RNA (shRNA)	68
5.10.10 Primers used as single guide RNA (sgRNA)	68
5.10.11 Primers used for amplification of genomic DNA after genome editing	68

5.11	Short interfering RNA	69
5.12	Plasmids	69
5.13	Bacteria	69
5.14	Cell lines	69
5.15	Solutions and Buffer	70
6.	Methods	
6.1	Molecular biology	75
6.1.1	Polymerase chain reaction	75
6.1.2	Mutagenesis PCR	75
6.1.3	RNA extraction	76
6.1.4	Reverse transcription of mRNA into DNA	76
6.1.5	Quantitative RT-PCR	76
6.1.6	Cloning	76
6.1.7	Digestion of DNA	77
6.1.8	Ligation	77
6.1.9	Transformation of DNA into bacteria and selection	77
6.1.10	DNA isolation und test digestion	77
6.1.11	Gel electrophoresis and gel purification	78
6.2	Biochemical methods	78
6.2.1	Cell lysis	78
6.2.2	Cell lysis and co-Immunoprecipitation experiments	78
6.2.3	In vivo ubiquitylation assay	79
6.2.4	SDS polyacrylamide gel electrophoresis (SDS-PAGE)	80
6.2.5	Western Blot or Immunoblot analysis	80
6.2.6	Reincubation of Western Blot membranes	81
6.2.7	Induction and purification of GST-tagged proteins	81
6.2.8	In vitro phosphorylation of USP9X by CDK1-Cyclin B	82
6.2.9	In vitro DUB activity assay using Ubiquitin-AMC	82
6.2.10	In vitro deubiquitination activity assay with HA-Ubiquitin-vinyl sulfone	83
6.3	Cell culture	84
6.3.1	Transfection of eukaryotic cells	84
6.3.2	Transfection of eukaryotic cells with short interfering RNA (siRNA)	85
6.3.3	Cell cycle synchronization and drug treatment	85

6.3.4	Viral transduction of eukaryotic cells	87
6.3.5	Generating HEK 293T cells stably expressing 6xHis-Ubiquitin	87
6.3.6	Preparation of cells for mass spectrometry in mitotic and asynchronous HEK 293T cells	88
6.3.7	Overexpression of FLAG-USP9X ^{WT} or FLAG-USP9X ^{S2563A} in HEK 293T cells for DUB activity assay using Ubiquitin-AMC or HA-Ubiquitin-vinyl sulfone	88
6.3.8	Flow cytometry	89
6.3.9	Generation of USP9X mutated U2-OS cells (USP9X ^{Mut}) using CRIPSR/Cas9	89
6.4	Biological assays	90
6.4.1	Enzyme-linked immunosorbent assay (ELISA) of IL-8 in cell culture supernatant	
6.4.2	Immunofluorescence	91
6.4.3	Normalization of protein levels in Western Blot and statistical analysis	92
7.	Literature	93
8.	Acknowledgement	107

Abbreviations

AA amino acids
ADP adenosin-5'-diphosphate
Amp Ampicillin
APAF apoptotic Protease-activating Factor 1
APC anaphase promoting complex
APS ammonium persulfate
As asynchronous
ATCC American Type Culture Collection
ATP adenosin-5'-triphosphate
BAX BCL2-Associated X Protein
BCL-2 B-cell lymphoma 2
BAK Bcl-2 homologous antagonist killer
BES N,N-Bis(2-hydroxyethyl)-2-aminoethanesulfonic acid
bp base pairs
BSA bovine serum albumin
Brd4 bromodomain-containing protein 4
BUB1 budding uninhibited by benzimidazole 1
BUB3 Budding uninhibited by benzimidazole 3
BUBR1 budding uninhibited by benzimidazole-related 1
°C degree Celsius
CDC20 cell division cycle protein 20
CDC14A/B/C cell division cycle protein 14A/B/C
CDC25 cell division cycle 25
CDH1 CDC20 homolog 1
CDK1 Cyclin depended kinase
CHX cycloheximide
CTCF CCCTC-binding factor
C-terminal carboxy terminal
CTNNB1 Catenin beta-1
ctrl control
CXCR CXC chemokine receptors
dist. distilled
DMEM Dulbecco's Modified Eagle Medium
DMSO dimethylsulfoxide
DNA desoxyribonucleic acid
dNTP 2'-desoxynukleosid-5'-triphosphat
DUB deubiquitinase
DTT dithiothreitol
E. coli escherichia coli
EDTA ethylenediaminetetraacetic acid
ELISA Enzyme Linked Immunosorbent Assay

EV empty vector
FACS fluorescence activated cell scanning/sorting
FBS fetal bovine serum
FEAR fourteen early anaphase release pathway
FLAG tag DYKDDDDK-tag
fw forward
Gag group specific antigen
G2P glycerol 2-phosphate disodium salt hydrate
GST glutathione S-transferase
HA-tag hemagglutinin tag
HECT Homologous to E6AP C-Terminus
HEK 293T human embryonic kidney cells
HeLa cells **Henrietta Lacks** cells
HEPES 4-(2-hydroxyethyl)-1-piperazineethanesulfonic acid
HRP horseradish peroxidase
hrs hours
HSF2 Heat shock factor protein 2
HSP90 heat shock protein 90
IF immunofluorescence
IL-8 interleucin 8
IP immunoprecipitation
IPTG Isopropyl β -D-1-thiogalactopyranoside
IRF7 Interferon regulatory factor 7
JAMMs JAB1, MPN, MOV-34 family
kD kilodalton
KIBRA Kidney/BRAin protein
KNL1 kinetochore scaffold 1
KTS amino acids lysine, threonine and serine
LB Luria-Bertani
Lys lysine
MAD 2 mitotic arrest deficient 2
MCC mitotic checkpoint complex
MCL1 induced myeloid leukemia cell differentiation protein
MJDs Machado–Josephin domain-containing protease
MEN mitotic exit network
MINDYs motif-interacting with ubiquitin-containing novel DUB family
Mit mitotic
mM (mmol/l) 10^{-3} mol/liter
Mps1 monopolar spindle 1
MS mass spectrometry
MTOC microtubule organizing center
NaVa Sodium orthovanadate (Na_3VO_4)
Noc nocodazole
nM (nmol/l) 10^{-9} mol/liter
NSCLC non-small cell lung cancer
N-terminal amino-terminal

OTUs ovarian tumor protease
PAGE polyacrylamide gel electrophoresis
PBS phosphate buffered saline
Pbx1 PBX Homeobox 1
PCR polymerase chain reaction
PI propidium iodide
PLK1 polo like kinase 1
PMSF phenylmethylsulfonyl fluoride
PP polypropylene
PP1 protein phosphatase 1
PP2A protein phosphatase 2A
P/S penicillin / streptomycin
PSM peptide spectrum match
PTM posttranslational modification
pUSP9X (S2563) phosphorylated USP9X on serine 2563
PVDF polyvinylidene fluoride
qPCR quantitative PCR
RING really interesting new gene
RNA ribonucleic acid
RPNP0 Ribosomal Protein Lateral Stalk Subunit P0
RT reverse transcription // room temperature
rv reverse
SAC spindle assembly checkpoint
SD standard deviation
SDS sodium dodecyl sulfate
SILAC stable isotope labeling by/with amino acids in cell culture
siRNA short interfering RNA
SIRT2 NAD-dependent protein deacetylase sirtuin-2
sec second
shRNA short hairpin RNA
Smad 4/7 SMAD Family Member 4/7
SOX 11 SRY-Box Transcription Factor 11
SWI 5 SWI5 Homologous Recombination Repair Protein
TAP tandem affinity purification
TEMED N,N,N',N'-Tetramethylethylenediamine
TGF β Transforming growth factor β
TLCK Tosyl-L-lysyl-chloromethyl ketone
TNF Tumor necrosis factor
TPCK Tosyl-phenylalanyl-chloromethyl ketone
TRIP13 thyroid receptor-interacting protein 13
TRIS tris(hydroxymethyl)aminomethane
TXNIP thioredoxin interacting protein
U unit
UCH ubiquitin carboxy-terminal hydrolase
UPS ubiquitin proteasome system
USP9X ubiquitin specific protease 9x

VEGF Vascular Endothelial Growth Factor
WCE whole cell extracts
wt wildtype
WT1 Wilms' tumor protein 1
w/v weight per volume
XIAP X-linked inhibitor of apoptosis
ZAP 70 Zeta-chain-associated protein kinase 70
 μg 10^{-6} gram
 μl 10^{-6} liter
 μmol 10^{-6} mol
 μM ($\mu\text{mol/l}$) 10^{-6} mol/liter)

1. Introduction

1.1 Mitosis and spindle assembly checkpoint (SAC)

Mitosis and the mitotic spindle assembly checkpoint (SAC) are highly organized and complex cellular processes which ensure correct distribution of chromosomes to daughter cells and which guarantee high fidelity cell division.

Mitosis comprises several phases which are characterized by specific processes and cellular reorganization. In short, in prophase the centrosomes are separated to induce microtubule-formation and to build the MTOC (microtubule organizing center). Furthermore, in prophase DNA is highly compacted and duplicated chromosomes are condensing. In prometaphase, the nuclear envelope breakdown occurs and spindle tubules are beginning to attach to the kinetochores of the chromosomes. In metaphase, attached microtubules align the chromosomes on the metaphase plate which means that they are located exactly between the two cell poles. During anaphase, the daughter chromosomes are separated and pulled to the cell poles by shortening of the microtubules. In telophase, a new nuclear envelope is established and the chromosomes begin to decondense followed by cytokinesis.

The essential checkpoint in mitosis which detects any erroneous chromosomal segregation and which impedes mitotic progression if any mistakes in chromosomal segregation are detected is the spindle assembly checkpoint (SAC) (Curtis, Ruda et al. 2020). In metaphase, the SAC is in charge of monitoring the attachment of microtubules to the kinetochores of chromosomes and any missing interaction of microtubules and kinetochores keeps the SAC activated and stalls mitotic progression (Musacchio 2011). As soon as all kinetochores are captured by microtubules, the spindle assembly checkpoint is silenced and cells can complete mitosis (Musacchio 2011).

The underlying molecular mechanisms of SAC activation are complex and to date not completely understood. Unattached kinetochores or reduced tension between the kinetochores of duplicated chromatids induce the activation of a machinery of the SAC which is called mitotic checkpoint complex (MCC) (Ruan, Lim et al. 2019). The MCC is a conglomerate of specific proteins, namely MAD2 (mitotic arrest deficient), CDC20 (cell division cycle 20), BUBR1 (budding uninhibited by benzimidazole related 1), BUB1 (budding uninhibited by benzimidazole 1) which inhibit the highly conserved ubiquitin ligase anaphase promoting complex (APC) as long as microtubule and kinetochore attachment has not been completed (Sudakin, Chan et al. 2001) (Figure 1).

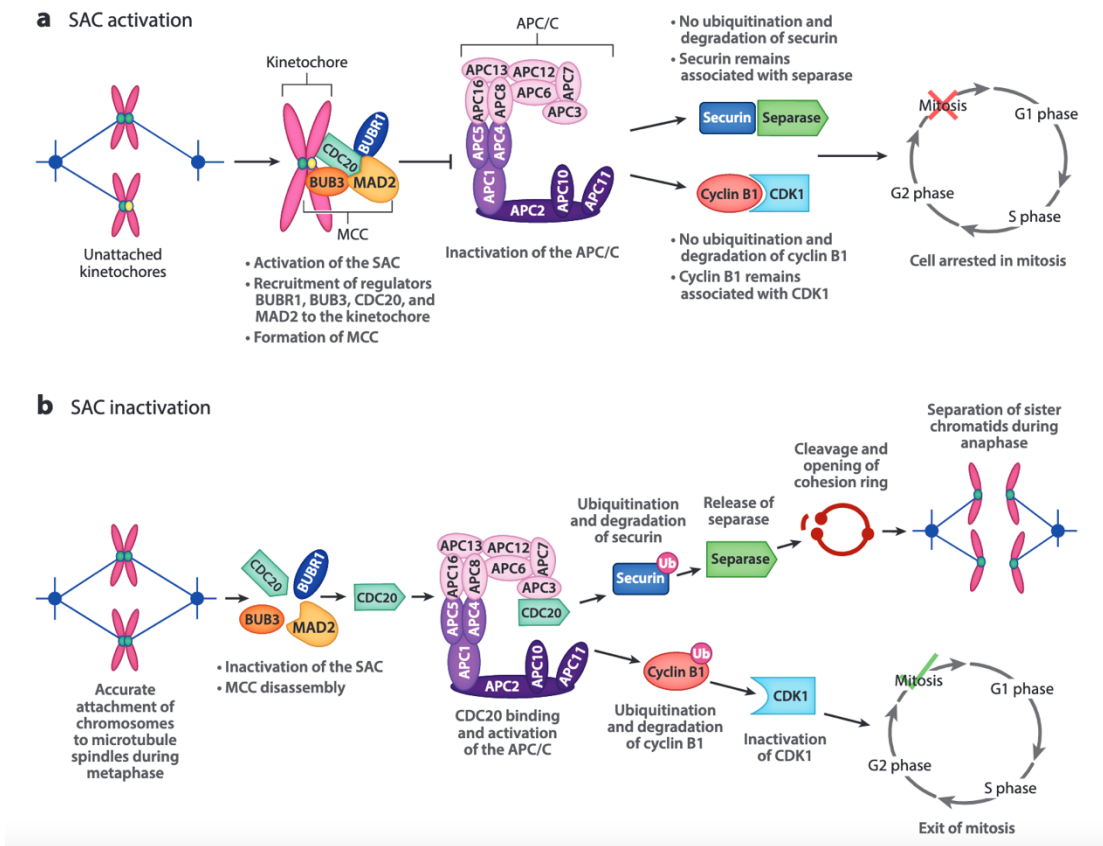


Figure 1 Activation and inactivation of the spindle assembly checkpoint Unattached kinetochores induce assembly of the mitotic checkpoint complex (MCC) comprising BUBR1, MAD2, CDC20 and BUB3 which inhibits activation of the anaphase promoting complex (APC) (upper part, left side). In consequence, the proteins securing and CyclinB1 preserve the state of metaphase and hamper progress into anaphase (upper part, right side). When the kinetochores are properly attached to the microtubules, the MCC is inactivated, CDC20 is liberated from the MCC and enhances the activity of the ubiquitin ligase anaphase promoting complex (lower part, left side). Consequently, the proteins securing and CyclinB1 are targeted for degradation by ubiquitylation which enables cells to enter anaphase (lower part, right side) (Curtis, Ruda et al. 2020).

Several kinases like PLK1, Mps1 or Bub1 are involved in the dynamics of the spindle assembly checkpoint (Musacchio 2015). One of the initial events in SAC formation is thought to be the phosphorylation of KNL1 by Mps1, which then recruits further MCC proteins to the kinetochores and which keeps the SAC activated (Primorac, Weir et al. 2013). As soon as all kinetochores are attached to microtubules KNL1 is dephosphorylated by the phosphatase PP2A-B56 (Espert, Uluocak et al. 2014). Additionally, the phosphatase PP1 is recruited to the kinetochores the dephosphorylate and inactive the kinase Mps1 and in second line to reduce phosphorylation of KNL1 (Moura, Osswald et al. 2017). Another means to terminate SAC function is the interaction of p31^{comet} and TRIP13 with the MCC which leads to disassembly of the CDC20 with the further MCC comprising proteins (Teichner, Eytan et al. 2011, Wang, Sturt-Gillespie et al. 2014). Therefore, when the MCC activity has fallen under a specific threshold, the APC binds to the protein CDC20 to ubiquitinate the protein securin, which is an inhibitor of the protease separase and therefore an inhibitor of sister chromatid separation, and CyclinB1, a coactivator of the kinase CDK1 (Hagting, den Elzen et al. 2002, Hornig, Knowles et al. 2002) (Figure 1). In consequence of degradation of securin and CyclinB1, cells can

progress with entering anaphase (Hagting , den Elzen et al. 2002). A functional mitotic spindle assembly checkpoint with high fidelity downstream signaling guarantees chromosomal integrity and any defect in these complex regulatory pathways can induce genomic instability which represents a hallmark of cancer (Hanahan 2022). Furthermore, the spindle assembly checkpoint is one of the central mechanisms in cell cycle that links cell division with cell fate decision and therefore mitotic survival (Curtis, Ruda et al. 2020). Under prolonged spindle assembly checkpoint activation, for example using a microtubule-interfering drug like paclitaxel or vinca alkaloids, cells can induce two substantially different cellular mechanisms to evade SAC activation: the first one is apoptosis by initiating the intrinsic apoptotic pathway in a BCL-protein family dependent manner, the second one is mitotic slippage, meaning completing mitosis without correct chromosomal segregation (Ruan, Lim et al. 2019).

Two essential regulatory means that influence mitotic apoptosis and mitotic slippage are the kinase activity of CDK1-CyclinB, a ubiquitination target of the APC, and the levels of proapoptotic proteins (Gascoigne and Taylor 2008, Ruan, Lim et al. 2019). Additionally, the two main SAC network proteins MPS1 and PLK1 have been found to improve or weaken mitochondrial membrane permeability and therefore regulate mitotic apoptosis (Lee, Lee et al. 2016, Zhang, Ling et al. 2016).

Another important role in intrinsic apoptotic signaling are mediated by the proapoptotic BCL-proteins BAX and BAK which dimerize and induce permeabilization of the mitochondrial outer membrane which in consequence leads to release of mitochondrial proteins into the cytosol (Lopez and Tait 2015). Dimerization of BAX and BAK is inhibited by the antiapoptotic proteins BCL2 and BCL-x_L and under prolonged SAC activation CDK1 phosphorylates BCL2 and BCL-x_L which blocks their function (Terrano, Upreti et al. 2010). One protein which is released from mitochondria in the process of apoptosis is cytochrome c which binds to the adaptor protein APAF-1 in the cytosol forming a complex called apoptosome (Lopez and Tait 2015). This complex has the ability to activate caspases representing the most downstream effectors of apoptosis and cleaving DNA, inducing nucleosome fragmentation and promoting phagocytosis (Lopez and Tait 2015).

1.2 The phosphatase CDC14B

The phosphatase Cdc14 is one of the essential mitotic phosphatases in budding yeast and reverses Cdk1-accomplished phosphorylation in mitosis (Visintin, Craig et al. 1998). More precisely, Cdc14 is activated after the spindle assembly checkpoint has been satisfied by shifting from the nucleolus -where its kept inactivated- to the cytoplasm by the Fourteen Early Anaphase Release (FEAR) pathway and the Mitotic Exit Network (MEN) (Bardin and Amon 2001, Yellman and Roeder 2015). The release in early anaphase from the nucleolus is promoted by the FEAR network by Cdk1-induced phosphorylation of Net1 (Azzam, Chen et al. 2004). Following the FEAR network, in late anaphase the MEN improves the export of Cdc14 from the nucleolus to the cytoplasm (Bardin and Amon 2001). When Cdc14 has reached an active state, it dephosphorylates among other proteins Sic, Swi5 and Cdh1/Hct1 and hampers function of cyclin-dependent kinases (CDKs) which forces mitotic cells to exit mitosis (Visintin, Craig et al. 1998). Cdh1 is a

coactivator of the major mitotic ubiquitin ligase called anaphase promoting complex (APC) and Cdh1 phosphorylation inhibits activity of the APC (Jaspersen, Charles et al. 1999). Therefore, Cdc14 activates the APC/Cdh1 complex which degrades mitotic proteins to induce mitotic exit (Yellman and Roeder 2015).

In human cells, mitotic exit is accomplished by the phosphatases PP1 and PP2A and the mitotic functions of the human orthologs of Cdc14 are still elusive and not completely understood (Wurzenberger and Gerlich 2011).

Three orthologs of the yeast Cdc14 are described in human named CDC14A, CDC14B and CDC14C (Trautmann and McCollum 2002, Rosso, Marques et al. 2008). Interestingly, in consequence of DNA damage the phosphatase CDC14B was demonstrated to translocate from the nucleolus to the cytoplasm to activate the anaphase promoting complex by dephosphorylation of CDH1 (Bassermann, Frescas et al. 2008). This suggests a similar role of CDC14B and the phosphatase Cdc14 in yeast towards the anaphase promoting complex but under different cellular conditions. In 2008 it could be shown that human cells which lack the phosphatase CDC14B have normal mitotic functions like spindle assembly and mitotic exit (Berdougo, Nachury et al. 2008). In contrast, another publication demonstrated that CDC14B promotes progression through mitosis by taking influence on the function of CDC25 and CDK1-Cyclin B (Tumurbaatar, Cizmecioglu et al. 2011). Furthermore, CDC14B stabilizes and bundles mitotic microtubules and improves mitotic exit by dephosphorylating SIRT2 (Dryden, Nahhas et al. 2003, Cho, Liu et al. 2005). If there are further mitotic signaling pathways in which CDC14B is involved remains to be studied.

In mouse embryonic fibroblasts, loss of CDC14B led to enhanced endogenous DNA damage and forced cells to enter senescence (Wei, Peddibhotla et al. 2011).

Upcoming work could indicate that CDC14B plays a central role in tumor biology. In microarray and immunohistochemistry analysis of clear cell renal cell carcinoma specimens, CDC14B was the most downregulated gene or protein found (Kim, Choi et al. 2014). Furthermore, in glioblastoma multiforme samples much lower expression of CDC14B was detected than in human healthy tissue (Galeano, Rossetti et al. 2013).

1.3 The kinase CDK1-Cyclin B

Cyclin-dependent kinases (CDKs) are a subgroup of serine/threonine kinases which require binding of specific cyclins for their activation and which have a large number of cellular functions (Malumbres 2014). The CDKs share the characteristic of S/T-P-X-K/R to be the consensus motif with the minimal consensus motif S/T-P (Errico, Deshmukh et al. 2010).

For instance, cell cycle is highly controlled by activity of the kinases CDK1, CDK4 and CDK5 and as proper cell cycle progression is pivotal and any disruption can induced cancer development, cell cycle dysregulation is seen as a hallmark of cancer (Malumbres 2014, Hanahan 2022). With more focus on mitosis, one of the essential mitotic kinases is CDK1 which is activated by association with Cyclin B1 in G2-phase and which is responsible for cells to enter mitosis (Nurse 1990). The protein levels of CDK1 were shown to be stable during cell cycle while its activity is mainly regulated by the abundance of the

activating protein Cyclin B1 (Morgan 1995). In recent publications, the importance of CDK1-Cyclin B1 was underlined as at least 551 proteins are phosphorylated in a CDK1-dependent manner in mitosis (Petroni, Adamo et al. 2016).

The substrates of mitotic CDK1-Cyclin B1 are involved in a wide range of cellular and mitotic processes like for example microtubule organization in yeast, Golgi apparatus function or apoptosis (Liakopoulos, Kusch et al. 2003, Preisinger, Körner et al. 2005, Allan and Clarke 2007). Furthermore, CDK1 plays a role in spindle assembly checkpoint (SAC) formation by phosphorylating of specific proteins of the SAC (Hayward, Alfonso-Pérez et al. 2019). Taking together, CDK1-Cyclin B1 can be seen as the major and essential kinase in mitosis (Nigg 1991).

Interestingly, CDK1 and CD14B have been found as counteracting pair in mitotic phosphoregulation of the protein KIBRA (Ji, Yang et al. 2012). It is tempting to speculate that KIBRA is not the only protein which is phosphorylated by the kinase CDK1 and dephosphorylated by the phosphatase CDC14B in mitosis.

Before cells can exit mitosis, the initial event and requirement is inactivation of CDK1-Cyclin B1 (Murray 2004). Therefore, the underlying processes is that the anaphase promoting complex (APC) activated by CDC20 ubiquitinates and targets Cyclin B for proteolysis which hampers activity of CDK1 (Musacchio 2015).

1.4 The Ubiquitin-proteasome system and USP9X

Ubiquitin is a protein comprised of 76 amino acids and which can be covalently attach to a wide range of target proteins for posttranslational modification (PTM) (Komander 2009). Ubiquitin is mainly covalently linked to a lysine residue of the target protein (Mattioli and Sixma 2014). The protein ubiquitin itself has seven lysine residues which means that ubiquitin can be ubiquitylated after it has been linked to a target protein which results in a polyubiquitin chain. In contrast to polyubiquitin chains, target proteins can also be only linked to one ubiquitin protein which is called monoubiquitylation (Swatek and Komander 2016).

Polyubiquitin chains are linked via different lysine residues of the ubiquitin proteins and depending on the lysine residue the chains exert different functions.

For example, polyubiquitin chains with lysine 48 (K48) as linker are described to target proteins for proteasomal degradation, also depending on chain length and the amount of ubiquitylated lysine residues of the target protein (Middleton and Day 2015). K48 linked ubiquitin chains were found to be the most abundant ubiquitin chains in cells (Yang, Zhao et al. 2021).

Another type of ubiquitin chain which has been widely investigated is the K63 linked polyubiquitin chain. Recent work could show that K63 linked ubiquitin chains exert their function in endocytosis, immunological processes and DNA repair (Husnjak and Dikic 2012). Beside this, K63 linked chains were described to regulate proteasomal degradation of the protein TXNIP (Ohtake, Tsuchiya et al. 2018).

Further ubiquitin chains with different ubiquitin lysine linkers like Lys 6, Lys 11, Lys 27, Lys 29 and Lys 33 are more and more understood. For example, K6 linked ubiquitin chains are involved in DNA replication and DNA repair, while K11 linked chains seem to play a

role in mitosis and cell division (Morris and Solomon 2004, Wickliffe, Williamson et al. 2011).

Interestingly, the protein ubiquitin can also be subjected to posttranslational modification like phosphorylation on threonine 14 and serine 20 and acetylation which raises the level of complexity of posttranslational modification (Husnjak and Dikic 2012).

The enzymatic cascade how ubiquitin is linked to the target proteins is highly regulated and comprises of a subset of different proteins.

First of all, an E1 enzyme binds to the C-terminus of a free and not attached ubiquitin via its active cysteine site under hydrolyzation of ATP to ADP and phosphate. In a second step, activated ubiquitin is transferred to a protein called E2 meaning that a bond between an active cysteine and the glycine of the C-terminus of ubiquitin is established. In a last step, an E3 ligase is involved. This protein interacts with the E2-ubiquitin complex and the possible substrate and leads to ubiquitylation of the substrate by initiating an isopeptide bond between the C-terminus of the ubiquitin protein and a lysine residue if the target protein (Figure 2) (Yang, Zhao et al. 2021).

As it can be seen here, substrate specificity is accomplished by the E3 ligases (Yang, Zhao et al. 2021). E3 ligases can be divided into different subgroups. One of this group comprises E3 ligases called HECT which harbor a specific domain called hect (homologous to the E6-AP carboxyl terminus) (Huibregtse, Scheffner et al. 1995).

The second group of E3 ligases is called RING-finger E3 ligases due to their RING domain (Zheng and Shabek 2017). This groups includes very diverse and in number the most E3 ligases (Deshaies and Joazeiro 2009).

The other two groups of E3 ligases are called U-box E3 ligases and RBR E3 ligases which are characterized by an in-between-Ring (IBR) flanked by two RING domains (Aguilera, Oliveros et al. 2000, Ryu, Cho et al. 2019).

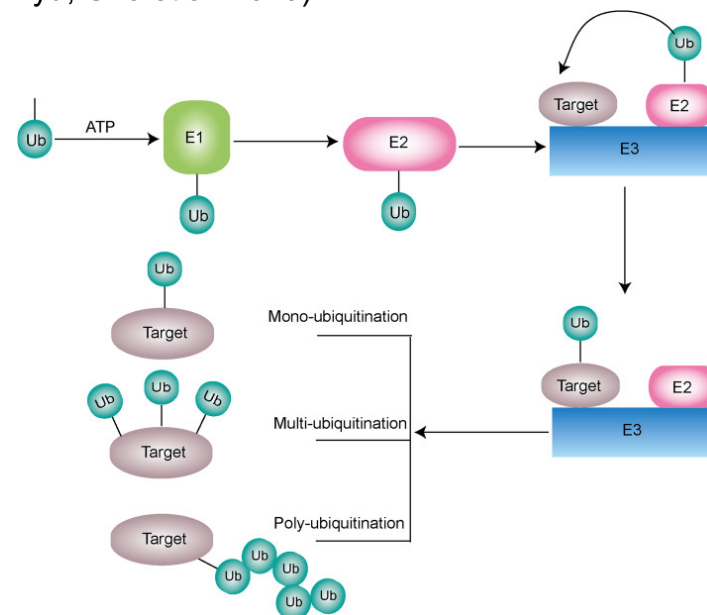


Figure 2 Process of protein ubiquitination Ubiquitin is activated by binding to the E1 enzyme under hydrolyzation of ATP to ADP. Next, the activated ubiquitin is transferred to E2. In a last step, an E3 leads to ubiquitylation. This results in monoubiquitylation, multi-monoubiquitylation or polyubiquitylation (Yang, Zhao et al. 2021).

The functions of ubiquitylation and the possible consequences for the target proteins have been described above. Nevertheless, a large number of ubiquitylated proteins are targeted for degradation by the 26S proteasome (Marshall and Vierstra 2019). The 26S proteasome is a 2.5MDa protein complex which comprises a 20S core protease and one or two 19S regulatory particles (Marshall and Vierstra 2019). The 20S has several active sites which are responsible for peptide cleavage and also called “proteolytic core” (Heinemeyer, Fischer et al. 1997). On the other hand, subunits of the 19S complex regulate substrate specificity of the 26S proteasome (Verma, Oania et al. 2004). Interestingly, the 26S proteasome is frequently targeted in cancer therapy. For example, the drug bortezomib reduces function of the 20S subunit of the 26S proteasome by reversibly inhibiting the peptidase activity of its beta5 subunit (Lü and Wang 2013).

Ubiquitylation of proteins is a posttranslational modification which was shown to be reversible (Komander, Clague et al. 2009). Counteracting the ubiquitin transferring E3-ligases, a subset of cellular enzymes exists which reverses ubiquitylation of proteins and which therefore take influence on a wide range of cellular processes by modifying the so-called “ubiquitin code” (Harrigan, Jacq et al. 2018). These proteins are peptidases and called deubiquitinases (DUBs) as they can reverse the isopeptide bond between the C-terminus of ubiquitin and the lysine of the target protein (Komander, Clague et al. 2009). To date, about 100 different DUBs have been described which can be divided into six different groups called USPs (ubiquitin-specific protease), UCHs (ubiquitin carboxy-terminal hydrolase), OTUs (ovarian tumor protease), MJDs (Machado–Josephin domain-containing protease), JAMMs (JAB1, MPN, MOV-34 family) and MINDYs (motif-interacting with ubiquitin-containing novel DUB family) (Harrigan, Jacq et al. 2018). Concerning the enzymatic activity of the deubiquitination enzymes, JAMMs are metalloproteases while all the others are cysteine proteases (Nijman, Luna-Vargas et al. 2005). The cellular function and biological relevance of those deubiquitination enzymes are extensive and very diverse. Deubiquitylation enzymes have been described to regulate cell cycle, DNA damage repair and signaling pathways like for example the Wnt signaling pathway (Fraile, Quesada et al. 2012).

The largest group of deubiquitylation enzymes are the ubiquitin-specific proteases (USPs) with more than 50 different enzymes (Quesada, Díaz-Perales et al. 2004). The unique biochemical characteristic of these USPs is the three-dimensional protein structure which consists of the Thumb, the Palm and the Finger (Hu, Li et al. 2002). The catalytic site which is the only similarity of these enzymes consists of a conserved cysteine and histidine motif and is flanked by the Thumb and the Palm while the Finger domain was described to interact with the ubiquitin protein (Fraile, Quesada et al. 2012, Murtaza, Jolly et al. 2015). Additionally, these USPs can harbor different domains or motifs like zinc-finger USP domains, ubiquitin-interacting motifs or ubiquitin-associated domains (Fraile, Quesada et al. 2012). Furthermore, binding of USPs to ubiquitin leads to a conformational change which primes the enzyme to cleave off the ubiquitin protein (Fraile, Quesada et al. 2012). How USPs recognize their substrate is still not completely understood, but one important factor for substrate recognition seems to be the amino acid sequence which flanks the active cysteine and histidine site of the corresponding USP (Murtaza, Jolly et al. 2015). Furthermore, an essential layer of regulation of enzymatic DUB activity towards substrates are posttranslational modifications like phosphorylation or deubiquitylation of DUBs (Wada and Kamitani 2006, Matsuoka, Ballif et al. 2007).

One highly conserved deubiquitinase of the USP-family is the enzyme called ubiquitin-specific protease 9X (USP9X) which has been described in *Drosophila* and which is found in mammals with a very conserved amino acid sequence (Murtaza, Jolly et al. 2015). This high grade of conservation suggests a central role of USP9X in cellular processes. With more detail to the structure of USP9X, it contains a ubiquitin like (UBL) domain in the N-terminal part of the protein as well as several nuclear localization sequences (Murtaza, Jolly et al. 2015).

The about 2700 amino acid large USP9X protein was described to be localized in the nucleus as well as in the cytoplasm (Murray, Jolly et al. 2004, Trinkle-Mulcahy, Boulon et al. 2008). This localization is variable and dependent on different cellular processes like cell adhesion (Murray, Jolly et al. 2004). The cellular processes that are regulated by USP9X are diverse. USP9X was described to influence endocytosis and protein trafficking by reversing autoubiquitylation of the protein Itch (Mouchantaf, Azakir et al. 2006). Furthermore, USP9X was shown to regulate cell polarity and tight junction formation by deubiquitylation of the protein Arf6 (Théard, Labarrade et al. 2010).

With more focus on cell survival and apoptosis, recent data have suggested anti- and proapoptotic functions of USP9X. USP9X interacts with and upregulates protein levels of ASK1 which induces cellular death in context of oxidative stress (Nagai, Noguchi et al. 2009). On the other hand, USP9X stabilizes mitotic XIAP and therefore enhances chemoresistance in lymphoma cells (Engel, Rudelius et al. 2016). Beside this, USP9X binds and deubiquitinates the BCL2 family protein MCL1 which in consequence promotes cellular survival (Schwickart, Huang et al. 2010). Additionally, USP9X is involved in neuronal processes and stem cell function (Agrawal, Chen et al. 2012, Stegeman, Jolly et al. 2013).

How USP9X is regulated in different cellular contexts is not well understood. One means of USP9X regulation could be phosphorylation of the DUB. USP9X was found to be phosphorylated on serine 1600 which further induces deubiquitination of the protein ZAP70 in lymphocytes (Naik and Dixit 2016). USP9X was shown to be phosphorylated in a TGF- β -dependent way and phosphorylated USP9X stabilizes the protein Ankyrin-G (Yoon, Parnell et al. 2020). The occurrence of further phosphorylation sites and the biological relevance of different posttranslational modifications of USP9X like SUMOylation or ubiquitylation need to be further investigated.

The research on USP9X has shed light on the role of USP9X in cancer cells. In a screen using in situ hybridization on tissue microarrays (ISH-TMA), USP9X was identified as a DUB which was significantly dysregulated in expression in different types of tumors (Luise, Capra et al. 2011). Furthermore, USP9X was shown to be overexpressed in lymphoma cells and solid tumors like breast cancer, kidney cancer and sarcoma (Schwickart, Huang et al. 2010, Murtaza, Jolly et al. 2015). In gastric cancer tissue, USP9X could be identified to be overexpressed and overexpression of USP9X significantly correlated with poorer survival of tumor patients (Fu, Xie et al. 2017).

1.5 The transcription factor Wilms' tumor protein 1 (WT1)

The Wilms' tumor protein 1 (WT1) is a transcription factor that was first found in 1990 encoded on the human chromosome 11 (Call, Glaser et al. 1990). Its name derives from a specific pediatric type of cancer called Wilms tumor where it was identified to be regularly homozygous deleted (Gessler, Poustka et al. 1990). The gene for WT1 is expected to encode for at least 36 isoforms of the protein WT1 which all harbor four C₂H₂ Kruppel-like zinc fingers which are necessary for DNA-binding (Hastie 2017). It was found to be an activator or a repressor of transcription depending on the cellular context and cell line (Menke, van der Eb et al. 1998, Lee, Huang et al. 1999). Splicing seems to be an important means to regulate function of WT1 (Hammes, Guo et al. 2001). The amino acids lysine, threonine and serine comprise a KTS motif which is flanked by zinc finger 3 and 4 and which was depicted to influence function of WT1 in kidney cells (Hammes, Guo et al. 2001). The transcription factor WT1 was characterized to bind dominantly to the consensus site 5'GCGTGGGAGT3' and data could show that especially the 3'thymidine and the alanine influence WT1 and DNA interaction (Nakagama, Heinrich et al. 1995).

Research assessing the biological relevance of WT1 has been an expanding field within the last decades. Recent work could indicate that WT1 plays a pivotal role in murine kidney development (Kreidberg, Sariola et al. 1993). In epicardial cells, WT1 is mainly inducing epithelial- mesenchymal transition via Snail and E-cadherin (Martínez-Estrada, Lettice et al. 2010). Beside this function in epicardial cells, WT1 was shown to repress expression of the chemokines Ccl5 and Cxcl10 directly and indirectly via the protein IRF7 (Velecela, Lettice et al. 2013).

One further important target gene of WT1 encodes for the protein Bcl-2 (Mayo, Wang et al. 1999) In primary cells of Wilms tumors, the protein level of WT1 and Bcl-2 correlate with each other and WT1 was demonstrated to regulate Bcl-2 expression via binding to the Bcl-2 promoter and therefore promoting tumor cell survival (Mayo, Wang et al. 1999). Interestingly, this binding was dependent on absence of the KTS motif between zinc finger 3 and 4 (Mayo, Wang et al. 1999). Among others, further genes which are regulated by WT1 on a transcriptional level identified by chromatin immunoprecipitation screens are Sox11, Smad7, Smad4 and Pbx1 (Hartwig, Ho et al. 2010).

Furthermore, WT1 has been shown to be highly modified by posttranslational modifications changing WT1 function. In vitro phosphorylation of the protein WT1 changes its ability to bind to DNA using gel mobility shift assays independent of the KTS motif (Ye, Raychaudhuri et al. 1996). Not only regulating interaction of WT1 with DNA, also subcellular localization is influenced by phosphorylation of WT1 meaning that phosphorylated WT1 is sequestered to the cytoplasm although the phosphorylation site has not been specified yet (Ye, Raychaudhuri et al. 1996).

Another work could identify phosphorylation of WT1 on serine 62 which is established by protein kinase B to inhibit WT1 ubiquitylation by the ubiquitin ligase F-box/WD repeat-containing protein 8 (FBXW8) which in consequence rescues WT1 from proteasomal degradation (Lee, Jeon et al. 2017).

HSP 90 was shown to take influence on ubiquitylation of WT1 (Bansal, Bansal et al. 2010). Inhibition of HSP90 with the reagent 17-AAG reduced protein levels of WT1 in a proteasome dependent way (Bansal, Bansal et al. 2010).

Another regulatory means of WT1 on posttranslational level is proteolytic cleavage of WT1. WT1 is cleaved by caspase 3 in leukemic cells in circumstances of apoptosis (Ruan, Gao et al. 2018). Cleavage was induced by treatment with etoposide and could be reversed by blocking general caspase activity and more specifically, by blocking activity of caspase 3 (Ruan, Gao et al. 2018).

Given the biological functions mentioned above, WT1 was assessed to be overexpressed in diverse cancer types.

In mice xenograft experiments with Ewing sarcoma cell lines, immunofluorescence of xenograft specimens could show that WT1 positively regulates angiogenesis in these tumor cells and furthermore, this work could demonstrate that WT1 promotes expression of VEGF in vitro (Katuri, Gerber et al. 2014). Interestingly, the only isoform of WT1 comprising amino acids of exon 5 and the KTS motif between zinc finger 3 and 4 induces expression of VEGF compared to a WT1 isoform lacking exon 5 and the KTS motif (Katuri, Gerber et al. 2014). Ewing sarcoma cell lines which were used for mice xenograft led to a higher tumor burden in the presents of WT1 (Katuri, Gerber et al. 2014).

In a murine leukemia model, WT1 has a fundamental role in cellular self-renewal via upregulation of the protein BCL₂C₂ by transcriptional means (Zhou, Jin et al. 2020). Performing flow cytometry and colony formation assays, overexpression of WT1 led to lower apoptotic rates in leukemic cell lines under treatment with WP1130, a deubiquitinase inhibitor (Zhou, Jin et al. 2020).

With more focus on clinical data, mRNA levels of WT1 in 10 osteogenic sarcoma patient samples compared to normal bone tissue were shown to be 3-fold upregulated performing a microarray-based analysis (Srivastava, Fuchs et al. 2006). Correlation of WT1-immunostaining in primary patient specimens and clinical data showed lower survival rate in patients with high WT1 expression and the authors suggest to conduct WT1-staining of tumor samples when diagnosed and to establish WT1-expression as a predictive maker in specific types of osteogenic sarcoma (Srivastava, Fuchs et al. 2006).

In non-small cell lung cancer cell lines, WT1 is an essential enhancer of cell migration (Wu, Zhu et al. 2013). In specimens of patients with NSCLC, high mRNA levels of WT1 positively correlate with occurrence of metastasis and lower survival rate of tumor patients (Wu, Zhu et al. 2013).

Taking the data above into account, WT1 is more and more found to exert rather oncogenic than tumor suppressive function. That WT1 is an oncogene is in contrast to early findings of WT1 where it was thought to be a tumor suppressor as loss of both alleles is necessary to promote cancer development (Knudson and Strons 1972). For better understanding of oncogenic and tumor suppressive function of WT1, Lee et al., brought up the explanation that the amino acid sequence CUG added to the protein synthesis initiation site of WT1 causes WT1 function rather to be oncogenic (Lee, Jeon et al. 2017).

1.6 The chemokine IL-8

Chemokines comprise a subgroup of about 40 proteins which resemble each other in structure and size (Gales, Clark et al. 2013). The known chemokines have a weight

between 8 and 14kDa and were initially found to regulate leukocyte function and inflammatory processes (Gales, Clark et al. 2013). Chemokines can attract and induce migration of neutrophils, lymphocytes and fibroblasts and play a pivotal role in orchestration of cellular immunological processes and tissue repair (Miller and Krangel 1992). Chemokines are described to exert their function via binding to a G-protein coupled receptor on the cellular membrane (Raman, Sobolik-Delmaire et al. 2011). Recent work could specify that different chemokines do not only regulate processes of the immune system but also play an important role in epithelial mesenchymal transition, angiogenesis, tumor growth and formation of metastasis (Sarvaiya, Guo et al. 2013).

One prominent chemokine is IL-8, also called CXCL-8, which belongs to the chemokine subgroup of C-X-C motif ligand chemokines (Rossi and Zlotnik 2000). The C-X-C motif comprises a variable amino acid between the first two cysteines in the amino acid sequence of the protein (Modi, Dean et al. 1990). Initially, one of the main functions of IL-8 was described to play a major role in acute inflammation as it attracts neutrophils to site of inflammation (Harada, Sekido et al. 1994). In recent publications IL-8 was shown to be secreted by fibroblast to regulate acute inflammation or by endothelial cells to hamper inflammation in adjacence to blood vessels (Gimbrone, Obin et al. 1989, Schröder, Sticherling et al. 1990). Furthermore, IL-8 is actively produced and secreted for example by monocytes, neutrophils and non-immunological cells like mesothelial cells (Guo, Zang et al. 2017).

The corresponding receptors for binding of IL-8 on the cellular membrane are CXCR1 and CXCR2 (Singh, Simões et al. 2013). The CXCR1 and CXCR2 do not only function as receptor for IL-8 as beside IL-8 also CXCL6 was described to bind to CXCR1, in comparison to the receptor CXCR2 that shows binding to for example CXCL1, CXCL5 and CXCL7 (Ahuja and Murphy 1996). The extracellular binding of IL-8 to the CXCR1 or CXCR2 receptor induces the formation of a heterotrimeric G-protein complex which leads to dissociation of the complex after binding guanosine triphosphate and potential activation of either the PI3K/Akt-, the PLC/PKC- or the Erk1/2-signaling pathway (Singh, Simões et al. 2013). A fourth signaling pathway which was shown to be activated by CXCR1 or CXCR2 signaling is the JAK-STAT pathway (Schraufstatter, Chung et al. 2001). Within the last years upcoming evidence brings up the idea that IL-8 does not only play a role in inflammatory processes but also in cancer biology.

In ovarian cancer cell lines IL-8 stimulation of SK-OV-3 cells improved cellular signaling via the Erk1/2 pathway (Venkatakrishnan, Salgia et al. 2000). In a bladder cancer cell line, IL-8 was highly expressed and promoted angiogenesis via upregulating the activity of matrix metalloprotease type 9 (Inoue, Slaton et al. 2000). Beside these effects, IL-8 binding to prostate cancer cell lines upregulated expression of the androgen receptor on the level of transcription (Seaton, Scullin et al. 2008).

In estrogen-receptor negative breast cancer cells IL-8 was highly expressed and actively secreted whereas this could not be shown for breast cancer cells with high estrogen receptor expression (Freund, Chauveau et al. 2003). Furthermore, IL-8 seems to potentiate invasiveness of breast cancer cell lines lacking expression of estrogen receptor (Freund, Chauveau et al. 2003). Supporting the idea of a central role of IL-8 signaling in breast cancer, staining of 43 breast cancer specimens performing immunohistochemical analysis showed expression of CXCR1 and CXCR2 in these tumor cells (Miller, Kurtzman et al. 1998). These data suggest a central role of IL-8 in cancer biology.

The regulators of IL-8 expression are diverse and have been described in previous publications. In breast cancer cells lines, IL-1 β was shown to induced expression of IL-8 (De Larco, Wuertz et al. 2001). Furthermore, treatment of tumor cells with TNF- α leads to the response of high IL-8 expression (Kasahara, Mukaida et al. 1991).

In non-cancer cells, more precisely in monocytes, IL-8 secretion was dependent on the absence or presence of the chemokines CCL2 and CCL5 (Azenshtein, Meshel et al. 2005). Furthermore and emphasizing the relevance of tumor environment, it was demonstrated that macrophages produce CXCR2 ligands which induce tumor formation of breast cancer cells (Bohrer and Schwertfeger 2012). Another work depicted the importance of chemokine loops and could show that mesenchymal stem cells can be stimulated to produced IL-7 which in consequence promotes secretion of IL-8 by tumor cells (Liu, Ginestier et al. 2011).

The regulation of CXCL8 gene expression has been intensively investigated within the last years. It could be shown that one main transcription factor which is responsible for CXCL8 expression is p65 NF- κ B under circumstances of IL-1 stimulation as treatment of tumor cells with IL-1- α induces binding of p65 NF- κ B to the promotor of CXCL8 (Hoffmann, Dittrich-Breiholz et al. 2002).

Another transcriptional regulator of CXCL8 in a more immunological context is the transcription factor C/EBP homologous protein (CHOP) (Vij, Amoako et al. 2008). Under stimulation of bronchial epithelial cells with prostaglandin E2 IL-8 expression was upregulated by binding of the transcription factor C/EBP homologous protein (CHOP) to the CXCL8 promoter (Vij, Amoako et al. 2008).

1.7 Mitotic bookmarking and active mitotic transcription

Within the last years the understanding of transcriptional activation and silencing in mitosis has changed. Until 2017, transcription in mitosis was expected to be completely silenced which is accomplished by a complex cascade of phosphorylation events by cyclin-dependent kinase (Prescott and Bender 1962, Rhind and Russell 2012). In general, mRNA levels seemed to be stabile during mitosis underlining the model of stalled transcription in mitosis and regulation of protein expression on the level of translation (Tanenbaum, Stern-Ginossar et al. 2015). Induced by phosphorylation, a great number of transcription factors were described to dissociate from DNA when cells enter mitosis, so for example Ets-1 and Sp1 (Martínez-Balbás, Dey et al. 1995, Delcuve, He et al. 2008). In contrast and in order to reactivate transcription after cells have passed through mitosis and to orchestra postmitotic transcription in space and time, a specific subset of transcription factors are bound to condensed mitotic DNA which is called mitotic bookmarking (Lodhi, Ji et al. 2016). Mitotic bookmarking was shown to enable a wave of highly active transcription after mitosis which is necessary for proper function of the daughter cell (Kadauke and Blobel 2013). Recent work has shown that at least 20 transcription factors are bound to condensed DNA in mitosis and one of their main functions is to conserve cell type specific gene expression after cell division and to preserve gene expression patters after mitosis with its high dynamics in chromatin formation (Zaidi, Lian et al. 2017). Two of these bookmarking transcription factors or DNA-

associated proteins are p300 and Runx2 (Young, Hassan et al. 2007, Wong, Byun et al. 2014).

One important regulatory means of mitotic bookmarking are epigenetic modifications. Phosphorylation of histones is one of the main regulatory events of chromatin condensation like phosphorylation of histone H3 on serine 10 and on serine 28 (Wang and Higgins 2013). Phosphorylation of histone H3 on serine 10 and serine 28 occurs in early mitosis and promotes condensation of chromosome (Goto, Tomono et al. 1999). Furthermore, histone modification like histone H3 and histone H4 acetylation together with histone H3 lysine 79 and histone H3 lysine 4 methylation are modifications which are highly conserved in mitotic cells compared to G0/G1-arrested cells (Kouskouti and Talianidis 2005). Histone modifications mentioned above take influence on the binding of specific proteins like transcription factors to DNA in mitosis (Egli, Birkhoff et al. 2008). Increasing the level of complexity, exchange of specific histones which associate with DNA like for example histone H3 is a main regulatory layer in epigenetics also throughout mitosis (Ng and Gurdon 2008).

With more focus on transcription factors and their role in mitotic bookmarking, an increasing number of transcription factors are described to be associated with specific areas of condensed DNA in mitosis. One of these transcription factors is the protein Brd4 which preserves binding to specific transcription starting sites in mitosis to ensure rapid transcriptional reactivation in G1 and interestingly, associating of Brd4 with DNA takes place in the last phase of mitosis with timely coincidence of histone H3 and H4 acetylation (Dey, Nishiyama et al. 2009). For instance, recent work could show that the transcription factor CTCF localizes to mitotic chromosomes which is mediated by zinc-finger domains and that binding of CTCF to condensed DNA is restricted to previously described target genes (Burke, Zhang et al. 2005).

A further interesting aspect of mitotic bookmarking was described by Xing et al. The protein HSF2 remains bound to the gene *hsp70i* in mitosis which induces interaction of the protein phosphatase A2 and condensing near the *hsp70i* gene (Xing, Wilkerson et al. 2005). This leads to dephosphorylation of condensin hampering its function and keeping the *hsp70i* gene accessible as DNA condensation is inhibited (Xing, Wilkerson et al. 2005). Another regulatory means of mitotic bookmarking is phosphorylation of transcription factors in their 2H2 zinc finger DNA-binding domains which for example influences binding the protein Ikaros to DNA (Dovat, Ronni et al. 2002).

In 2017 the concept of mitotic bookmarking and mitotic transcription began to change. Palozola et al., could show that cells preserve low level transcription of a subset of genes in mitosis (Palozola, Donahue et al. 2017). First of all, active transcription of RNA could be inhibited by using the RNA-polymerase inhibitor alpha-amanitin in mitosis (Palozola, Donahue et al. 2017). Furthermore, mitotic or nocodazole-released cells were incubated with 5-ethynyluridine (EU) to label newly synthesized RNA which was further purified and analyzed by RNA Sequencing (Palozola, Donahue et al. 2017). Genes found that were higher expressed in mitotic cells than in asynchronous cells are involved in focal adhesion, extracellular region and transcription (Palozola, Donahue et al. 2017).

2. Aim of the study

Correct mitosis and a functioning spindle assembly checkpoint are pivotal for cell division and disturbance of mitotic cell cycle progression can lead to mitotic catastrophe and cell death (Castedo, Perfettini et al. 2004). In case of erroneous mitosis, high fidelity mitotic signaling mediates cell fate decision to prevent genomic instability and development of cancer (Dominguez-Brauer, Thu et al. 2015). Among others, essential mitotic processes and the spindle assembly checkpoint are regulated by posttranslational modifications like phosphorylation and ubiquitylation (Manic, Corradi et al. 2017, Watson, Brown et al. 2019). One of the central mitotic regulators in budding yeast is the phosphatase Cdc14 by antagonizing Cdk1- mediated phosphorylation of Cdh1 (Visintin, Craig et al. 1998). A role of the human ortholog of Cdc14 named CDC14B has been described in G2 DNA damage checkpoint response but its role in mitosis and mitotic substrates remain elusive (Bassermann, Frescas et al. 2008, Wei, Peddibhotla et al. 2011).

Given the poorly described mitotic function of the phosphatase CDC14B in human cells, the aim of this study was to identify possible substrates of CDC14B which are part in mitotic signaling pathways. To this end, an unbiased mass spectrometry of mitotic CDC14B interacting proteins was performed. After the target protein USP9X was verified, phosphor-proteomic analysis was performed to detect the dephosphorylation site of USP9X regulated by CDC14B. Further, to complete the understanding of phosphorylation of USP9X on serine 2563 the relevant kinase and the biochemical effects were identified. To find possible mitotic substrate of the deubiquitinase USP9X, a mitotic ubiquitome-analysis was performed, followed by verifying WT1 as substrate by stability, binding and ubiquitylation assays. In a subsequent step, RNA sequencing identified IL8 as the downstream target of the transcription factor WT1 in mitotic cells.

Overall, this project identifies a new signaling axis in mitosis which regulates mitotic survival that can serve as a potential new therapeutic target structure in cancer therapy.

3. Results

The results of this project were mainly gained in the research group of Prof. Florian Bassermann at Klinikum rechts der Isar and TranslaTUM (TUM). Parts of the experiments were performed by collaborators or co-workers in the laboratory. For a better understanding of the project, data of our collaborators and co-workers are included. This data is appropriately labeled in text and figure legends and the corresponding remarks of the experimental setup and procedure are kept short and are reduced to a necessary extend.

3.1 CDC14B interacts with USP9X in mitotic cells

The following experiments were performed by Vanesa Fernández-Sáiz and Katharina Clemm von Hohenberg aiming for a better understanding of the mitotic function of the phosphatase CDC14B and its involvement in mitotic signaling pathways. To this end, an unbiased proteome-wide screen with mass spectrometric analysis was conducted. Therefore, CDC14B which was tagged with a Strep- and FLAG-tag or control vector were overexpressed in HEK 293T. Further, cells were either arrested in G2/M or kept asynchronous followed by tandem affinity purification. Using mass spectrometry interacting proteins of CDC14B were analyzed by Christian Johannes Gloeckner and most significant hits are listed below (Table 1). This yielded USP9X as a potential interacting protein of CDC14B with cell cycle regulated binding enhanced in mitosis. To verify the *in vivo* interaction of CDC14B and USP9X, FLAG-tagged CDC14B was overexpressed in HEK 293T cells which were arrested in mitosis using the microtubule-targeting drug nocodazole or which were kept asynchronous. Immunoprecipitation and immunoblot analysis performed by Katharina Clemm von Hohenberg confirmed pronounced mitotic interaction of CDC14B and USP9X in HEK 293T cells with immunoblot analysis (Figure 3).

Gene	TAP control	TAP CDC14B (AS)	TAP CDC14B (G2/M)
CDC14B	0	24	22
USP9X	0	4	7
RPL3	0	2	3
RPL17	0	0	3
RPL8	0	0	2
RPL23A	0	2	2
RPS32	0	0	2

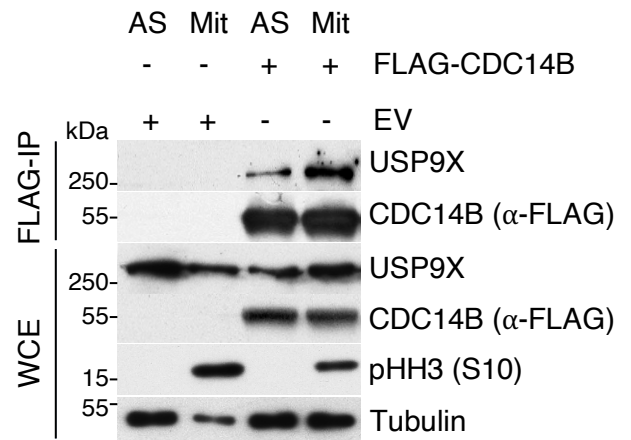


Table 1 CDC14B interacts with USP9X in mitotic cells Mass spectrometric analysis of the CDC14B interactome by tandem purification (TAP) from HEK 293T cells which were either kept asynchronous (AS) or arrested in G2/M. Proteins are depicted which scored for most significant change between asynchronous and G2/M arrested cells. Numbers of unique peptides are indicated. **Figure 3** Co-immunoprecipitation of FLAG-tagged CDC14B with endogenous USP9X from HEK 293T cells. Cells were treated with nocodazole (Mit) or kept asynchronous (AS). EV stands for empty vector. Immunoprecipitates (FLAG-IP) and whole cell extracts (WCE) were analyzed with indicated antibodies. Experiments were performed by Fernández-Sáiz and Clemm von Hohenberg. Tubulin is used as loading control and pHH3 Serine 10 (pHH3 (S10)) as cellular marker for mitosis. (kDa: kilo Dalton).

3.2 Stable isotope labeling of amino acids in cell culture (SILAC) under CDC14B overexpression

In order to investigate the dephosphorylation activity of the phosphatase CDC14B towards USP9X an unbiased proteomic approach using the method of stable isotope labeling of amino acids in culture (SILAC) was performed. Cells were either cultured in heavy medium (“H”) meaning that the amino acids lysine and arginine containing stable isotopes were added to the medium or cells were cultured in light medium (“L”) meaning that unlabeled lysine and arginine were added to the medium. Control vector or vector coding for FLAG-tagged CDC14B were expressed by Clemm von Hohenberg in HEK 293T cells followed by mitotic synchronization with nocodazole. Mass spectrometry of cell lysates was done by Christian Johannes Gloeckner. Results of mass spectrometry indicated that mitotic USP9X is phosphorylated on serine 2563 in a CDC14B dependent way (Table 2, Figure 4).

Ratio H/L normalized	Position	Peptides	Gene name
4,4188	2563	3	USP9X
	1226	1	USP9X

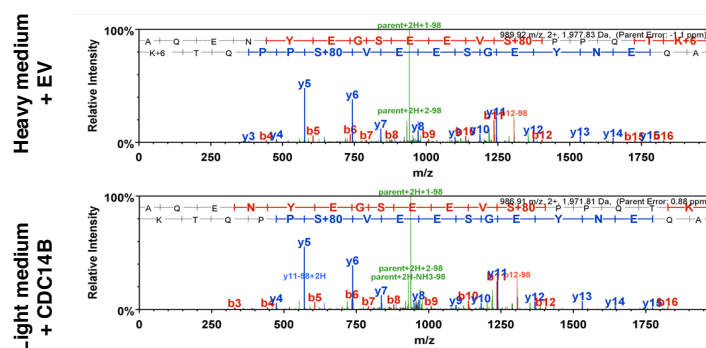


Table 2 Stable isotope labeling of amino acids in culture (SILAC) under CDC14B overexpression Mass spectrometric phosphor-analysis of SILAC in HEK 293T cells which overexpressed either CDC14B or empty vector. Control cells (EV = expression vector) were cultured in heavy (“H”), CDC14B overexpressing cells in light (“L”) medium. Normalized ratio of phosphopeptide intensity in light and heavy condition, the corresponding position on USP9X and the number of analyzed peptides are depicted. **Figure 4** Mass spectra of the USP9X phosphopeptides showing the relative intensity of phosphopeptides on the y-axis, and mass-to-charge ratio on the x-axis. Data was generated by Clemm von Hohenberg und Gloeckner.

3.3 CDC14B dephosphorylates USP9X on serine 2563 in mitosis

In order to confirm the results of the mass spectrometry screen and to demonstrate that CDC14B reverses the mitotic phosphorylation of USP9X on serine 2563 experiments changing CDC14B activity were performed. For Western Blot experiments a custom-made antibody to detect phosphorylation of USP9X on serine 2563 was produced. USP9X knockdown experiments in U2-OS cells showed specific binding of the antibody to endogenous USP9X (Figure 5). U2-OS cells were treated with siRNA against USP9X as 6.3.2. Afterwards, cells were synchronized with a thymidine block followed by arrest in mitosis using nocodazole as described in 6.3.3. Mitotic cells were harvested by mitotic shake-off, lysed in okadaic acid containing lysis buffer and samples were subjected to SDS-polyacrylamide gel electrophoresis and Western Blot. Next, transferred proteins were immunoblotted first with the custom-made USP9X antibody detecting the phosphorylation of USP9X on serine 2563. Then, the same membrane was re-incubated with an antibody targeting USP9X to evaluate whole protein levels as described in 6.2.6. This experiment could show the specificity of the phosphorylation specific antibody against USP9X.

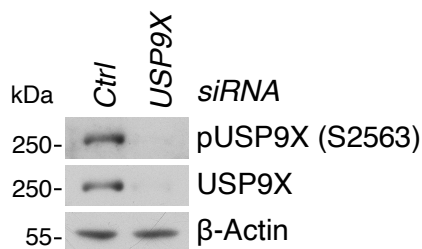


Figure 5 Validation of USP9X antibody against serine 2563 phosphorylation Immunoblot with the custom-made antibody against USP9X serine 2563 phosphorylation after cells were transfected with either *control* or *USP9X* siRNA in U2-OS cells. The signal for pUSP9X (S2563) is generated by the custom-made phosphorylation specific antibody, the USP9X signal by commercial antibody. Beta actin is used as loading control. (kDa: kilo Dalton).

In the next steps, CDC14B levels were lowered by transfecting U2-OS cells with siRNA targeted against *CDC14B* as described in 6.3.2. Afterwards, cells were synchronized in mitosis using thymidine supplemented medium followed by nocodazole treatment as described in 6.3.3. Mitotically arrested cells were harvested performing a mitotic shake-off, lysed in okadaic acid containing lysis buffer, separated by molecular weight by SDS-PAGE and visualized by Western Blot and immunoblot, respectively. This experiment could demonstrate that knockdown of *CDC14B* in mitotic U2-OS cells leads to enhanced phosphorylation of USP9X on serine 2563 suggesting CDC14B to be the mitotic phosphatase of USP9X (Figure 6a). Cyclin B1 is a protein which is highly expressed in mitosis, degraded when cells exit mitosis and therefore usable as a protein marker for mitosis (Afonso, Castellani et al. 2019). Cellular levels of Cyclin B1 are equal between *control* and *CDC14B* knockdown cells ruling out an effect on USP9X phosphorylation generated by different stages of cell cycle. Another mitotic marker used in this experiment is the kinase PLK1 which is highly expressed in mitotic cells (Anger, Kues et al. 2003). As we did not have any antibody directed against CDC14B, cells were aliquoted after harvesting. One part was subjected to Western Blot, the other part was used to validate knockdown of *CDC14B* by quantitative RT-PCR. Therefore, mRNA was extracted from cells as described in 6.1.3. Then, quantitative RT-PCR was done with the primers listed in 5.10. The mRNA levels were decreased in *CDC14B* siRNA treated cell to a about 30% compared to control cells (Figure 6b).

Vice versa, overexpression of FLAG-tagged CDC14B in HeLa cells as described in 6.3.1 leads to reduced phosphorylation of USP9X on serine 2563. Samples for Western Blot and immunoblotting were prepared as described above (Figure 6c).

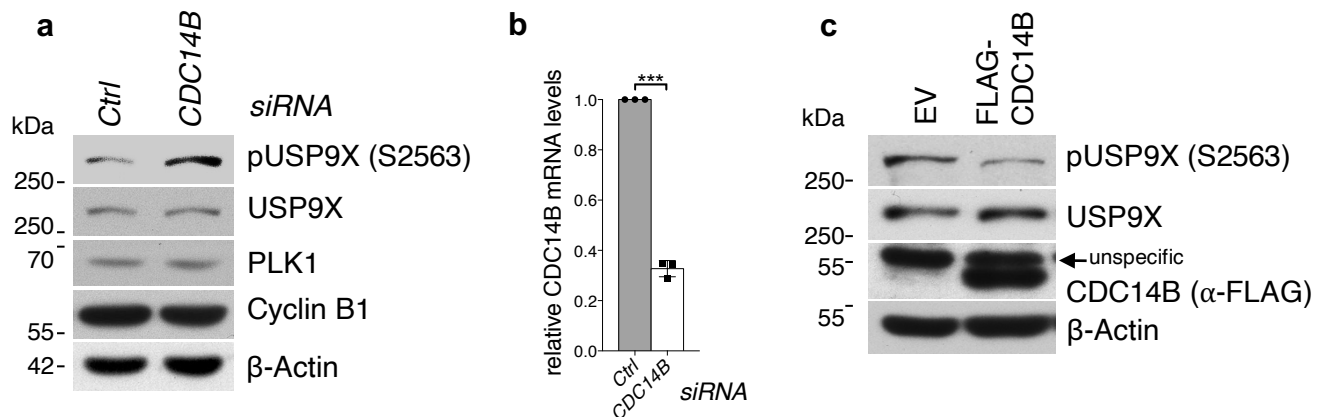


Figure 6 CDC14B dephosphorylates USP9X on serine 2563 in mitosis (a) Immunoblot analysis of U2-OS cells that were treated with siRNA directed against *CDC14B* or with *control* siRNA. Cells were synchronized as described in the main text. Samples were probed with the indicated antibodies after Western Blot. PLK1 and Cyclin B1 are mitotic cell cycle markers. β-Actin is used as loading control. **(b)** Quantitative RT-PCR showing knockdown of *CDC14B* in *CDC14B* siRNA treated cells compared to *control* siRNA treated cells on mRNA level. Data from three biological triplicates are shown. Y-axis shows mRNA levels normalized to control sample, x-axis depicts different siRNA conditions. Significance calculated with Ratio paired t-test with $**p=0.0045$. **(c)** Immunoblot analysis confirming reduced phosphorylation of USP9X on serine 2563. HeLa cells were either transfected with a FLAG-tagged *CDC14B* coding plasmid or empty vector (EV). Samples were analyzed by Western Blot followed by incubation with indicated antibodies. The signal for pUSP9X (S2563) is generated by the custom-made phosphorylation specific antibody, the USP9X signal by commercial antibody. FLAG-tagged *CDC14B* overexpression is depicted with an antibody against the FLAG-peptide. β-Actin is used as loading control. (kDa: kilo Dalton).

3.4 USP9X phosphorylation on serine 2563 is highly regulated during cell cycle

To address the question if USP9X phosphorylation on serine 2563 is a mitosis specific, a cell cycle analysis of the respective phosphorylation site in U2-OS cells was conducted. To perform cell cycle analysis which expands one entire cell cycle, cells were either synchronized in G1/S-phase or in mitosis followed by a release out of both blockages. First, U2-OS cells were synchronized in G1/S-phase with a double thymidine block. After cells had been released from G1/S-phase blockage, cells were harvested at the indicated time points. This experimental setup is capable to identify phosphorylation of USP9X on serine 2563 in G1/S-phase and G2 phase. Precise description of synchronization steps can be found in 6.3.3.

For a better understanding of phosphorylation of USP9X on serine 2563 in the cell cycle phases mitosis, mitotic exit and G1-phase U2-OS cells were arrested in mitosis using the spindle poison nocodazole and released as described in 6.3.3. Cells were harvested at the indicated time points.

Harvested cell pellets were lysed in an okadaic acid containing lysis buffer, subjected to SDS-PAGE, Western Blot and immunoblotting. These experiments could be shown that phosphorylation of USP9X on serine 2563 occurs to a much higher extend in mitotic cells than in G1 or S-Phase cells while protein levels of USP9X are quite stable during cell cycle (Figure 7). To confirm the corresponding cell cycle stage of the analyzed U2-OS cells immunoblots for specific proteins which are expressed or modified in a cell cycle dependent manner were conducted. Histone H3 phosphorylation on serine 10 (pHH3) is a marker for mitosis, high Cyclin E levels correlate with cell accumulation in G1-S-phase (Sherr and Roberts 1995, Hendzel, Wei et al. 1997) (Figure 7). Cyclin B1 and PLK1 expression pattern have been specified above.

Taken together, these experiments show for the first time that phosphorylation of USP9X on serine 2563 is a highly regulated, cell cycle dependent posttranslational modification.

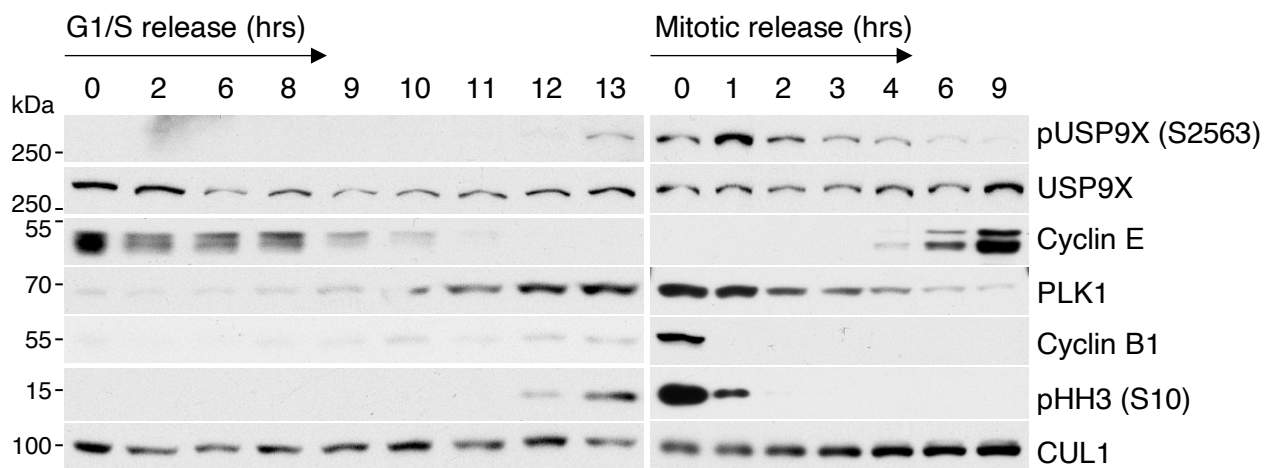


Figure 7 USP9X phosphorylation on serine 2563 is highly regulated during cell cycle U2-OS cells synchronized in G1/S-phase (left part) using a double thymidine block or arrested in mitosis using nocodazole (right part). Cells were further released from the respective cell cycle blockage and collected at the time points shown (hrs=hours after release). Immunoblot analysis was performed using indicated antibodies. CUL1 is used as loading control. (kDa: kilo Dalton).

3.5 CDK1 phosphorylates USP9X on serine 2563 in mitosis

Given the data that USP9X is dephosphorylated by CDC14B on serine 2563 in mitosis, the next aim was to identify the corresponding kinase of USP9X. Recent publications describe CDC14B to oppose the function of CDK1 towards different target proteins. (Tanguay, Rodier et al. 2010, Ji, Yang et al. 2012). Supporting the idea of CDK1 to be the mitotic kinase of USP9X on serine 2563, CDK1 is one of the main regulating kinases in mitosis and furthermore, serine on position 2563 of USP9X lies within the known consensus site of CDK1 (Malumbres 2014). This consensus site of CDK1 comprises a serine or threonine as phosphorylation site followed by the amino acid proline (Figure 8).

CDK1 recognition site

USP9X protein: (2557) G S E E V S P P Q T K D Q Stop
CDK1 Consensus site: S/T P

Figure 8 USP9X harbors a CDK1 consensus site on position 2563/2564 C-terminus of USP9X with serine 2563 (green) shown in top line and CDK1 consensus site depicted in lower line (S/T followed by proline in amino acid sequence)

In a first step, the functional role of CDK1 towards USP9X was investigated. Therefore, U2-OS cells were synchronized in mitosis using nocodazole as described in 6.3.3. Then, arrested cells were treated with the selective CDK1 inhibitor RO-3306 for 0,5h at a final concentration of 9µM (Vassilev, Tovar et al. 2006). Further cells were harvested, lysed and subjected to Western Blot followed by immunoblotting. This experiment indicates that CDK1 inhibition leads to decreased phosphorylation of USP9X on serine 2563 (Figure 9a).

To verify the effect of USP9X hypo-phosphorylation under RO-3306 treatment as direct consequence of reduced CDK1 activity and CDK1 as the direct kinase of USP9X an in vitro phosphorylation assay with radioactively labeled ATP was conducted.

First, plasmids carrying either a GST-tagged C-terminal truncated USP9X wildtype (USP9X^{WT}) or a GST-tagged C-terminal truncated USP9X mutant (USP9X^{S2563A}) were transformed into E.Coli BL21 bacteria. The truncated versions of USP9X consist of the amino acids ranging from position 2165 to 2570 of USP9X. The GST-tagged C-terminal truncated USP9X mutant (USP9X^{S2563A}) harbors a mutation on position 2563 with an exchange of serine to alanine representing a non-phosphorylatable mutant. After transformation, expression of wildtype and mutated GST-tagged C-terminal truncated USP9X or GST-empty (GST) was induced using IPTG overnight, followed by cell lysis and purification of GST-tagged C-terminal truncated USP9X variants or GST-empty. The extended description of experimental procedure is described in 6.2.7. Upon purification, GST-empty (GST), GST-tagged truncated USP9X wildtype (USP9X^{WT}) or GST-tagged truncated USP9X mutant (USP9X^{S2563A}) were incubated with radioactive [alpha-P32]ATP and CDK1-Cyclin B as described in 6.2.8. This experiment could show for the first time

that USP9X is phosphorylated on serine 2563 by CDK1 in vitro. The non-phosphorylatable variant of USP9X with a mutation on serine 2563 (USP9X^{S2563A}) is phosphorylated to a much lesser extent than the wildtype form of USP9X. The in vitro phosphorylation experiment was performed in technical duplicates and quantified (Figure 9b,c).

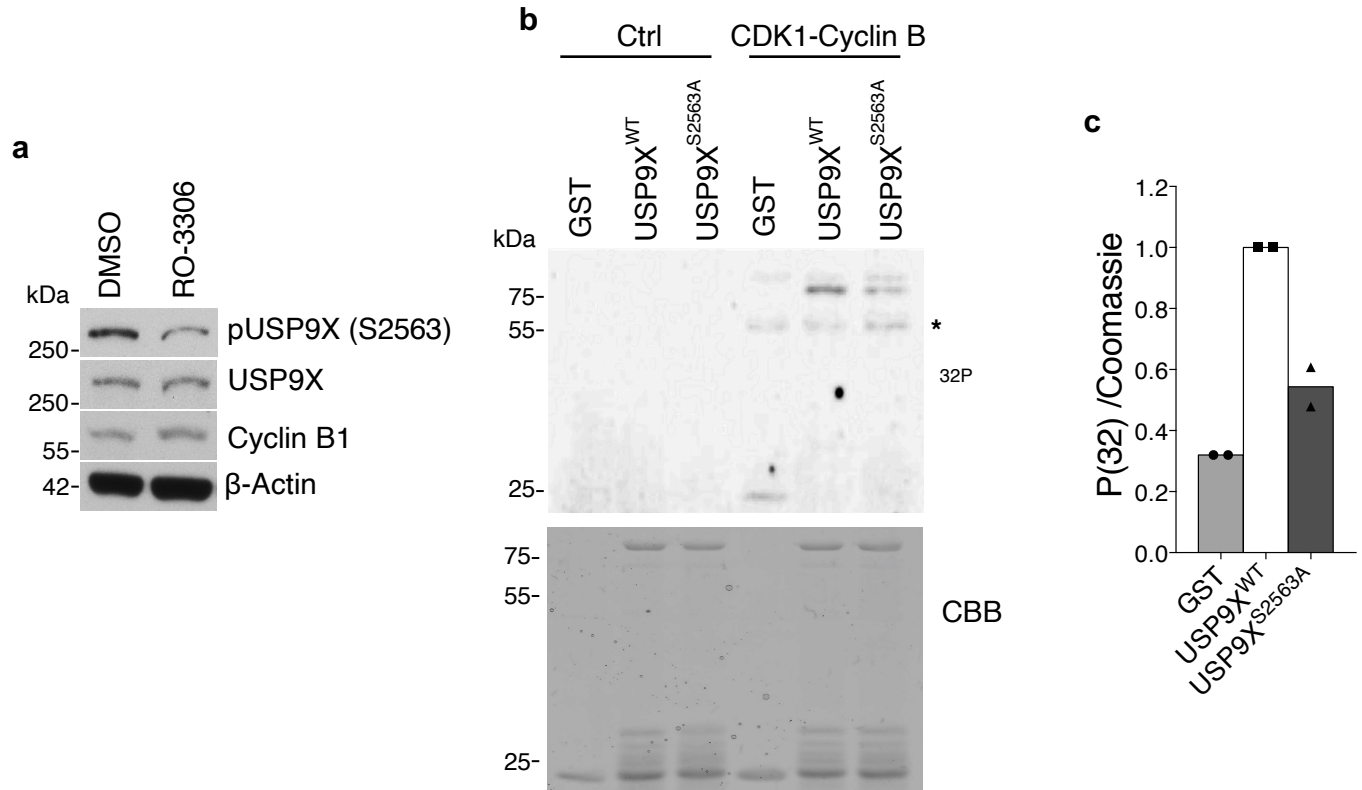


Figure 9 CDK1 phosphorylates USP9X on serine 2563 in mitosis and in vitro (a) Immunoblot analysis depicting that USP9X phosphorylation on serine 2563 is dependent on activity of CDK1. U2-OS cells were synchronized in mitosis using nocodazole and treated either with DMSO or RO-3306 for 30min. Samples were lysed, subjected to SDS-PAGE, Western Blot and immunoblotting with indicated antibodies. β-Actin is used as loading control. **(b)** In vitro phosphorylation assay of truncated variants of USP9X wildtype and mutant. First three lanes are incubated with no CDK1-Cyclin B (Ctrl), lane 4-6 are subjected to CDK1-Cyclin B activity. Upper blot shows radioactive signal (32P) emitted by ATP, lower blot shows a Coomassie brilliant blue (CBB) for whole protein levels. In the upper blot, radioactive signal at the weight of 25kDa in lane 4 is background signal generated by GST-protein. USP9X generates a radioactive signal at the weight of 75kDa. *= Cyclin B. (kDa: kilo Dalton). **(c)** Radioactive signals of two individual experiments were quantified using the software ImageJ. Y-axis depicts radioactive signal intensity normalized to the corresponding signal in the Coomassie brilliant blue, x-axis shows different reaction conditions. Means of two experiments are shown.

3.6 USP9X phosphorylation on serine 2563 regulates its enzymatic activity

In order to investigate the functional consequence of serine 2563 phosphorylation of USP9X deubiquitylation activity assays depending on the phosphorylation status of serine 2563 were performed.

To this end, in vitro USP9X deubiquitylation activity was assessed using HA-Ubiquitin-vinyl sulfone (HA-Ubiquitin-VS). HA-Ubiquitin-VS consists of HA-tagged Ubiquitin and a covalently attached vinyl sulfone molecule (Borodovsky, Kessler et al. 2001). HA-Ubiquitin-VS can be cleaved in vitro by active deubiquitinases which leads to irreversible modification of the active site and inactivation of the DUB (Borodovsky, Kessler et al. 2001). In consequence, the complex comprising HA-Ubiquitin-VS and the deubiquitinase can be immunoprecipitated by targeting the HA-tag. Afterwards, quantification of captured and former active deubiquitinase can be done by Western Blot (Borodovsky, Kessler et al. 2001). For further information see 6.2.10. The more deubiquitinase is purified by immunoprecipitation the higher the in vitro enzymatic activity.

In mitosis we expect the wildtype form of USP9X (USP9X^{WT}) to be highly phosphorylated compared to a non-phosphorylatable USP9X mutant harboring an exchange of serine 2563 to alanine (USP9X^{S2563A}). Assuming that serine 2563 phosphorylation regulates enzymatic activity of USP9X, the most pronounced difference in activity between the USP9X^{WT} and USP9X^{S2563A} can be expected in mitosis.

For in vitro deubiquitylation activity assay, HEK 293T cells overexpressing either empty vector (EV), FLAG-tagged USP9X^{WT} or FLAG-tagged USP9X^{S2563A} were synchronized in mitosis using nocodazole. Further, cells were harvested and respective lysates subjected to in vitro deubiquitylation assay using HA-Ubiquitin-VS and HA-immunoprecipitation followed by Western Blot and immunoblotting. Experimental procedure is described in 6.2.10. This experiment could verify that the USP9X^{S2563A} mutant is less immunoprecipitated by HA-immunoprecipitation than the wildtype and therefore shows lower in vitro enzymatic activity than the phosphorylated form of USP9X (Figure 10a). An equal experiment was done in S-phase synchronized cell lysates where only very low levels of USP9X phosphorylation on serine 2563 occur (Figure 7). As expected, no difference of USP9X immunoprecipitation and therefore enzymatic activity was seen between USP9X^{WT} and USP9X^{S2563A} in S-Phase cell lysates (Figure 10b).

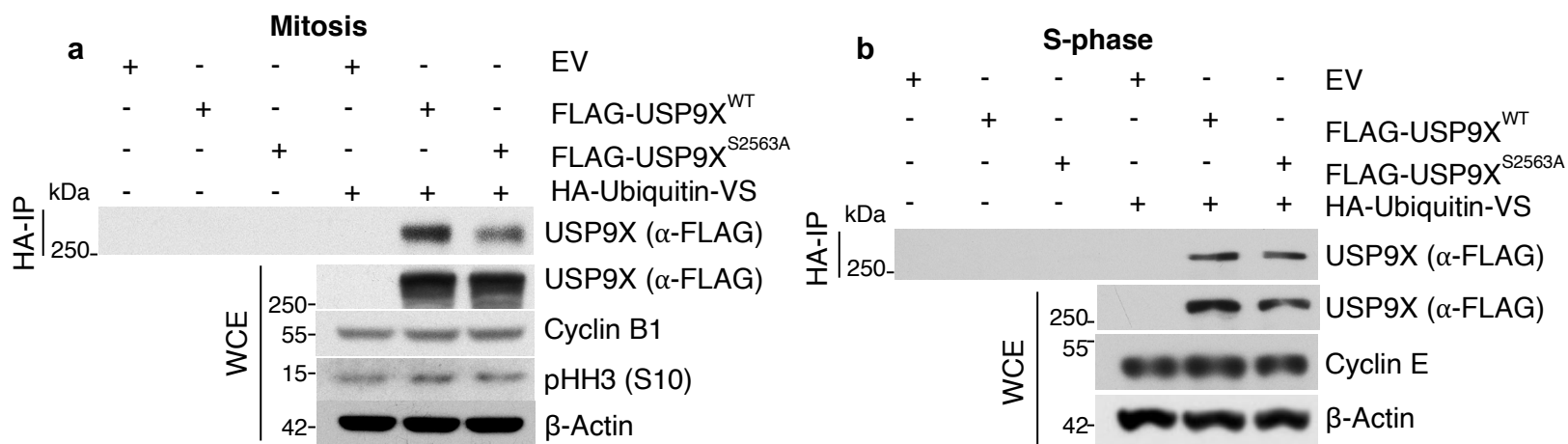


Figure 10 USP9X phosphorylation on serine 2563 regulates its enzymatic activity (a) In vitro deubiquitylation assay using HA-Ubiquitin-VS showing activity of USP9X^{WT} and USP9X^{S2563A} in HEK 293T cells which were synchronized in mitosis using nocodazole. HEK 293T cells were transfected with empty vector (EV), FLAG-USP9X^{WT}, FLAG-USP9X^{S2563A} as shown above and cells were treated with nocodazole for mitotic arrest. Afterwards, cells were harvested and lysates were either used as whole cell extract (WCE) or subjected to incubation with HA-Ubiquitin-VS or control reagent. Further, lysates were used for HA-immunoprecipitation, SDS-PAGE, Western Blot and immunoblotting with the indicated antibodies. β -Actin is used as loading control. **(b)** In vitro deubiquitylation assay using HA-Ubiquitin-VS showing comparable activity of USP9X^{WT} and USP9X^{S2563A} in S-phase arrested cells. Experimental setup as described in (a). β -Actin is used as loading control. (kDa: kilo Dalton).

To corroborate the results in Figure 10a, a different assay to measure *in vitro* deubiquitinating activity of USP9X was performed. Therefore, the substrate Ubiquitin-AMC was incubated with FLAG-tagged USP9X^{WT} or FLAG-tagged USP9X^{S2563A} which were purified from mitotically arrested HEK 293T cells. Activity of USP9X as deubiquitinase against Ubiquitin-AMC leads to liberation of AMC which generates a fluorescence signal as parameter for enzymatic activity (Dang, Melandri et al. 1998). The exact experimental setup and procedure is described in 6.2.9. Using a serial dilution of Ubiquitin-AMC the value of V_{max} which reflects the maximum of enzymatic reaction activity was calculated. This assay could show that V_{max} of USP9X^{WT} is 36,69 μ M/min compared to USP9X^{S2563A} with a V_{max} of 31,06 μ M/min suggesting a regulatory function of serine 2563 phosphorylation concerning activity of USP9X (Figure 11). Taken together the results above show that the USP9X serine 2563 residue is phosphorylated in mitosis which further regulates the enzymatic activity of USP9X.

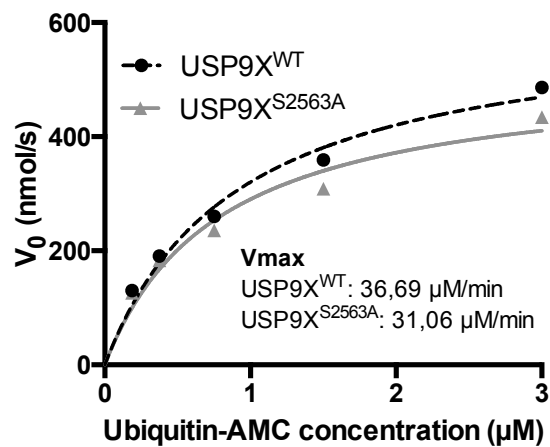


Figure 11 USP9X phosphorylation on serine 2563 regulates its enzymatic activity *in vitro* Enzyme kinetics of FLAG-tagged USP9X^{WT} and FLAG-tagged USP9X^{S2563A}. HEK 293T cells overexpressing FLAG-tagged USP9X^{WT} or FLAG-tagged USP9X^{S2563A} were arrested in mitosis, cells lysed and FLAG-tagged proteins purified performing an immunoprecipitation followed by elution. Afterwards, proteins were incubated with increasing concentrations of Ubiquitin-AMC and enzymatic activity with the corresponding substrate concentrations are depicted. V_{max} of USP9X^{WT} is 36.69 μ M/min or 31.06 μ M/min of USP9X^{S2563A}. Y-Axis depicts the reaction speed, the x-axis increasing concentrations of Ubiquitin-AMC per reaction. Results of one experiment are shown.

3.7 USP9X dependent ubiquitome analysis in mitotic HEK 293T cells

To identify possible substrate(s) of the deubiquitinase USP9X in mitosis and therefore USP9X phosphorylation dependent substrates, an unbiased SILAC-based proteomic screen was performed. The rationale was to purify the whole cellular ubiquitome. In more detail, this approach aimed to identify ubiquitylated proteins- in mitotic and asynchronous 6xHis-Ubiquitin-overexpressing HEK 293T cells under conditions of USP9X knockdown compared to control.

“SILAC” stands for “stable isotope labeling by amino acids in cell culture” and describes a technique where cells are cultured in cell culture medium that is supplemented with amino

acids carrying specific isotopes (Ong and Mann 2007). This leads to incorporation of with isotope labeled amino acids into newly translated proteins. In consequence, purified proteins from different cellular conditions (for example asynchronous vs mitotic cells) can be measured by mass spectrometric analysis and using differently labeled amino acids for each condition facilitates assignment of proteins to specific samples (Ong and Mann 2007).

First, we generate a stably expressing 6xHis-Ubiquitin HEK 293T cell line. The procedure of generating this cell line, transfection and ubiquitin purification is described in 6.3.5 and 6.2.2. Summarized briefly, HEK 293T cells were transduced with a pLenti-puro vector carrying the sequence for 6xHis-tagged Ubiquitin and a gene coding for puromycin resistance. In a next step, cells were selected for puromycin resistance and for further culturing cells were either kept in DMEM which was supplemented with L-Lysine D4 0,4mM and L-Arginine 13C 0,8mM (DMEM “medium”) or in DMEM with L-Lysine 13C 15N 0,4mM and L-Arginine 13C 15N 0,8mM (DMEM “heavy”). Further, the amino acid proline was added to a final concentration of 2mM. After 5 passages, cells grown in “medium” DMEM were transfected with *control* short hairpin (*shcontrol*) and cells grown in “heavy” DMEM with short hairpin against *USP9X* (*shUSP9X*) using Lipofectamine™ 2000. Afterwards, one half of each condition was either treated with nocodazole for mitotic arrest or kept asynchronous. 3,5h before harvesting, Bortezomib was added to inhibit the 26S proteasome and to enrich ubiquitylated proteins. After harvesting, cells were lysed under denaturing conditions. Lysis and ubiquitin purification under denaturing conditions using high concentrations of urea reduces contamination of not ubiquitylated, unspecific proteins. Denaturation avoids purification of proteins that are bound to ubiquitinated proteins and therefore only indirectly enriched in the sample for ubiquitome analysis. Further, lysates were either used as whole cell extract or subjected to purification by Ni-NTA-Agarose followed by washing before mass spectrometry (Figure 12a). The whole procedure is described in 6.2.2. Mass spectrometry was performed by Christian Johannes Gloeckner and Felix von Zweydf.

Western Blot of 6x-His-Ubiquitin overexpressing cells compared to control cells was done to evaluate levels of ubiquitin overexpression. As seen in Figure 12b in whole cell extracts (WCE) ubiquitin levels are comparable between control cells and 6x-His-Ubiquitin overexpressing cells meaning physiological expression of ubiquitin. Cell lysates were separated in SDS-PAGE, Western Blot and immunoblotted with indicated antibodies. Figure 12b also shows immunoblot analysis of purified ubiquitome (Ni-NTA-AP) immunoblotted for ubiquitin and excludes any contamination in the empty vector sample (EV) where no 6x-His-ubiquitin was overexpressed.

Validation of USP9X knockdown is depicted in Figure 12c. An aliquot of HEK 293T cells which was used for mass spectrometry was lysed and proteins separated by SDS-PAGE, subjected to Western Blot followed by immunoblotting with indicated antibodies.

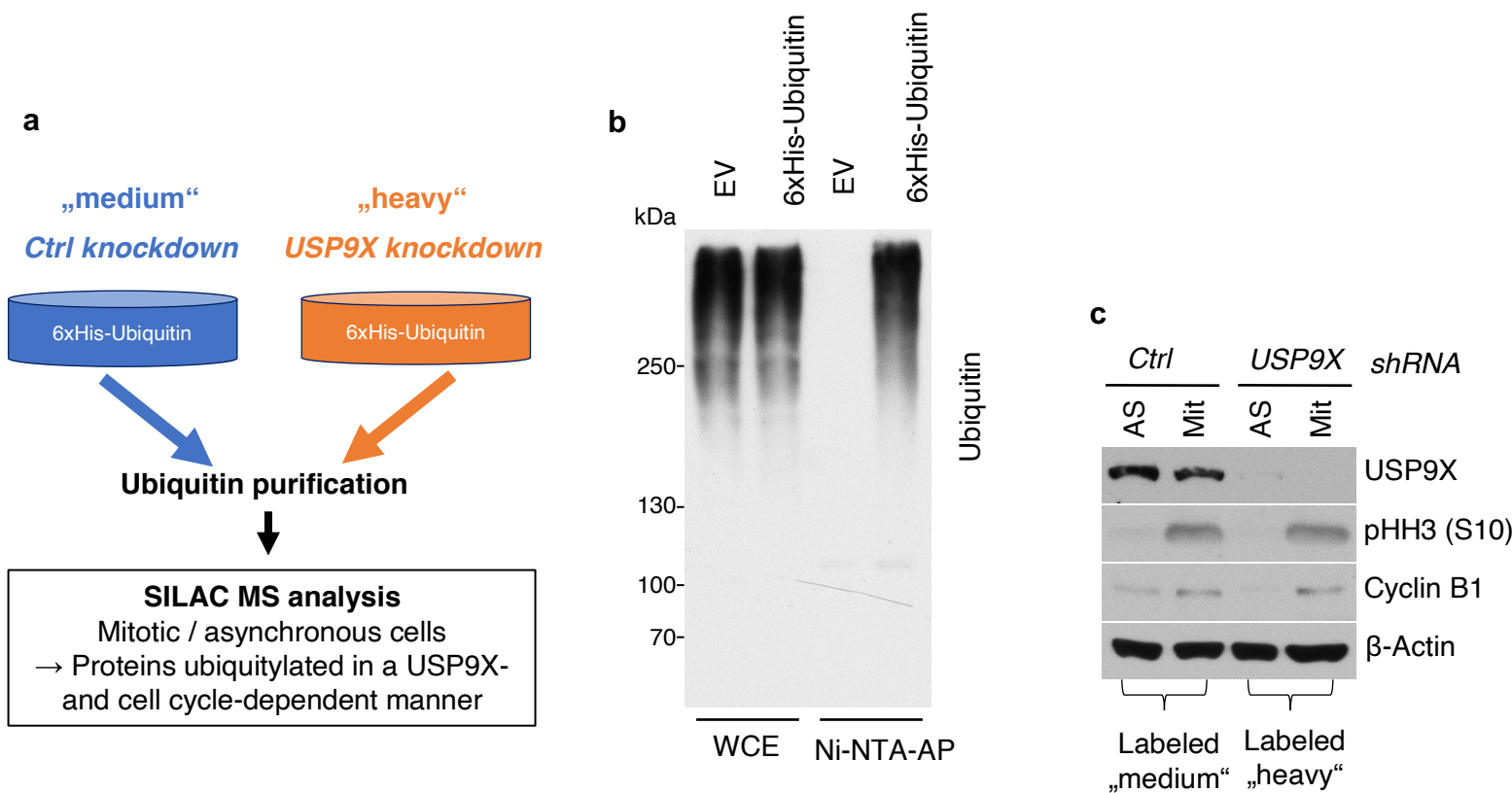


Figure 12 USP9X dependent ubiquitome analysis in mitotic HEK 293T cells (a) Setup of SILAC-based mass spectrometry of ubiquitome in stably 6xHis-Ubiquitin expressing HEK 293T cells under control or USP9X knockdown in mitosis or asynchronous cells. Cells in “medium” DMEM were treated with *shcontrol*, cells in “heavy” DMEM transfected with *shUSP9X*. Following ubiquitin purification, proteins were sent for mass spectrometry to identify differently ubiquitylated proteins comparing USP9X knockdown and control knockdown. (b) Immunoblot analysis of transduced HEK 293T cells with either control vector (EV) or a 6xHis-Ubiquitin-carrying construct. Samples were lysed under denaturing conditions using urea containing buffer followed by Ni-NTA-Agarose purification (Ni-NTA-AP) or used for whole cell extract (WCE). Afterwards samples were subjected to SDS-PAGE, Western Blot and incubation with indicated antibodies. (c) Immunoblot of stably expressing HEK 293T cells showing USP9X knockdown. HEK 293T cells were treated with indicated shRNAs, synchronized in mitosis using nocodazole (Mit) or kept asynchronous (AS), and subjected to Western Blot and immunoblot with indicated antibodies. (kDa: kilo Dalton).

3.8 Mass spectrometry yields Wilms’ tumor protein 1 (WT1) as possible mitotic substrate of USP9X

To find any possible substrate of USP9X in mitosis, ubiquitome analysis under loss of USP9X was performed as described above. Mass spectrometry yielded Wilms’ tumor protein 1 (WT1) as a possible mitotic substrate of USP9X. Ubiquitylated WT1 was purified to a significantly higher extend in mitotic USP9X knockdown cells compared to control cells suggesting higher ubiquitylation of WT1 under loss of USP9X (Figure 13a). Ubiquitylated WT1 was also purified in asynchronous cells but the fold change comparing USP9X and control knockdown condition was lower than in mitotic cells meaning a cell cycle specific activity of USP9X towards WT1 (Figure 13b). Interestingly, in the asynchronous condition β-catenin (CTNNB1) was purified significantly more under USP9X knockdown compared to control cells. This result validated the mass spectrometric approach as CTNNB1 has been described as substrate of USP9X in recent publications (Murray, Jolly et al. 2004, Yang, Zhang et al. 2016). (Table 3). Mass

spectrometry, data analysis and graph-creating were done by Christian Johannes Gloeckner and Felix von Zweydford.

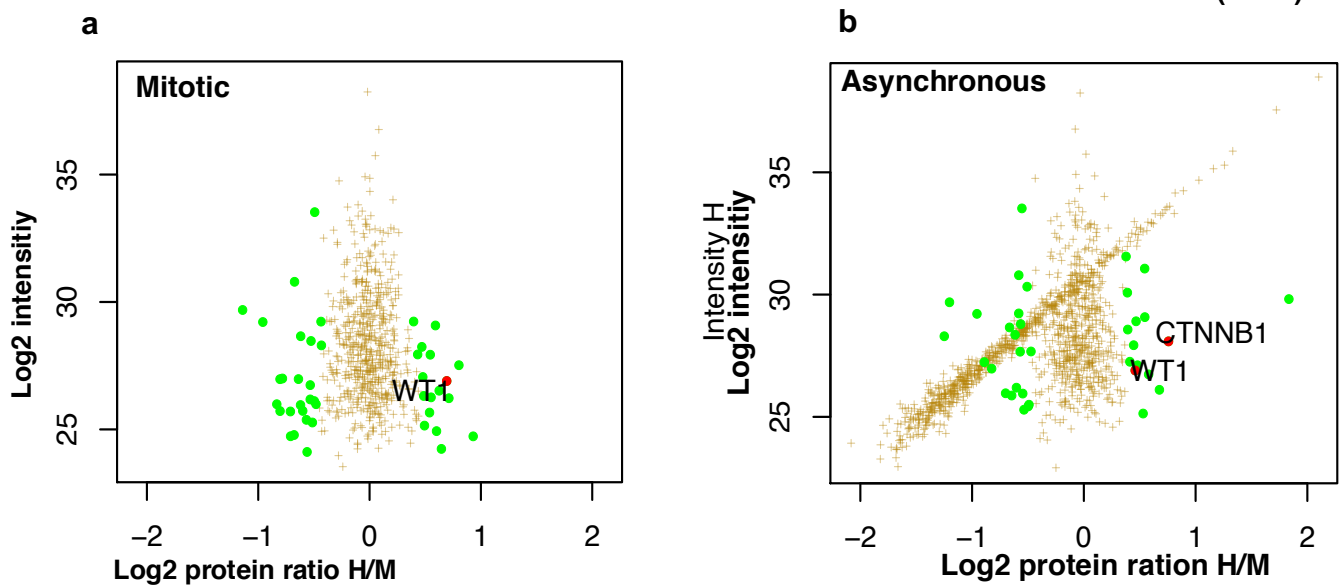


Figure 13 Mass spectrometry yields Wilms tumor protein 1 (WT1) as possible mitotic substrate of USP9X (a) Mass spectrometric analysis of purified, ubiquitylated proteins under USP9X knockdown in mitotic, stably expressing 6xHis-Ubiquitin HEK 293T cells compared to control knockdown cells. On the y-axis log 2 signal intensity of proteins in mass spectrometry is depicted, on the x-axis log 2 ratio of peptide amounts of analyzed proteins from USP9X knockdown cells (“H”) and control knockdown cells (“M”). Green dots represent proteins that are differently purified between the two conditions in a significant way. Significance B test at $p=0.01$ was applied. One of the most promising hits to be enriched in the USP9X knockdown sample compared to control sample was WT1, also called Wilms’ tumor protein 1, marked with a red dot. Log2 ratio= 0,6930521. Analysis performed and data gained by Christian Johannes Gloeckner and Felix von Zweydford. **(b)** Mass spectrometric analysis of purified ubiquitylated proteins under USP9X knockdown in asynchronous, stably expressing 6xHis-Ubiquitin HEK 293T cells. For description of graph see (a). As significant hits, CTNNB1 and with a lower ratio than in mitotic cells WT1 is displayed, both marked with a red dot. Log2 ratio for WT1= 0,4937498. Analysis performed and data gained by Christian Johannes Gloeckner and Felix von Zweydford.

Log 2 ratio H/M normalized	Condition	Protein name	Gene name
0,7575354	asynchronous	Catenin beta-1	CTNNB1
0,6930521	Mitosis	Wilms’ tumor protein 1	WT1
0,4937498	asynchronous	Wilms’ tumor protein 1	WT1

Table 3 Mass spectrometry yields Wilms’ tumor protein 1 (WT1) as possible mitotic substrate of USP9X Mass spectrometric analysis of purified, ubiquitylated proteins under USP9X knockdown (H) or control knockdown (M) in asynchronous or mitotic stably expressing 6xHis-Ubiquitin HEK 293T cells. Log 2 ratio of H/M, meaning USP9X to control knockdown ratio is shown in different conditions. Results for Catenin beta-1 (CTNNB1) and WT1 are displayed. Analysis performed and data gained by Christian Johannes Gloeckner and Felix von Zweydford.

3.9 USP9X interaction with WT1 is enhanced in mitosis

In order to confirm the results of the mass spectrometric ubiquitome analysis that WT1 is a cell cycle dependent substrate of the deubiquitinase USP9X, interaction experiments were performed.

Hence, FLAG-tagged WT1 was expressed in HEK 293T cells using the calcium phosphate method and treated with nocodazole to arrest cells in mitosis before harvesting. Lysates were subjected to immunoprecipitation using ANTI-FLAG® M2 Affinity Gel, SDS-PAGE, Western Blot and immunoblotting as described in 6.2.2 Binding of endogenous USP9X to FLAG-tagged WT1 enhances in mitosis compared to asynchronous cells (Figure 14a) Furthermore, interaction of FLAG-tagged WT1 with USP9X increases in a similar manner as phosphorylation of USP9X on serine 2563 is increasing. This suggests a serine 2563 phosphorylation-dependent binding of USP9X to WT1. Vice versa, it could be shown that interaction of endogenous WT1 with FLAG-tagged USP9X increases when cells are arrested in mitosis compared to untreated cells (Figure 14b). Experimental setup of Figure 14a was exactly the same as for Figure 14b except the time points of harvesting and overexpression of FLAG-USP9X instead of FLAG-tagged WT1.

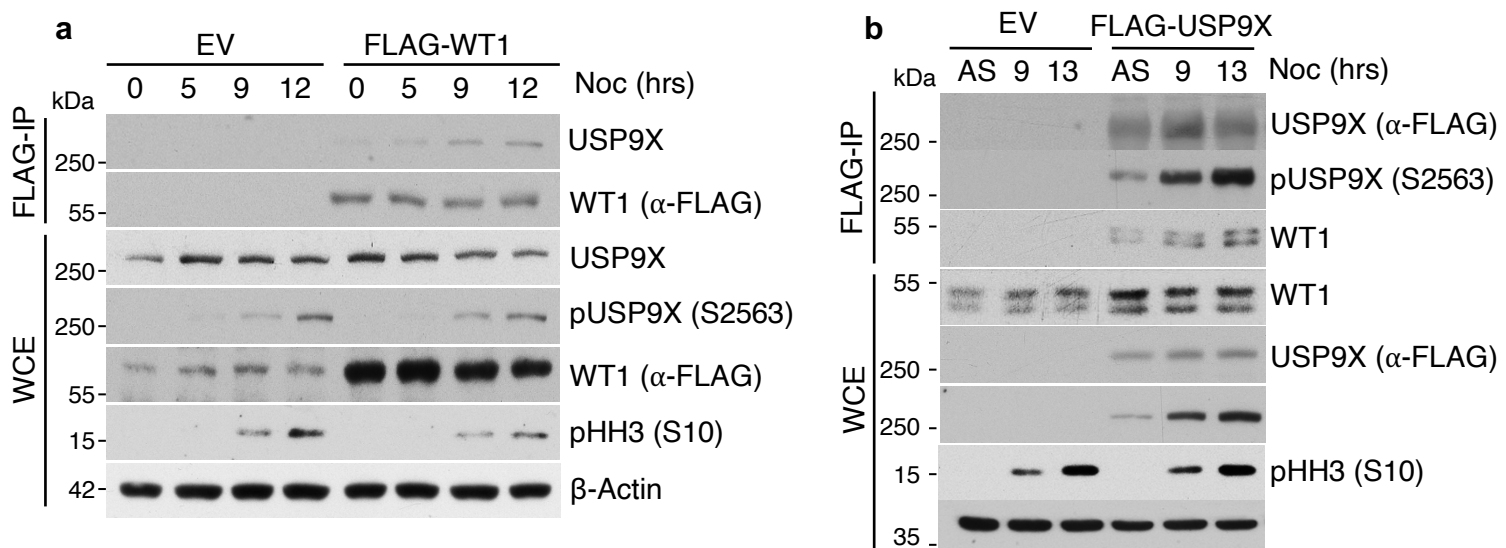


Figure 14 USP9X interaction with WT1 is enhanced in mitosis (a) Immunoblot of immunoprecipitation of FLAG-tagged WT1 with co-immunoprecipitated endogenous USP9X. HEK 293T cells were either transfected with EV (empty vector) or a FLAG-tagged WT1 (FLAG-WT1) carrying construct and treated with nocodazole (Noc) for the indicated time points before harvesting (hrs=hours). Cells were lysed and subjected to immunoprecipitation using ANTI-FLAG® M2. Whole cell eluates (WCE) and immunoprecipitates (FLAG-IP) were further analyzed by SDS-PAGE, Western Blot and immunoblot using the indicated antibodies. **(b)** Immunoblot of immunoprecipitation of FLAG-tagged USP9X with co-immunoprecipitated endogenous WT1. HEK 293T cells were either transfected with EV (empty vector) or a FLAG-tagged USP9X carrying construct (FLAG-USP9X) and treated with nocodazole (Noc) for the indicated time points before harvesting (hrs=hours). Cells were lysed and subjected to immunoprecipitation using ANTI-FLAG® M2. Whole cell eluates (WCE) and immunoprecipitates (FLAG-IP) were further analyzed by SDS-PAGE, Western Blot and immunoblot using the indicated antibodies. (kDa: kilo Dalton).

As overexpression of proteins for immunoprecipitation is prone to generate unspecific interaction with different other proteins due to high protein levels, endogenous

immunoprecipitation and co-immunoprecipitation was done. Therefore, HEK 293T cells were arrested in mitosis by culturing in nocodazole containing media, lysed and either incubated with control IgG antibody or antibody against WT1 as described in 6.2.2. Further, immunocomplex or lysates were separated by SDS-PAGE and analyzed by Western Blot and immunoblotting. As depicted in Figure 15 endogenous WT1 and endogenous USP9X interact in mitosis.

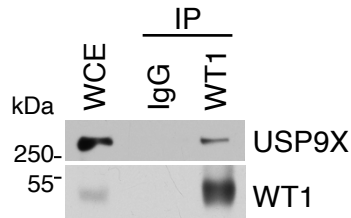


Figure 15 Endogenous USP9X interacts with endogenous WT1 in mitosis Immunoblot of immunoprecipitation of endogenous WT1 and endogenous USP9X. Therefore, HEK 293T cells treated with nocodazole, lysed, incubated with IgG or anti-WT1 antibody for immunoprecipitation and analyzed by Western Blot. WCE= whole cell extract, IP= immunoprecipitation, IgG= Immunglobuline G. (kDa: kilo Dalton).

3.10 WT1 binding to USP9X in mitosis is modulated by serine 2563 phosphorylation

Given the results above, interaction between USP9X and WT1 in mitosis could be demonstrated. The next question was, if binding of WT1 to USP9X depends on the phosphorylation status of USP9X on serine 2563. To this end, FLAG-tagged USP9X^{WT} and FLAG-tagged USP9X^{S2563A} were overexpressed in HEK 293T cells and cells were either synchronized in mitosis by nocodazole treatment for 15h or kept asynchronous and further harvested. Next, cells were lysed and FLAG-tagged USP9X^{WT} or FLAG-tagged USP9X^{S2563A} were immunoprecipitated using ANTI-FLAG® M2 as described in 6.2.2. Afterwards, samples were subjected to SDS-PAGE, Western Blot and immunoblotting. Co-immunoprecipitation and therefore interaction of WT1 with USP9X^{S2563A} is reduced compared to phosphorylated USP9X^{WT} in mitosis suggesting USP9X phosphorylation on serine 2563 to modulate interaction with WT1 (Figure 16a). In unsynchronized cells with low phosphorylation of USP9X^{WT} no difference in binding of WT1 to FLAG-tagged USP9X^{WT} or FLAG-tagged USP9X^{S2563A} is detected (Figure 16a).

In a next step, interaction of WT1 to FLAG-tagged USP9X^{WT} and FLAG-tagged USP9X^{S2563A} was quantified. Immunoblot signal of WT1 and of FLAG representing USP9X^{WT} or USP9X^{S2563A} were scanned, quantified using the ImageJ software and ratio of WT1 values and FLAG values were calculated. Quantification of three independent experiments resulted in a significant difference in binding of WT1 to FLAG-tagged USP9X^{WT} compared FLAG-tagged USP9X^{S2563A} (Figure 16b).

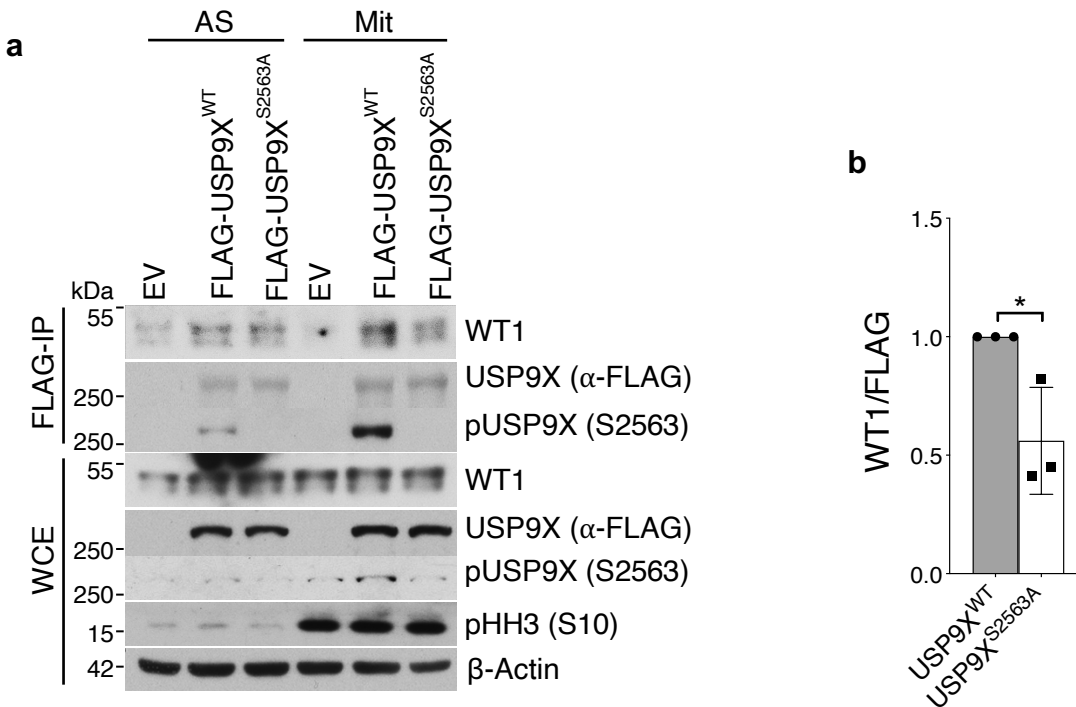


Figure 16 WT1 binding to USP9X in mitosis is modulated by serine 2563 phosphorylation (a) Immunoblot of immunoprecipitated FLAG-tagged USP9X^{WT} and FLAG-tagged USP9X^{S2563A} with co-immunoprecipitation of WT1 in HEK 293T cells. Empty vector (EV), FLAG-tagged USP9X^{WT} or FLAG-tagged USP9X^{S2563A} were transfected and overexpressed in HEK 293T cells which were further kept asynchronous (AS) or mitotically arrested with nocodazole for 15h (Mit). Afterwards cells were harvested and proteins purified by immunoprecipitation and co-immunoprecipitation. SDS-PAGE, Western Blot and immunoblot of whole cell extracts (WCE) and co-immunoprecipitated proteins (FLAG-USP9X^{WT} and FLAG-USP9X^{S2563A}) were performed as indicated. (kDa: kilo Dalton). **(b)** Quantification of WT1 binding to FLAG-tagged USP9X^{WT} and FLAG-tagged USP9X^{S2563A}. Results of three independent experiments which were conducted as in (a) are shown. Y-axis shows signal intensity of WT1 normalized to the FLAG signal, x-axis stands for different conditions. Mean and standard deviations are depicted, t-test was applied with *p=0.02797309.

3.11 USP9X stabilizes WT1 in mitosis by rescuing WT1 from proteasomal degradation

As it can be seen in Figure 14b, USP9X overexpression leads to higher abundance of WT1 suggesting a stabilizing function of USP9X towards WT1.

To evaluate the WT1 proteins levels under USP9X knockdown a cycloheximide time course was conducted. To this end, U2-OS cells were treated with *control* or *USP9X* siRNA and synchronized in mitosis as described in 6.3.2. Next, mitotic shake-off was done and cells were either harvested for time point “0” or further kept in cell culture and treated with cycloheximide at a concentration of 100µg/ml. Cycloheximide inhibits protein synthesis and can be used to investigate protein stability independent of transcription and translation of proteins (Baliga, Pronczuk et al. 1969). To show that loss of WT1 in the cycloheximide time course was due to degradation of WT1 by the 26S proteasome we inhibited the proteasome using the reagent bortezomib (Lü and Wang 2013). To avoid cleavage of WT1 by caspase 3 we additionally added the pan-caspase inhibitor Z-VAD-

FMK at a concentration of 10 μ M (Ruan, Gao et al. 2018). The exact description of the experimental setup can be found in 6.3.2 and 6.3.3. Lysates were subjected to SDS-PAGE, Western Blot and immunoblotting.

Stability of WT1 under loss of USP9X is reduced in a cycloheximide time course compared to control cells (Figure 17a). The most pronounced difference in protein stability can be seen after 6h of treatment with cycloheximide. Furthermore, bortezomib increases WT1 protein levels suggesting proteasomal degradation of WT1 in mitosis. The fact that WT1 is degraded by the proteasome is in congruence with recent publications (Bansal, Bansal et al. 2010). Additionally, WT1 levels under *USP9X* siRNA treatment were quantified. WT1 signal of immunoblots and of loading control were scanned and quantified using the ImageJ software. WT1 values were normalized to loading control and to time point "0". Quantification of three independent experiments resulted in a significant difference in WT1 levels under *USP9X* knockdown compared to control cells (Figure 17b).

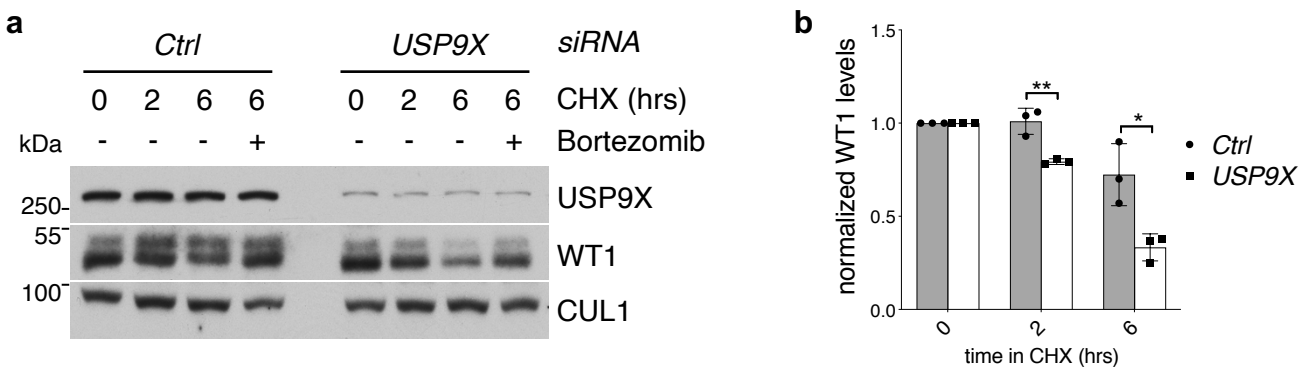


Figure 17 USP9X stabilizes WT1 in mitosis by rescuing WT1 from proteasomal degradation (a) Immunoblot of cycloheximide time course showing WT1 stability under USP9X knockdown. U2-OS cells were treated with *control* or *USP9X* siRNA, arrested in mitosis using thymidine and nocodazole for 11hrs before mitotic shake-off was performed. Mitotic cells were further treated with cycloheximide, bortezomib (where indicated) and Z-VAD-FMK. After indicated incubation time, cells were collected, lysed and subjected to Western Blot and immunoblot with the indicated antibodies. (kDa: kilo Dalton). **(b)** Quantification of WT1 protein levels under USP9X knockdown. Quantification of three independent experiments as described in (a) are shown. Y-axis depicts quantified WT1 signals which were scanned, quantified using ImageJ software and normalized to loading control of the respective experiment (β -Actin or CUL1) and to time point 0. X-axis shows different time points of harvesting. Mean and standard deviations as error bars are shown. t-test was applied with * $p=0.020367$; ** $p=0.006350$. Grey bar represent *control* siRNA samples, white bars represent *USP9X* siRNA samples.

3.12 USP9X deubiquitinates mitotic WT1 in a phosphorylation dependent manner

Summarizing the results above, USP9X interacts with WT1 depending on USP9X phosphorylation of serine 2563 and USP9X rescues WT1 from proteasomal degradation in mitosis. In order to answer the question if USP9X stabilizes WT1 via its deubiquitylation activity, an *in vivo* ubiquitylation assay of WT1 under expression of FLAG-tagged USP9X^{WT} and FLAG-tagged USP9X^{S2563A} was conducted.

First, HEK 293T cells were transfected with plasmid carrying FLAG-tagged USP9X^{WT} or FLAG-tagged USP9X^{S2563A}, 2xStrep-tagged WT1 and HA-tagged Ubiquitin using the

transfection reagent Lipofectamine™ 2000. Second, HEK 293T cells were synchronized in mitosis using nocodazole. Additionally, bortezomib was added to inhibit proteasomal degradation and to enrich ubiquitylated WT1. To prevent caspase dependent cleavage of WT1, cell culture medium was supplemented with caspase inhibitor Z-VAD-FMK. After 14 hours incubation with both reagents, cells were harvested, directly lysed under denaturing conditions using SDS and high temperature followed by 2xStrep affinity purification using Strep-Tactin® Superflow. For further description please see 6.2.3 and 6.3.1. Whole cell extracts and affinity purified WT1 were subjected to SDS-PAGE, Western Blot and immunoblotting.

This experiment shows for the first time that WT1 is deubiquitylated by FLAG-USP9X in mitosis (Figure 18). Further, deubiquitylation activity of USP9X towards WT1 depends on USP9X phosphorylation of serine 2563.

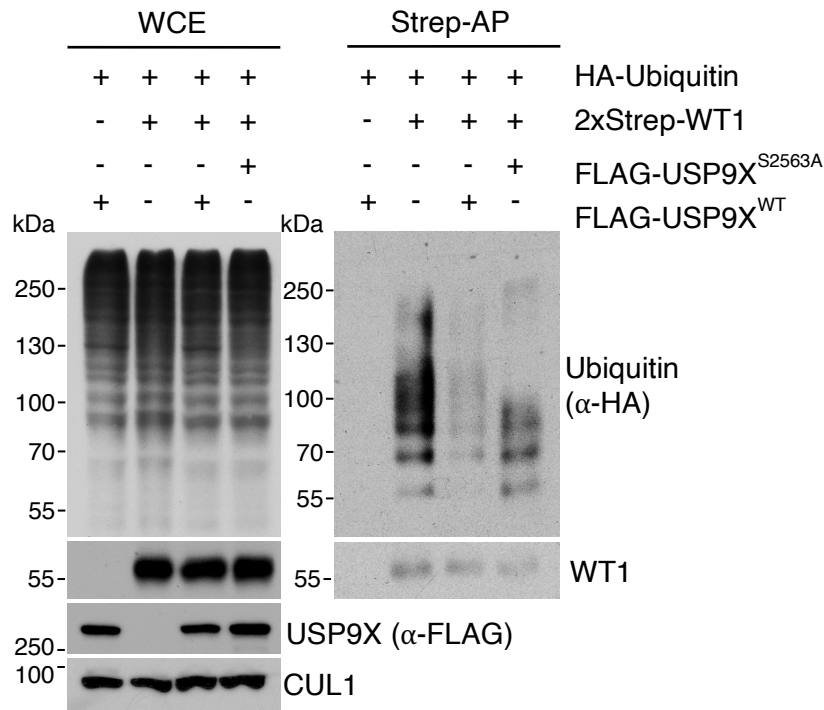


Figure 18 USP9X deubiquitinates mitotic WT1 in a phosphorylation dependent manner Immunoblot of in vivo ubiquitylation assay of WT1 under overexpression of FLAG-tagged USP9X^{WT} and FLAG-tagged USP9X^{S2563A}. HEK 293T were transfected with FLAG-tagged USP9X^{WT} or FLAG-tagged USP9X^{S2563A}, 2xStrep-tagged WT1 (2xStrep-Wt1) and HA-tagged Ubiquitin (HA-Ubiquitin) carrying plasmids, synchronized in mitosis using nocodazole for 14 hours and treated with bortezomib to inhibit proteasomal degradation and with the caspase inhibitor Z-VAD-FMK to avoid caspase-3 mediated cleavage of WT1. HEK 293T cells were harvested, lysed under denaturing conditions and Strep affinity (Strep-AP) purification was performed. Afterwards SDS-PAGE, Western Blot and immunoblotting with indicated antibodies was done. Immunoblot analyses of whole cell extract on the left and (WCE) and affinity purified WT1 (right) are shown. (kDa: kilo Dalton).

3.13 USP9X knockdown leads to enhanced ubiquitination of WT1 in mitosis

In contrast to overexpression, knockdown of USP9X leads to higher levels of ubiquitylated FLAG-tagged WT1 in mitotic HEK 293T cells (Figure 19). HEK 293T cells were either transfected with *control* or *USP9X* shRNA-containing plasmid, FLAG-tagged WT1 and HA-tagged Ubiquitin using Lipofectamine™ 2000. Further, cells were synchronized in mitosis using nocodazole together with bortezomib for 14h. Afterwards, cells were harvested, lysed under denaturing conditions and FLAG immunoprecipitation using ANTI-FLAG® M2 Affinity Gel was performed. Samples were subjected to SDS-PAGE, Western Blot analysis and immunoblotting with the indicated antibodies. The description of the experimental procedure and transfection is described in 6.3.1 and 6.2.3.

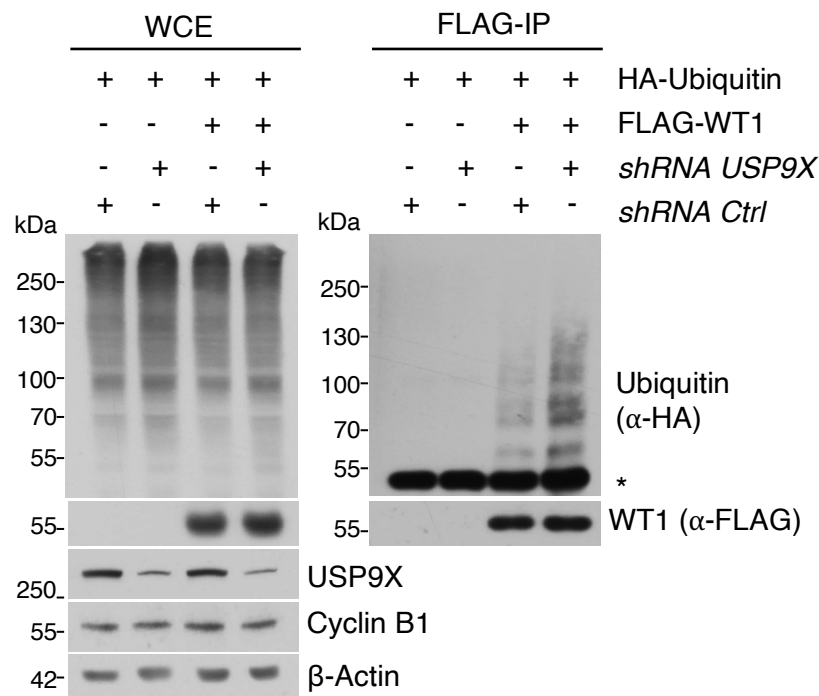


Figure 19 USP9X knockdown leads to enhanced ubiquitination of WT1 in mitosis Immunoblot of in vivo ubiquitylation of WT1 under *USP9X* knockdown. HEK 293T cells were transfected with *control* or *USP9X* shRNA-containing plasmid, FLAG-tagged WT1 (FLAG-WT1) and HA-tagged Ubiquitin (HA-Ubiquitin) synchronized in mitosis using nocodazole and bortezomib for 14 hours. Afterwards, cells were lysed under denaturing conditions and immunoprecipitation using ANTI-FLAG® M2 Affinity Gel was performed. Immunoblot analyses of whole cell extract on the left and (WCE) and immunoprecipitated WT1 (right) are shown. * Indicates immunoglobulin heavy chain detected by the secondary antibody. (kDa: kilo Dalton).

3.14 USP9X inhibition with WP1130 destabilizes WT1 in mitosis

Besides *USP9X* knockdown and overexpression experiments, experiments with inhibition of *USP9X* using the unspecific and commercially available DUB inhibitor WP1130 were

performed. Therefore, U2-OS cells were synchronized in mitosis by treatment with nocodazole. Then, mitotic shake-off was performed and cells were either treated with WP1130 or with DMSO for 3h before harvesting. Additionally, Z-VAD-FMK was added to inhibit caspase-3 dependent cleavage of WT1. This data confirmed the stabilizing function of USP9X towards WT1 in mitosis (Figure 20).

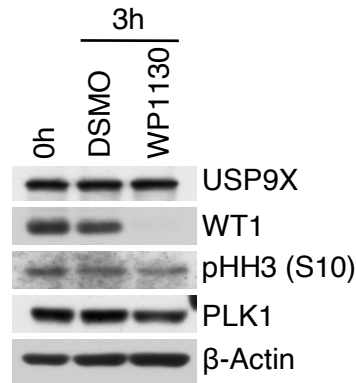


Figure 20 USP9X inhibition with WP1130 destabilizes WT1 in mitosis Immunoblot showing WT1 destabilization under inhibition of USP9X using the inhibitor WP1130. U2-OS cells were treated with nocodazole for synchronization in mitosis. Then, mitotic cells were either collected (0h), or treated with DMSO or WP1130 for 3h. Z-VAD-FMK was added to inhibit caspase-3 dependent cleavage of WT1. Lysates were analyzed by SDS-PAGE, Western Blot and immunoblotting with the indicated antibodies. (kDa: kilo Dalton).

3.15 USP9X and WT1 colocalize in mitotic cells

To determine not only interaction but also colocalization of USP9X and WT1, indirect immunofluorescence (IF) of U2-OS cells was conducted.

Initially, the antibody against USP9X was tested and validated for the following immunofluorescence experiments. To this end, U2-OS cells were plated on a poly-D-lysine hydrobromide coated IF-Chamber slide to ensure proper attachment of mitotic cells on cell culture dish. Subsequently, cells were transfected either with *control* or *USP9X* siRNA to generate a USP9X knockdown. 72h after transfection, cells were subjected to immunofluorescence preparation and incubation with antibody against USP9X followed by staining with AlexaFluor488 secondary antibody and Hoechst to visualize DNA. In the next steps, indirect immunofluorescence was done using a Leica SP8 Confocal Laser Scanning Microscope. Working steps of IF-Chamber slide coating, immunofluorescence and microscopy are described in 6.4.2.

Figure 21a shows a specific indirect immunofluorescence signal in control cells with a distinct lower signal in USP9X knockdown cells suggesting specific binding of the USP9X antibody to endogenous USP9X in the immunofluorescence setting.

In order to investigate USP9X colocalization to WT1, U2-OS were plated on an IF-Chamber slide after slides have been coated using poly-D-lysine hydrobromide. Then, cells were transfected with a FLAG-tagged WT1 carrying construct using Lipofectamine™ 2000 and treated with nocodazole for 15 hours. Afterwards, cells were fixed and stained using the validated USP9X antibody or FLAG antibody to visualize overexpressed WT1.

All steps are described in 6.4.2. To ensure proper attachment of mitotic cells on coated IF-chamber slides washing steps of immunofluorescence preparation were done very carefully. Figure 21b shows two representative cells with USP9X and overexpressed WT1 colocalization in mitotic U2-OS cells with a Pearson's coefficient of 0,57. Pearson's coefficient was calculated from colocalization in 17 cells.

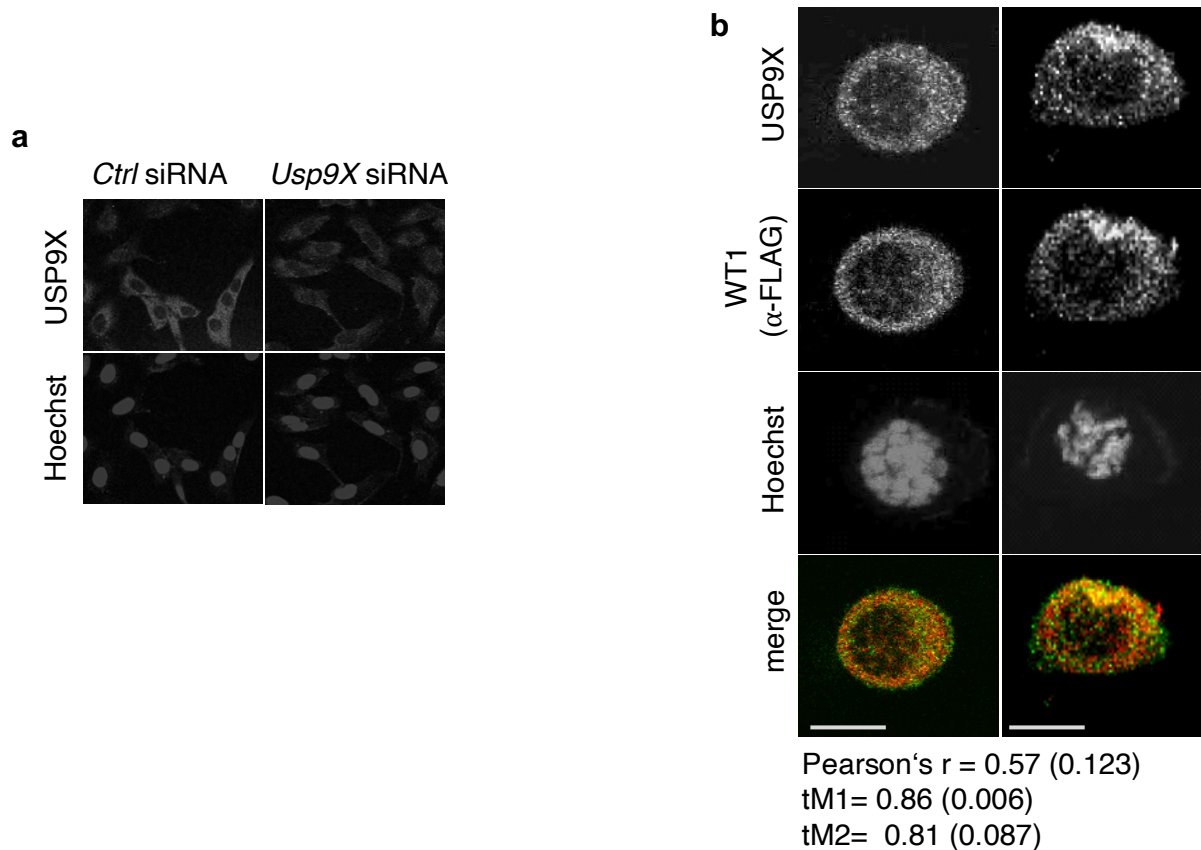


Figure 21 USP9X and WT1 colocalize in mitotic cells (a) Indirect immunofluorescence of endogenous USP9X using the USP9X antibody. U2-OS cells were either treated with *Usp9X* siRNA or *control* siRNA and incubated with a USP9X specific antibody and an AlexaFluor488 secondary antibody. Hoechst staining was used to visualize DNA. **(b)** Indirect immunofluorescence of U2-OS that were transfected with FLAG-WT1 and synchronized in mitosis. Afterwards, cells were fixed and stained with the indicated antibodies. Mean and SD values for Pearson's coefficient and the Manders' coefficients (tM1 and tM2) were calculated from 17 samples. The value for tM1 indicates the intensity of all analysed pixels from channel 1 in which the signal for channel 2 is above background, divided by the total intensity from channel 1. The value for tM2 indicates the intensity of all analysed pixels from channel 2 in which the signal for channel 1 is above background, divided by the total intensity from channel 2. Merge= overlapping signal of FLAG and USP9X.

3.16 RNA sequencing of mitotic U2-OS cells under WT1 knockdown and in USP9X^{Mut} U2-OS cells

Recent work by Palozola, K. C. et al showed that transcriptional activity of specific genes is preserved and not completely stalled during mitosis (Palozola, Donahue et al. 2017). Further, a subset of transcription factors remain bound to condensed DNA during mitosis to ensure highly cell cycle regulated activation of transcription, a process which is called mitotic bookmarking (Lodhi, Ji et al. 2016)

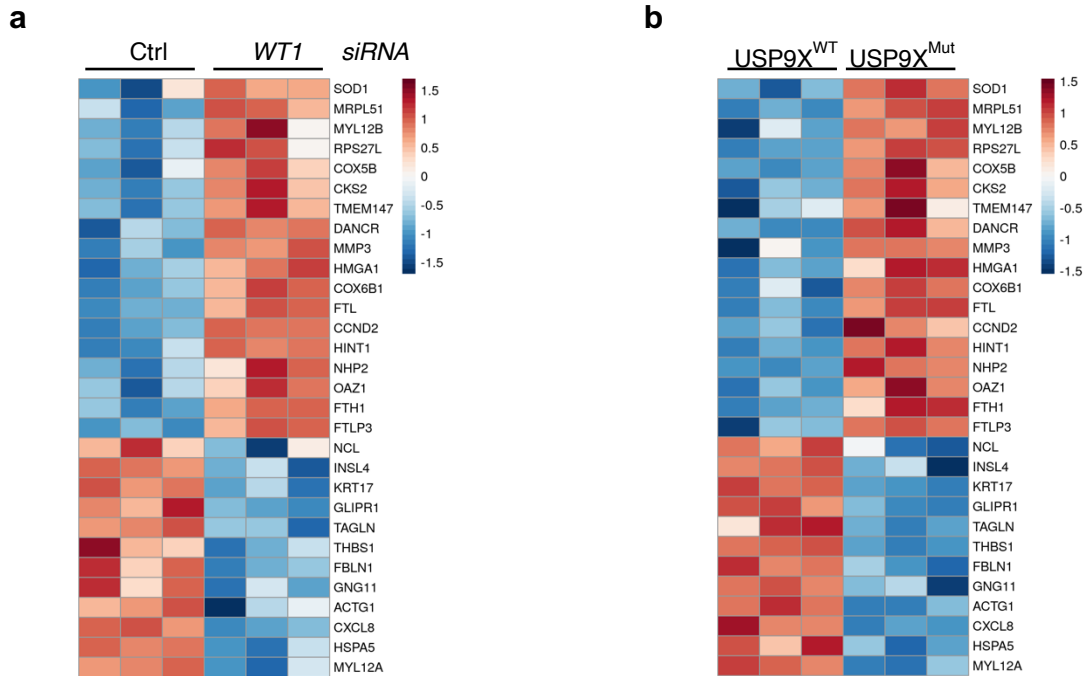


Figure 22 RNA sequencing of mitotic U2-OS cells under WT1 knockdown and in USP9X^{Mut} U2-OS cells (a) Heatmap of RNA sequencing analyses showing genes which are differentially expressed in mitotic *control* siRNA treated cells versus *WT1* siRNA treated U2-OS cells. Each column represents an independent biological replicate. Genes that are higher expressed under *WT1* knockdown are displayed on the top (colour red means higher gene expression than in control condition), genes that are lower expressed under loss of *WT1* are listed on the bottom (colour blue means lower gene expression than in control condition). Data and graphs generated by Thomas Engleitner. **(b)** Heatmap of RNA sequencing analyses showing genes which are differentially expressed in mitotic USP9X^{WT} cells compared to USP9X^{Mut} U2-OS cells. Each column represents an independent biological replicate. Genes that are higher expressed in USP9X^{Mut} cells are displayed on the top (colour red means higher gene expression than in control condition), genes that are lower expressed in USP9X^{Mut} are listed on the bottom (colour blue means lower gene expression than in control condition). Data and graphs generated by Thomas Engleitner.

To investigate whether *WT1* is an active transcription factor in mitosis and to find genes which are regulated during cell cycle and by *WT1*, RNA sequencing analysis (RNA-Seq) in mitotic cells was performed. Therefore, U2-OS cells were treated either with *control* or *WT1* siRNA and arrest in mitosis using nocodazole to identify genes that are regulated in a *WT1*-dependent manner. Mitotic cells were shaken-off, harvested on ice and directly frozen. RNA extraction was performed as described in 6.3.1.

Additionally, RNA sequencing of an U2-OS cell line which was genetically modified using CRISPR/Cas9 system to disrupt the minimal consensus recognition site of CDK1 surrounding serine 2563 of USP9X (USP9X^{Mut} cells) was conducted. As control condition an unmodified U2-OS cell line was used (USP9X^{WT}). The genetic alteration of the USP9X^{Mut} cell line was homozygous and the sequence is depicted in 6.3.9. As USP9X^{Mut} cells lack USP9X phosphorylation on serine 2563, the disrupted phosphorylation site mimics high CDC14B activity and therefore low USP9X activity. Using this USP9X^{Mut} cell line phosphorylation dependent alteration in transcription could be monitored. Synchronization, harvesting and RNA isolation was done exactly as for *WT1* knockdown cells.

Extracted RNA was handed over and subjected to RNA sequencing by Thomas Engleitner and Roland Rad. Statistical analysis and generation of heatmaps was done by Thomas Engleitner. Genes with a significant change of expression not only in response to WT1 knockdown compared to *control* siRNA but also in USP9X^{Mut} cells compared to USP9X^{WT} cells are shown in Figure 22a and Figure 22b. Further, genes with significant alteration in each paired condition were ranked reflecting differences in transcription (Table 4). This ranking was done by Katharina Clemm von Hohenberg. After combined ranking from RNA sequencing analyses of WT1 siRNA cells and USP9X^{Mut} cells, CXCL8, the gene coding for IL-8, scored as highest ranked gene of significantly modified genes (Table 4).

gene name	rank USP9X ^{Mut} vs. USP9X ^{WT}	rank WT1 vs. Ctrl siRNA	relative rank USP9X ^{Mut} vs. USP9X ^{WT}	relative rank WT1 vs. Ctrl siRNA	relative combined rank
CXCL8	27	1	0.9323	0.9818	0.9571
KRT17	51	16	0.8722	0.7091	0.7906
THBS1	12	32	0.9699	0.4182	0.6941
INSL4	155	13	0.6115	0.7636	0.6876
FBLN1	124	34	0.6892	0.3818	0.5355
TAGLN	171	37	0.5714	0.3273	0.4494
GLIPR1	185	39	0.5363	0.2909	0.4136
MYL12A	292	46	0.2682	0.1636	0.2159
HSPA5	359	47	0.1003	0.1455	0.1229

Table 4 Ranked genes of RNA sequencing of mitotic U2-OS cells under WT1 knockdown and in USP9X^{Mut} U2-OS cells List of genes which were ranked depending of their significantly different expression in control versus WT1 knockdown U2-OS and USP9X^{WT} compared to USP9X^{Mut} U2-OS cells. Only genes which showed a positive correlation between expression and USP9X phosphorylation or WT1 level, respectively, are depicted. List was assembled by Katharina Clemm von Hohenberg.

3.17 WT1 and USP9X regulate mRNA levels of IL-8 in mitosis

In order to validate the result of the RNA sequencing analysis that IL-8 expression is regulated by USP9X, more specific by USP9X serine 2563 phosphorylation, and WT1, quantitative RT-PCR experiments were performed. To this end, U2-OS cells were transfected either *control* siRNA, WT1 siRNA, USP9X siRNA or WT1 and USP9X siRNA as described in 6.3.2. Further, these cells and USP9X^{WT} or USP9X^{Mut} U2-OS cells were synchronized in mitosis using nocodazole and harvested as described in 6.3.3. Harvested cells were lysed and RNA was extracted following description in 6.1.3. Afterwards, mRNA was reversely transcribed as explained in 6.1.4 to generate cDNA which was further subjected to quantitative RT-PCR using IL-8 oligonucleotides listed in 5.10 and following steps of quantitative RT-PCR. IL-8 mRNA levels are significantly reduced under loss of WT1 or USP9X but no additional effect is seen under double knockdown of WT1 and

USP9X (Figure 23a). This indicates that WT1 and USP9X act in the same pathway with the CXCL8 gene as downstream target. Additionally, mRNA levels of IL-8 are reduced in USP9X^{Mut} compared to USP9X^{WT} suggesting regulation of CXCL8 gene in mitosis dependent on USP9X serine 2563 phosphorylation (Figure 23b).

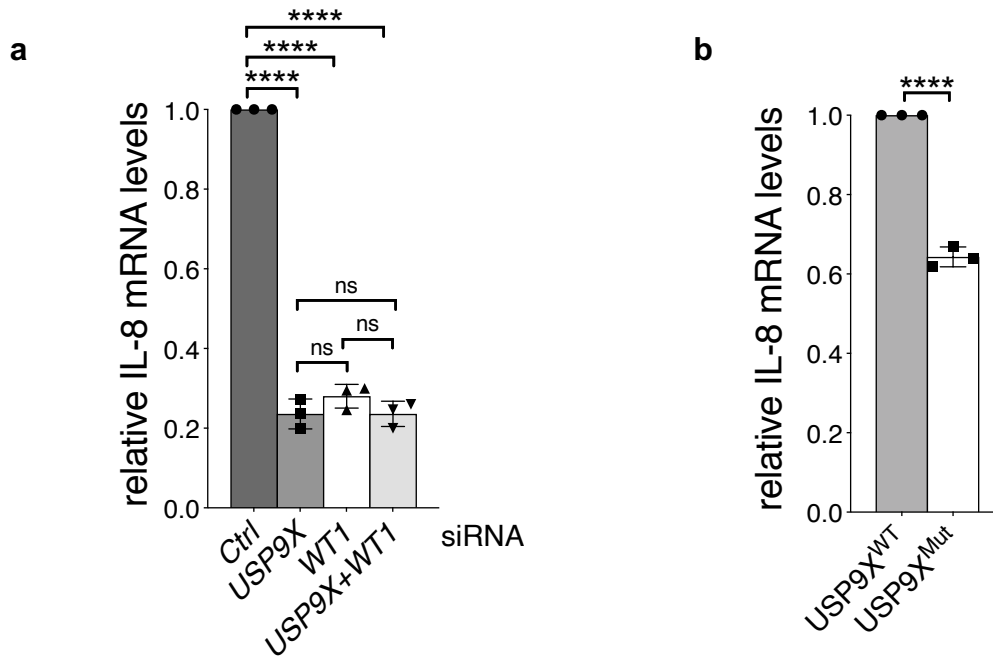


Figure 23 WT1 and USP9X regulate expression of IL-8 in mitosis (a) Graph depicting results of quantitative RT-PCR from mitotic U2-OS cells which were treated with *control*, *WT1*, *USP9X* or *WT1* and *USP9X* siRNA and synchronized in mitosis using nocodazole. Loss of WT1 or USP9X leads to reduced IL-8 mRNA levels, but double knockdown cells do not show further decrease in mRNA compared to single knockdown. Mean is shown from n=3 biologically independent experiments. Y-axis shows relative mRNA levels normalized to control sample, x-axis shows different siRNA conditions. One-way ANOVA was applied with ****p<0.0001 followed by Dunnett's test with ****p<0.0001 (p(USP9X vs. WT1)=0.211; p(USP9X vs. USP9X+WT1)>0.9999; p(WT1 vs. USP9X+WT1)=0.2061) (b) Graph depicting results of quantitative RT-PCR showing reduced IL-8 mRNA in USP9X^{Mut} versus USP9X^{WT} U2-OS cells under mitotic arrest with nocodazole. Y-axis shows relative mRNA levels normalized to control sample, x-axis shows USP9X^{WT} and USP9X^{Mut} sample. Mean is shown from n=3 biologically independent experiments. One sample t-test was applied with **p<0.002.

3.18 WT1 binds to the CXCL8 promoter in mitosis

The results above verify that USP9X and WT1 influence mRNA levels of IL-8 in mitosis. The following question was if WT1 is the transcription factor of the gene CXCL8 which would support the model that USP9X regulates IL-8 transcription via stabilization of WT1. First, we compared the WT1 binding motif according to the Homo sapiens COmprehensive MOdel Collection (HOCOMOCO) web tool (<http://hocomoco11.autosome.ru>) to the genomic sequence at the transcriptional start site of the CXCL8 gene. To depict this graphically we assembled a position weight matrix of the two sequences which underlined accordance of WT1 binding motif and CXCL8 transcriptional start (Figure 24).

WT1 consensus binding motif: 

CXCL8 genomic sequence: **5' TAGGGTGATGATAT 3'**

 *Transcription start CXCL8*

Figure 24 Position weight matrix of the WT1 binding motif according Position weight matrix of the WT1 binding motif according to the Homo sapiens COmprehensive MOdel Collection (HOCOMOCO) web tool (<http://hocomoco11.autosome.ru>) and the genomic sequence of the CXCL8 gene at the transcriptional start site.

To confirm that the transcription factor WT1 binds to the CXCL8 promoter in mitotic cells, chromatin immunoprecipitation (ChIP) and luciferase reporter assays were performed by Oleksandra Karpiuk. The results of these experiments are included in this thesis only for a better understanding of the mechanism how WT1 regulates expression of IL-8. As the experiments were not done and data was not generated by me, experimental setup and explanations are not described in detail.

For ChIP of WT1, U2-OS cells were synchronized in mitosis using nocodazole for 16h. Afterwards cells were trypsinized and crosslinked with formaldehyde. Afterwards, cells were centrifuged, washed and frozen at -80°C. For lysis, pellets were resuspended in lysis buffer for ChIP to isolate nuclei which were further lysed in lysis buffer for nuclei. Next, nuclei were sonicated, centrifuged and supernatant was incubated overnight with antibodies to WT1 and IgG followed by incubation with protein A Sepharose. Subsequently, samples were washed and to isolate DNA samples were mixed with Chelex resin, decrosslinked followed by RNase A and Proteinase K treatment. Further, samples were subjected to quantitative RT-PCR with primers in list 5.10. Figure 25a shows binding of the transcription factor WT1 to the chromatin region harboring the promoter of CXCL8 in mitotic cells.

For the luciferase reporter assay, CXCL8 promoter was cloned into a promoterless NanoLuc vector (pNL1.1). U2-OS cells were transfected with CXCL8 promoter containing pNL1.1 vector or pNL1.1 control vector together with WT1 expression vector, followed by cell cycle arrest in mitosis and luminescence measurement. WT1 regulates expression of IL-8 by binding to the CXCL8 promoter generating a luminescence signal significantly higher than in control cells (Figure 25b).

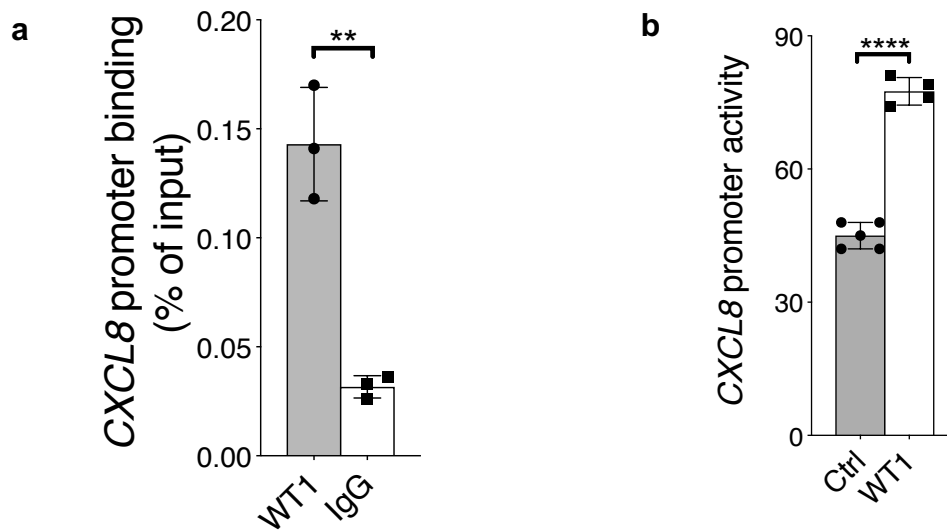


Figure 25 WT1 binds to the CXCL8 promoter in mitosis (a) Graph showing chromatin immunoprecipitation (ChIP) of WT1 occupancy on the CXCL8 promoter in U2-OS cells synchronized in mitosis with nocodazole. ChIP signal was quantified using RT-PCR and occupancy of WT1 was normalized to total input DNA. Mean from n=3 biologically independent experiments is shown. Ratio paired t-test was applied with **p=0.00277. Data was generated by Aleksandra Karpiuk. (b) Graph showing CXCL8 reporter assay done in U2-OS cells that were synchronized in mitosis using nocodazole. Cells were transfected with luciferase reporter construct harboring the human CXCL8 promoter or an empty reporter construct and a WT1 overexpressing vector as indicated. Luminescence signal was normalized to the background luminescence of the empty reporter construct. Mean from n=4 biologically independent experiments is shown. Ratio paired t-test was applied with ****p<0.0007. Throughout this figure standard deviations are displayed as error bars. Data was generated by Aleksandra Karpiuk.

3.19 WT1 and USP9X regulate abundance of IL-8 protein in mitosis

WT1 seems to regulate expression of IL-8 mRNA by direct binding to the promoter of CXCL8 (Figure 23 and 25). Furthermore, WT1 activity towards IL-8 expression is influenced by USP9X and USP9X phosphorylation on serine 2563 (Figure 23b). The next aim was to show that in consequence this regulatory pathway changes extracellular amount of IL-8 protein abundance. To this end, we transfected U2-OS cells with *control*, *WT1*, *USP9X* or *WT1* and *USP9X* siRNA using Lipofectamine™ 2000 as described in 6.3.2 Afterwards, cells were synchronized in mitosis and after 14h treatment an aliquot of 2ml of medium was taken and frozen at -80°C for measurement of secreted IL-8. Additionally, cells were harvested by mitotic shake-off.

For measurement of IL-8 amount in cell culture supernatant we used a commercially available enzyme-linked immunosorbent assay (ELISA). Before analysis, supernatants were thawed at room temperature and working steps for ELISA are described in 6.4.1. For measurement 100µl of supernatant were used and each condition was done as technical duplicate. Absorbance at a wave length of 450nm with a reference filter at a wave length of 600nm was measured. To get the absolute amounts of secreted IL-8 protein a standard curve using a serial dilution of IL-8 protein was calculated. USP9X and WT1 knockdown leads to lower extracellular levels of IL-8 secreted by U2-OS cells, but no additional effect under double siRNA treatment with *USP9X* and *WT1* is seen (Figure 26a). Furthermore, *USP9X^{Mut}* cells secrete IL-8 protein to a much lower extent than *USP9X^{WT}* (Figure 26b). This underlines the model that USP9X whole cellular levels, USP9X serine 2563 phosphorylation and WT1 play a pivotal role in expression and secretion of IL-8 in mitotic U2-OS cells.

To determine intracellular IL-8 abundance and to verify knockdown of USP9X and WT1 in cells of Figure 26a, b, collected cells were lysed, proteins separated by SDS-PAGE, subjected to Western Blot and incubated with indicated antibodies. Not only mRNA and extracellular levels of IL-8 are reduced under loss of USP9X or WT1, also intracellular IL-8 protein levels are lowered (Figure 26c). This rules out that intracellular IL-8 protein cannot be secreted under *USP9X* or *WT1* knockdown and that lower extracellular levels are due to higher intracellular capture of IL-8.

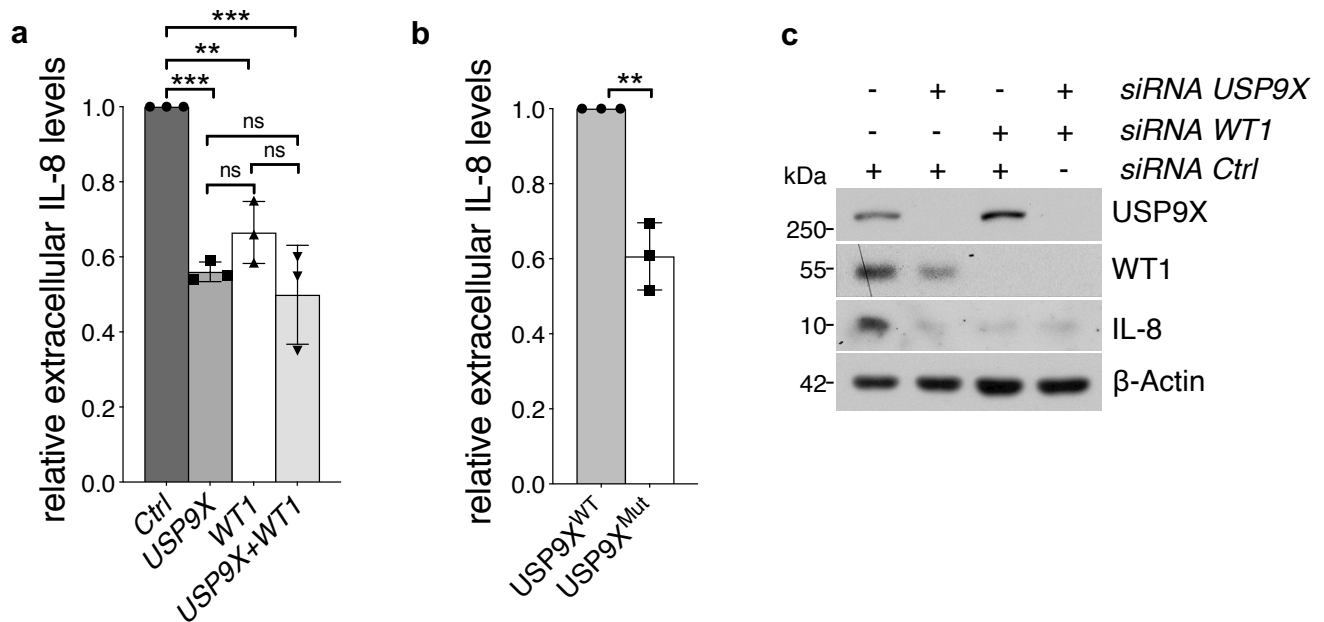


Figure 26 WT1 and USP9X regulate abundance of IL-8 protein in mitosis (a) Graph showing ELISA of secret IL-8 protein of mitotically arrested U2-OS cells. U2-OS cells were treated with *USP9X*, *WT1*, or double siRNA versus control siRNA. Means are shown from three biologically independent experiments. One way ANOVA was applied with *** $p=0.0002$ followed by Dunnett's test with *** $p(\text{Ctrl vs. USP9X})=0.0004$, ** $p(\text{Ctrl vs. WT1})=0.021$, *** $p(\text{Ctrl vs. USP9X+WT1})=0.0002$; $p(\text{WT1 vs. USP9X})=0.3081$, $p(\text{WT1 vs. USP9X+WT1})=0.0791$, $p(\text{USP9X vs. USP9X+WT1})=0.6772$. (b) Graph showing results of ELISA of secret IL-8 protein of mitotically arrested USP9X^{Mut} compared to USP9X^{WT} U2-OS cells. Means are shown from three biologically independent experiments. Ratio paired t-test was applied with * $p=0.0277$. (c) Immunoblot analysis of mitotic U2-OS cells that were transfected with control, *USP9X*, *WT1* or *USP9X* and *WT1* siRNA and arrested in mitosis using nocodazole. Cells were subjected to lysis, Western Blot and immunoblotting with the respective antibodies. (kDa: kilo Dalton).

3.20 Actinomycin D inhibits active transcription of IL-8 in mitosis

In order to investigate if IL-8 is actively transcribed in mitosis, mitotically arrested U2-OS cells were treated with the RNA polymerase inhibitor actinomycin D. This inhibitor stalls active transcription in mitosis abruptly. Further, under WT1 knockdown which lowers transcription of IL-8 mRNA a reduced effect of actinomycin D on transcription of IL-8 is expected. U2-OS cells were transfected with control or *WT1* siRNA using Lipofectamine™ 2000 as described in 6.3.2 and arrested in mitosis with nocodazole. After 15h treatment, mitotic cells were shaken off and replated onto a fresh cell culture dish. Next, either DMSO

or actinomycin D were added to nocodazole containing medium of each condition and incubation lasted for further 3 hours. Afterwards, cells were harvested and mRNA was extracted and quantitative RT-PCR done as described in 6.1.3-6.1.5.

Figure 27 indicates that the CXCL8 gene is actively transcribed in mitosis as treatment of *control* cells with actinomycin D decreases mRNA levels of IL-8. Furthermore, no significant difference of actinomycin D treatment compared to DMSO was detected in WT1 knockdown cells as transcription of IL-8 is already impaired in those cells.

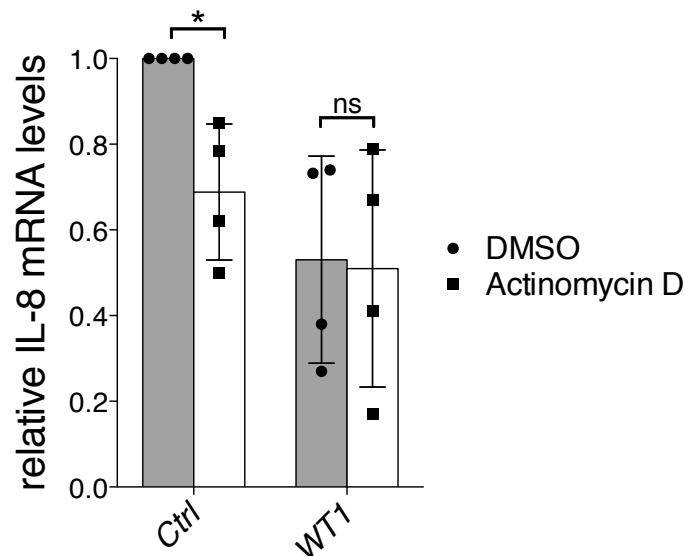


Figure 27 Actinomycin D inhibits active transcription of IL-8 in mitosis Graph depicting results of quantitative RT-PCR from mitotic U2-OS cells which were treated with *control* or *WT1* siRNA and DMSO or actinomycin D. After 15 hours incubation with nocodazole, mitotic cells were shaken off. Further, cells of each condition were divided, kept in nocodazole and simultaneously treated with either DMSO or actinomycin D. After 3 hours, cells were harvested, mRNA extracted and quantitative RT-PCR for analysis of IL-8 mRNA was done. Mean and standard deviations as error bars are shown from four independent experiments. One sample t-test (*control* siRNA) and ratio paired t-test (*WT1* siRNA) were applied with $*p(\text{Ctrl siRNA})=0.0293$, $p(\text{WT1 siRNA})=0.478$.

3.21 IL-8 regulates mitotic survival in U2-OS cells

Given the data above, the next aim was to investigate the biological role of IL-8 in mitotic survival. Recent work could show that IL-8 can regulate tumor growth and cell survival via an autocrine manner (Brew, Erikson et al. 2000) (Guo, Zang et al. 2017). Therefore, U2-OS cells were treated with *CXCL8* siRNA or *control* siRNA using Lipofectamine™ 2000 as described in 6.3.2. After further 48h, medium was removed and nocodazole containing medium was added and cells incubated for 8h. Afterwards, mitotic shake-off was performed and cells harvested. Then, cell lysis was done, lysates subjected to SDS-PAGE and Western Blot and samples analyzed by immunoblot with the indicated antibodies. Mitotically arrested cells using nocodazole express IL-8 to a higher extend than untreated cells (Figure 28a). Additionally, knockdown of IL-8 leads to higher levels of activated meaning cleaved caspase 3 indicating a higher rate of apoptotic cells in the population of

CXCL8 knockdown cells (Figure 28a). Antibodies detecting cleaved caspase 3 are widely used for quantifying apoptosis by immunoblotting (Hartmann, Hunot et al. 2000). Quantification of three independent experiments underlines that CXCL8 knockdown leads to statistically significant higher levels of cleaved caspase representing more activation of apoptotic pathways (Figure 28b).

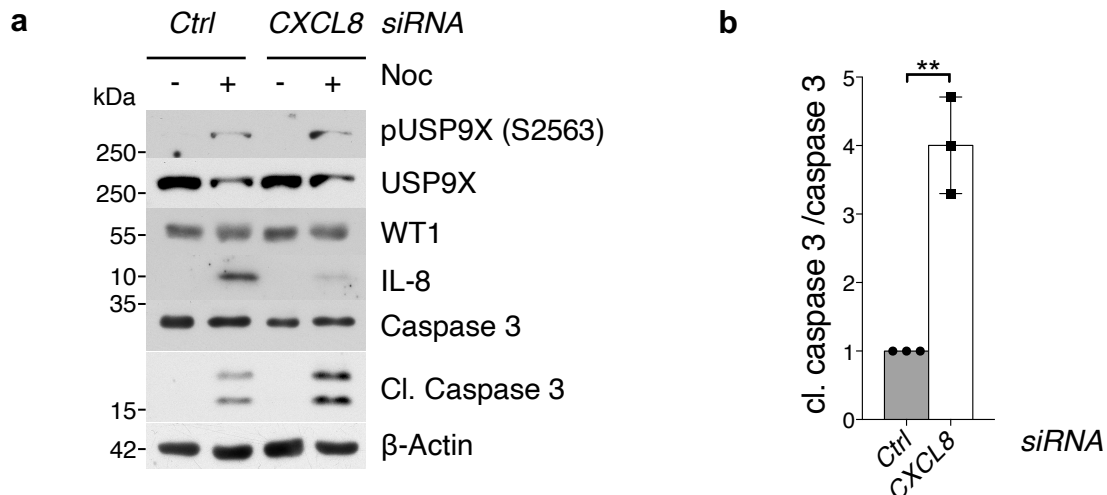


Figure 28 IL-8 regulates mitotic survival in U2-OS cells (a) Immunoblot of mitotic cells that were treated with CXCL8 or *control* siRNA and arrested in mitosis using nocodazole for 8h. U2-OS cells were treated with indicated siRNAs followed by nocodazole treatment. Samples were collected, lysed and analysed by Western Blot and immunoblot with the indicated antibodies. Cl. Caspase 3= cleaved Caspase 3. (kDa: kilo Dalton) **(b)** Graph with quantification of cleaved caspase 3 normalized to caspase 3 levels. Data of three independent experiments as described in (a) are shown. The y-axis indicates ration of cleaved caspase 3 and caspase 3, x-axis shows different conditions. Mean and standard deviations are displayed, t-test was applied with $**p=0.00179672$.

3.22 Blocking CXCR1 and CXCR2 receptor using reparixin incudes mitotic apoptosis

As mentioned above, IL-8 regulated tumor growth via an autocrine manner (Brew, Erikson et al. 2000). Taking this and the results of Figure 28 into account, inhibition of the CXCR1/2 receptor which is the receptor of IL-8 signaling should lead to apoptosis in mitotic cells (Brat, Bellail et al. 2005). To this end, U2-OS cells were either treated with DMSO or reparixin at a final concentration of 200µM, a non-competitive inhibitor of CXCR1 and CXCR2 (Bertini, Allegretti et al. 2004). After 40 h of incubation, nocodazole was added and cells were harvested after 8h incubation. Additionally, non-treated, asynchronous U2-OS cells were harvested. Then, cells were lysed, subjected to SDS-PAGE, Western Blot and immunoblot. Blocking of CXCR1 and CXCR2 signaling leads to higher activation of caspase 3 measured by levels of cleaved caspase 3 (Figure 29a) Quantification of three independent experiments indicates that IL-8 induced signaling plays a significant role in mitotic survival of mitotic U2-OS cells (Figure 29b).

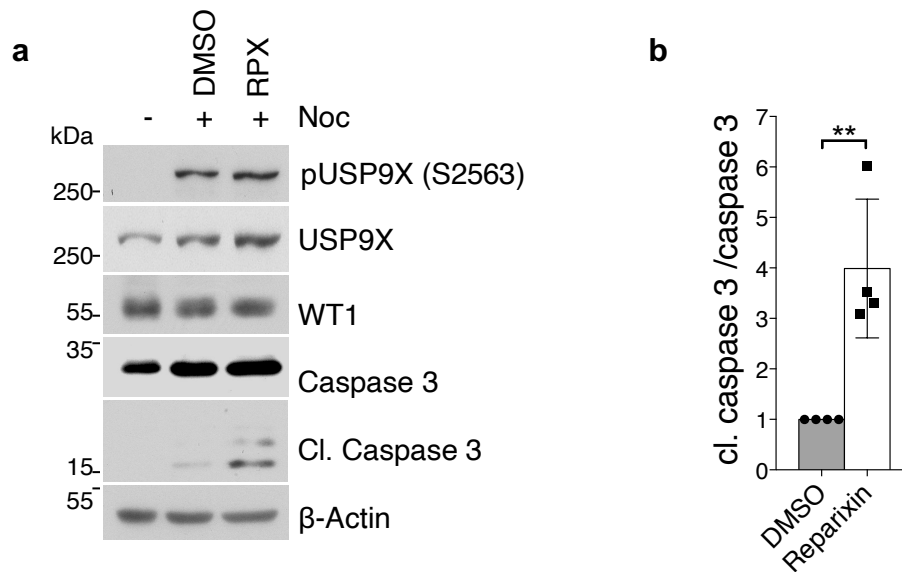


Figure 29 Blocking CXCR1 and CXCR2 receptor using reparixin incudes mitotic apoptosis (a) Immunoblot of mitotic U2-OS cells that were treated with DMSO or reparixin (RPX) and nocodazole (Noc) (8 hours). Blockage of CXCR1 and CXCR2 was performed for 40h, then nocodazole was added for 8 hours before cells were harvested. (kDa: kilo Dalton) **(b)** Quantification of cleaved caspase 3 normalized to caspase 3. Results of three independent experiments conducted as described in (a) are shown. The y-axis indicates ration of cleaved caspase 3 and caspase 3, x-axis shows different conditions. Mean and standard deviations are displayed, t-test was applied with * $p=0.02918964$.

3.23 Mitotic apoptosis induced by *CXCL8* knockdown can be rescued by exogenous IL-8

Suggesting the model that secreted IL-8 is a stimulus for cell survival in an autocrine manner, addition of exogenous IL-8 should rescue the effect of *CXCL8* siRNA treatment (Brew, Erikson et al. 2000). To verify this hypothesis, U2-OS cells were transfected with *control* or *CXCL8* siRNA using Lipofectamine™ 2000 as described in 6.3.2. 48h after transfection, cells were treated with nocodazole for 8h. 48h before harvesting, recombinant, commercially available IL-8 as added to cell culture medium of *CXCL8* knockdown cells. IL-8 concentration was titrated using final concentrations of 0,3ng/ml, 3ng/ml and 15ng/ml. Afterwards, cells were harvested by mitotic shake-off, lysed, proteins separated using SDS-PAGE following Western Blot and immunoblotting with indicated antibodies (Figure 30). This experiment shows that amount of cleaved caspase 3 and therefore apoptosis can be rescued in *CXCL8* knockdown cells by reconstitution of IL-8 signaling by adding exogenous IL-8 protein.

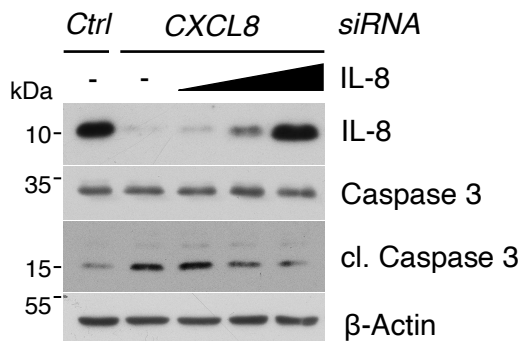


Figure 30 Mitotic apoptosis induced by CXCL8 knockdown can be rescued by exogenous IL-8 Immunoblot showing that exogenous IL-8 rescues mitotic apoptosis in IL-8 depleted cells. U2-OS cells were treated with the indicated siRNAs and incubated with exogenous IL-8 for the last 48 hours. Nocodazole treatment was performed for 8 hours. Cl. Caspase 3= cleaved Caspase 3. (kDa: kilo Dalton).

3.24 WT1 knockdown induces apoptosis in mitotic U2-OS cells which can be rescued by exogenous IL-8

Based on the experiment described in Figure 30, U2-OS cells were depleted of WT1 using *WT1* siRNA which was transfected with Lipofectamine™ 2000 as described in 6.3.2. After 48h, nocodazole was added to cell culture medium to induce mitotic arrest for 8 h followed by mitotic shake-off. To rescue the effect of WT1 mediated loss of extracellular IL-8, exogenous IL-8 was added to cells 48h before harvesting. Then, cells were lysed, subjected to SDS-PAGE, Western Blot and immunoblot. Figure 31a depicts that cleaved caspase 3 levels and therefore cellular apoptotic rate decreases under 15ng/ml of exogenous IL-8. This indicates that WT1 regulates mitotic survival via expression of IL-8 which exerts its function via binding to CXCR1 and CXCR2 and following intracellular signaling. ELISA experiments to verify addition of IL-8 and to measure extracellular levels of IL-8 in cell culture supernatants are shown in Figure 31b.

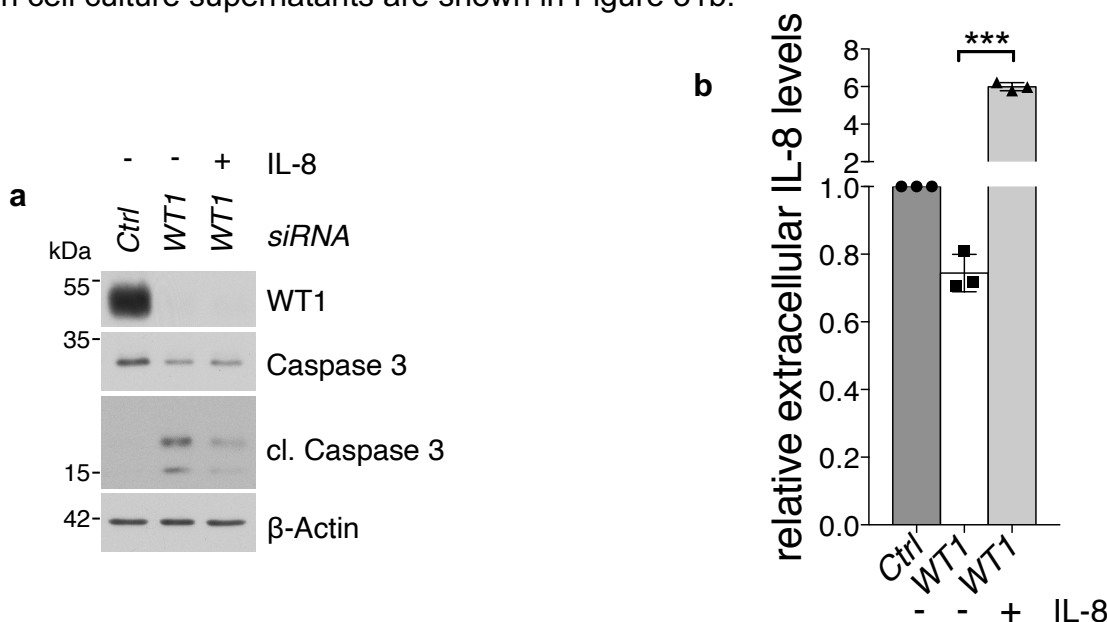


Figure 31 WT1 knockdown induces apoptosis in mitotic U2-OS cells which can be rescued by exogenous IL-8 (a) Immunoblot showing rescue of WT1 knockdown induced mitotic apoptosis by exogenous IL-8. U2-OS cells were treated with indicated siRNAs followed by addition of exogenous IL-8 at a final concentration of 15ng/ml for the last 48 hours. To induce mitotic arrest, cells were treated with nocodazole for 8 hours. Cl. Caspase 3= cleaved Caspase 3. (kDa: kilo Dalton) (b) ELISA depicting reconstitution of extracellular IL-8 in WT1 depleted cells. Results of three biological replicates are depicted. Mean and standard deviations are shown, ratio paired t-test was applied with *** $p < 0.0002$.

3.25 WT1 and IL-8 act in the same signaling pathway to regulated cell survival in mitosis

In order to demonstrate that WT1 regulates mitotic survival via IL-8 expression, U2-OS cells were treated with *WT1*, *CXCL8* or *WT1* and *CXCL8* siRNA using Lipofectamine™ 2000. After 48h, U2-OS cells were arrested in mitosis using nocodazole followed by mitotic shake-off, cell lysis, SDS-PAGE, Western Blot and immunoblotting. WT1 depletion leads to a substantial increase of apoptosis in mitotically arrested cells (Figure 32). Furthermore, IL-8 reduction by *CXCL8* knockdown does not further induce apoptosis under WT1 depletion suggesting that WT1 and IL-8 play a role in the same signaling pathway (Figure 32). WT1 knockdown as the upstream regulator of IL-8 leads to a more pronounced effect on cleaved caspase than IL-8 knockdown (Figure 32).

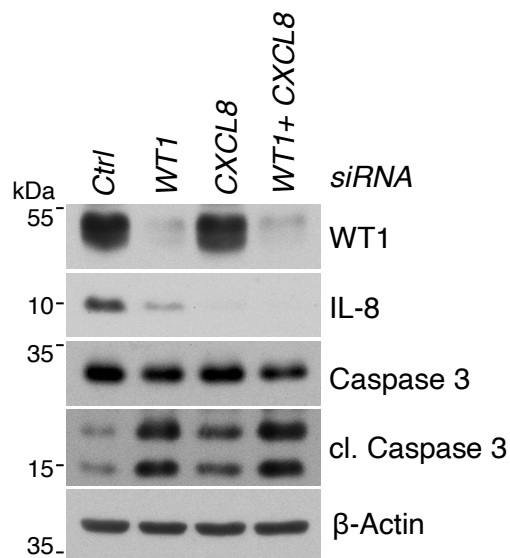


Figure 32 WT1 and IL-8 act in the same signaling pathway to regulated cell survival in mitosis Immunoblot showing WT1, *CXCL8* or *WT1* and *CXCL8* depleted U2-OS cells using siRNA followed by nocodazole treatment for 8h. IL-8 knockdown does not induce further apoptosis in WT1 depleted cells. WT1 knockdown leads to a more pronounced effect on cleaved caspase than IL-8 knockdown. Cl. Caspase 3= cleaved Caspase 3. (kDa: kilo Dalton)

3.26 Regulation of cell survival in mitosis by IL-8 is not restricted to microtubule-targeting drugs

For investigation of cell survival under different conditions of siRNA treatment U2-OS cells were arrested in mitosis using the microtubule-targeting drug nocodazole. In order to rule out that the effects seen only occur under spindle poison treatment and to demonstrate that IL-8 also regulates mitotic survival in untreated cells with physiological mitosis following experiment was performed. U2-OS cells were transfected with *CXCL8* siRNA using the Lipofectamine™ 2000 method as described in 6.3.2. After changing the medium to remove transfection reagents, thymidine was added and cells grown for further 24

hours. Then, medium was aspirated and cells release cells from G1/S-phase by washing cells once with medium and twice with DPBS. After 12 hours growth in normal medium, thymidine was added again for 24 hours. In the next step, cells were release as described above and collected mitotic shake-off was performed after 14 hours for harvesting. Then, cells were lysed, subjected to SDS-PAGE, Western Blot and immunoblotting. IL-8 is expressed in mitosis independent of forced spindle assembly checkpoint activation using nocodazole (Figure 33). Additionally, IL-8 knockdown induces apoptosis measured by cleaved caspase 3 and by cleavage of PARP 1 (Soldani and Scovassi 2002) independent of nocodazole suggesting that the pro-survival effect of IL-8 is relevant irrespective of mitotic stress force spindle assembly checkpoint activation.

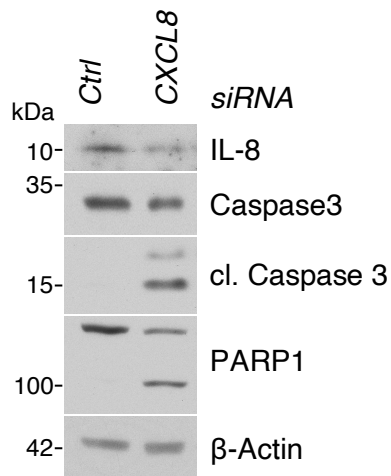


Figure 33 Regulation of cell survival in mitosis by IL-8 is not restricted to microtubule-targeting drugs
 Immunoblot analysis of mitotic U2-OS using a double thymidine block and which were treated with *control* or *CXCL8* siRNA. IL-8 pro-survival effect is independent of nocodazole as spindle poison and occurring in undisturbed mitosis. Cl. Caspase 3= cleaved Caspase 3. (kD: kilo Dalton).

3.27 Effect of WT1 and IL-8 on mitotic cell survival is not restricted to U2-OS cells

The biological effects seen of mitotic survival under *WT1* and *CXCL8* siRNA treatment were detected in U2-OS cells. To generalize the biological relevance of WT1 and IL-8 to other cell lines, knockdown experiments of WT1 and CXCL8 in A549 lung cancer cell line were conducted. Therefore, A549 cells were transfected with siRNA against *WT1* or *CXCL8*, and synchronized in mitosis using nocodazole after 48 hours. Nocodazole treatment was stopped after 8 hours performing a mitotic shake-off to harvest mitotic cells. Cells were lysed and analyzed after SDS-PAGE, Western blot and immunoblotting. Loss of WT1 or IL-8 in lung cancer A549 cells induces apoptosis measured by activation and cleavage of caspase 3 (Figure 34).

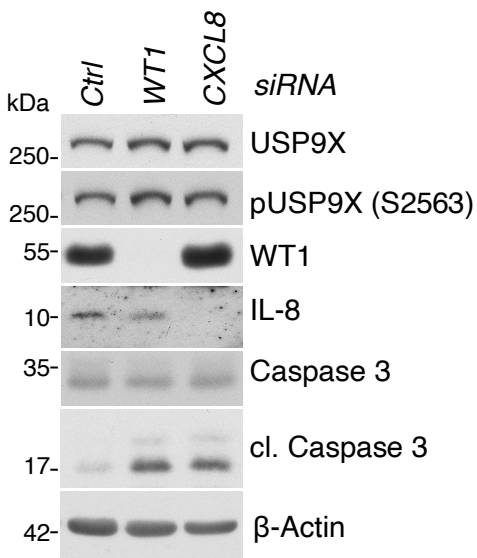


Figure 34 Effect of WT1 and IL-8 on mitotic cell survival is not restricted to U2-OS cells Immunoblot showing mitotic apoptosis under *CXCL8* or *WT1* siRNA treatment versus control knockdown in A549 lung cancer cells. Cells were arrested in mitosis using nocodazole for 8 hours. Cl. Caspase 3= cleaved Caspase 3. (kDa: kilo Dalton).

3.28 USP9X serine 2563 phosphorylation influences mitotic survival

In order to show that USP9X phosphorylation on serine 2563 is responsible for survival of U2-OS cells in mitosis, USP9X^{WT} U2-OS cells were either kept asynchronous or treated with nocodazole for 3, 10, 12, 14 and 16 hours to arrest cells in mitosis for indicated time ranges before harvesting by mitotic shake-off. For comparison, USP9X^{Mut} U2-OS cells were subjected to the same procedure. Afterwards, cells were lysed, and SDS-PAGE, Western Blot and immunoblot was conducted. First of all, USP9X phosphorylation cannot be detected on serine 2563 (Figure 35a). Furthermore, USP9X levels are not significantly changed between the two cell lines (Figure 35a). Additionally, treatment of USP9X^{Mut} U2-OS cells leads to higher levels of cleaved caspase 3 than in USP9X^{WT} standing for higher apoptotic rates in USP9X^{Mut} cells (Figure 35a). These results indicate that USP9X serine 2563 phosphorylation regulates cell survival in mitosis. In this experiment, no clear difference in cleaved caspase 3 levels could be seen in asynchronous and U2-OS cells treated for 3h with nocodazole. This could be due to a very weak immunoblot signal of cleaved caspase 3 (Figure 35a). To differentiate survival in asynchronous cells, USP9X^{WT} U2-OS cells and USP9X^{Mut} U2-OS cells were either kept untreated or arrested in mitosis using nocodazole for 32 hours. Afterwards, cells were shaken-off and subjected to flow cytometry using PI-staining. Gating and cell analysis was performed as described in 6.3.8. In this experiment shown in Figure 35b no difference in apoptosis comparing asynchronous USP9X^{WT} and USP9X^{Mut} U2-OS cells could be detected. In contrast, under treatment with nocodazole, mitotic arrest and therefore phosphorylation of USP9X serine 2563 was induced in USP9X^{WT} U2-OS cells. USP9X^{Mut} U2-OS cells expressing the non-phosphorylatable USP9X mutant show higher apoptotic rate due to loss of USP9X phosphorylation. Raw data were analyzed using the software FlowJo.

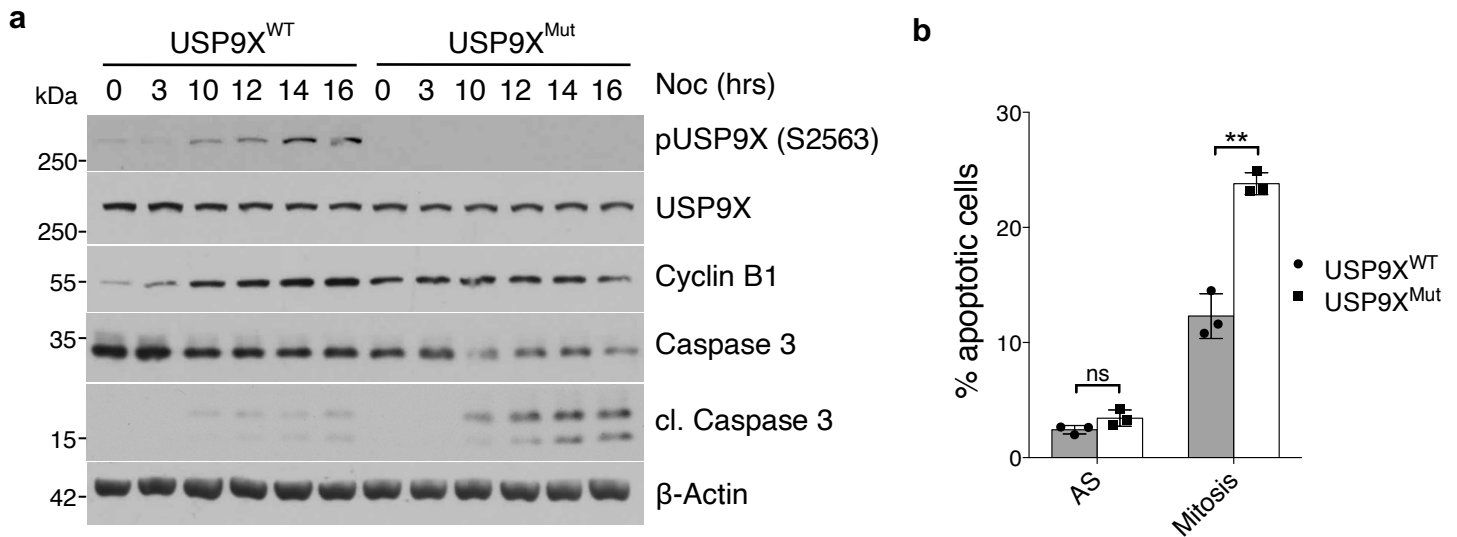


Figure 35 USP9X serine 2563 phosphorylation influences mitotic survival (a) Immunoblot showing mitotic apoptosis in USP9X^{Mut} compared to USP9X^{WT} U2-OS cells. Cells were either kept asynchronous or treated with nocodazole (Noc) for the indicated time for mitotic arrest. Cl. Caspase 3= cleaved Caspase 3. (kDa: kilo Dalton). **(b)** Graph depicting flow cytometry results showing mitotic apoptosis in USP9X^{Mut} U2-OS cells and USP9X^{WT} U2-OS cells that were kept asynchronous or treated with nocodazole for 32 hours. Afterwards mitotic shake-off was performed, cells stained with propidium iodide and measured by flow cytometry. Mean is shown from n=3 biologically independent.

3.29 USP9X serine 2563 phosphorylation influences mitotic survival via WT1

Given the biological results above that WT1 and IL-8 regulate mitotic survival and the founding that WT1 is stabilized by serine 2563 phosphorylated USP9X, the next aim was to investigate if the antiapoptotic effects of WT1 and IL-8 are regulated via phosphorylated USP9X. Therefore, USP9X^{Mut} U2-OS cells or USP9X^{WT} U2-OS cells were transfected with *WT1* or *control* siRNA using LipofectamineTM 2000 as described in 6.3.2. 48 hours after transfection, cells were synchronized in mitosis using nocodazole. For collection of mitotic cells, mitotic shake-off was performed. Afterwards, cells were lysed, proteins separated by SDS-PAGE and Western Blot followed by immunoblot was done. Loss of WT1 in USP9X^{WT} cells induces mitotic apoptosis (Figure 36). In USP9X^{Mut} cells lower levels of WT1 can be seen in mitosis, suggesting that USP9X phosphorylation on serine 2563 regulates WT1 abundance (Figure 36). Furthermore, knockdown of WT1 in mitotic USP9X^{Mut} cells does not enhance apoptosis which can be interpreted that USP9X phosphorylation on serine 2563 regulates mitotic survival via WT1 and IL-8.

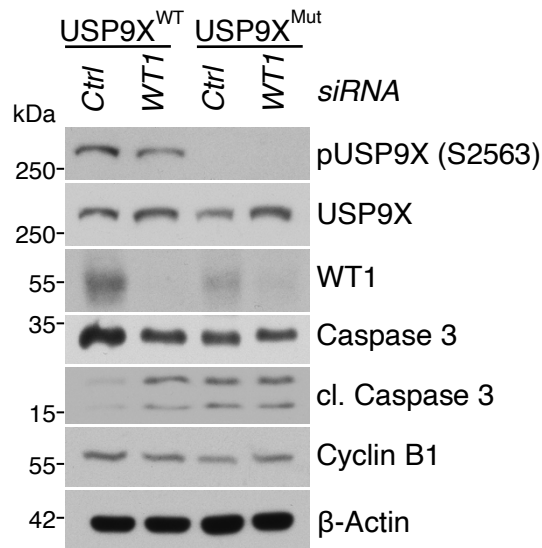


Figure 36 USP9X serine 2563 phosphorylation influences mitotic survival via WT1 Immunoblot of USP9X^{WT} and USP9X^{Mut} U2-OS cells which were transfected with *control* or *WT1* siRNA and arrested in mitosis using nocodazole. Immunoblots show an increased mitotic apoptosis by WT1 knockdown only in USP9X phosphorylatable U2-OS (USP9X^{WT}) cells and not in mutated USP9X cells (USP9X^{Mut}). Cl. Caspase 3= cleaved Caspase 3. (kDa: kilo Dalton).

3.30 Flow cytometry using PI-staining underlines that USP9X serine 2563 phosphorylation regulates mitotic survival via WT1

As shown in Figure 36, USP9X serine 2563 phosphorylation regulates mitotic survival via stabilizing WT1. To underline these results which were produced by Western Blot and immunoblotting, flow cytometry analysis using PI-staining to investigate mitotic survival was conducted. Therefore, U2-OS cells were treated with siRNA and synchronized in mitosis as described in Figure 36. Afterwards, mitotic cells were shaken-off, centrifuged and pellet was resuspended with DPBS carefully. This washing procedure was repeated once. Next, cells were resuspended with 1ml DPBS which was supplemented with propidium iodide (PI) to a final concentration of 1µg/ml. Finally, cells were subjected flow cytometry using a CyAn ADP LxP8 cytometer to distinguish between PI-positive and PI-negative cells. For analysis of cell viability, counted cells were displayed in a graph with sideward scatter (SSC) for cell granularity on the x-axis and forward scatter (FSC) representing cell size on the y-axis. Next, cell debris was excluded by gating the cell population of interest. Cells of interest are circled in Figure 37a in the upper panel (“intact cells”). Afterwards, circled cells were blotted for positive PI-signal representing apoptotic cells. PI-signal was measured in the FL3 channel using the cytometer. Absolute PI-positive cell counts are shown in the lower panel of Figure 37a. Raw data were analyzed using the software FlowJo. Also measured with flow cytometry *WT1* siRNA treatment of U2-OS cells induces mitotic apoptosis (Figure 37a).

Quantification and statistical analysis of three independent experiments using flow cytometry and PI-staining is shown in Figure 37b. These results are in accordance with Figure 36 that non phosphorylatable USP9X serine 2563 U2-OS cells have different apoptotic rates in mitosis under *control* siRNA treatment. This phenotype is abolished as soon as USP9X^{Mut} U2-OS cells and USP9X^{WT} U2-OS cells were treated with *WT1* siRNA indicating that USP9X serine 2563 phosphorylation is one of the most upstream regulatory events in this signaling pathway.

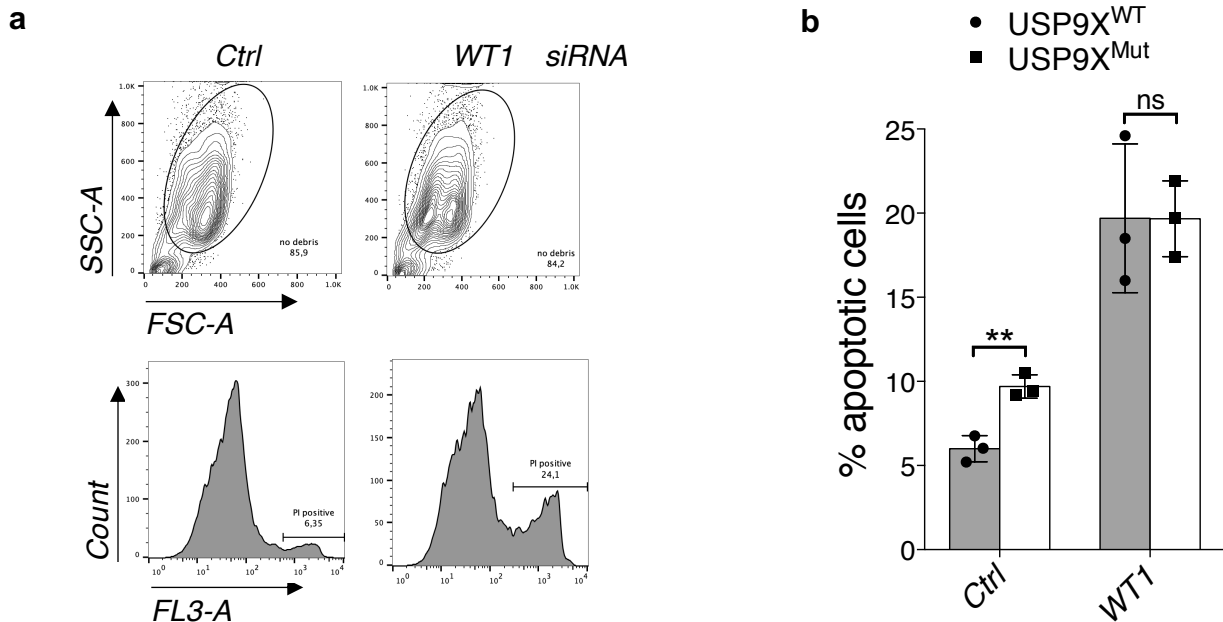


Figure 37 Flow cytometry using PI-staining underlines that USP9X serine 2563 phosphorylation regulates mitotic survival via WT1 (a) Graph depicting flow cytometry and gating strategy of mitotic U2-O. Cells were treated as in figure 36 and finally subjected to PI-staining and flow cytometry. Counted cells were displayed in a graph with sideward scatter (SSC) for cell granularity on the x-axis and forward scatter (FSC) representing cell size on the y-axis (upper panel). Cell debris was gated out and intact cells circled in the upper panel (“intact cells”). For further analysis only “intact cells” were used. FL3 high and therefore PI-positive cells are represented in the lower panel (lower panel) on the right side and are marked with a bar (PI positive). Control and WT1 knockdown samples are representatively shown. (b) Graph depicting mitotic apoptosis in USP9X^{WT} and USP9X^{Mut} U2-OS cells following control or WT1 knockdown. USP9X^{WT} and USP9X^{Mut} U2-OS cells were treated as in figure 37a and subjected to flow cytometry with PI-staining. PI-positive cells were analyzed for each sample. Error bars display standard deviations from n=3 biologically independent experiments. Unpaired t-test was applied with **p(Ctrl siRNA)=0.00363687; p(WT1 siRNA)=0.99127578.

3.31 CDC14B regulates mitotic survival via USP9X phosphorylation in U2-OS cells

To investigate whether CDC14B is the upstream regulator of the USP9X-WT1-IL-8 axis, USP9X^{WT} U2-OS cells or USP9X^{Mut} U2-OS cells were transfected with *CDC14B* siRNA or *control* siRNA and kept asynchronous or arrested in mitosis for 14 hours as described in 6.3.2 and 6.3.3. Afterwards, mitotic cells were shaken-off and lysis, SDS-PAGE, Western Blot and immunoblot were performed. First of all, Figure 38 shows that USP9X phosphorylation on serine 2563 is enhanced under knockdown of the phosphatase CDC14B. Furthermore, higher phosphorylation leads to more abundance of WT1 which upregulates IL-8 expression, respectively (Figure 38). This accumulates in induction of apoptosis detected by cleavage of caspase 3. USP9X^{Mut} U2-OS cells show no clear difference in WT1 and IL-8 levels upon loss of CDC14B which is in line with our model that CDC14B cannot exert dephosphorylation of serine 2563 of USP9X in mitosis in USP9X^{Mut} U2-OS cells. Additionally, no increase in apoptotic induction can be seen in USP9X^{Mut} U2-OS cells under *CDC14B* siRNA treatment.

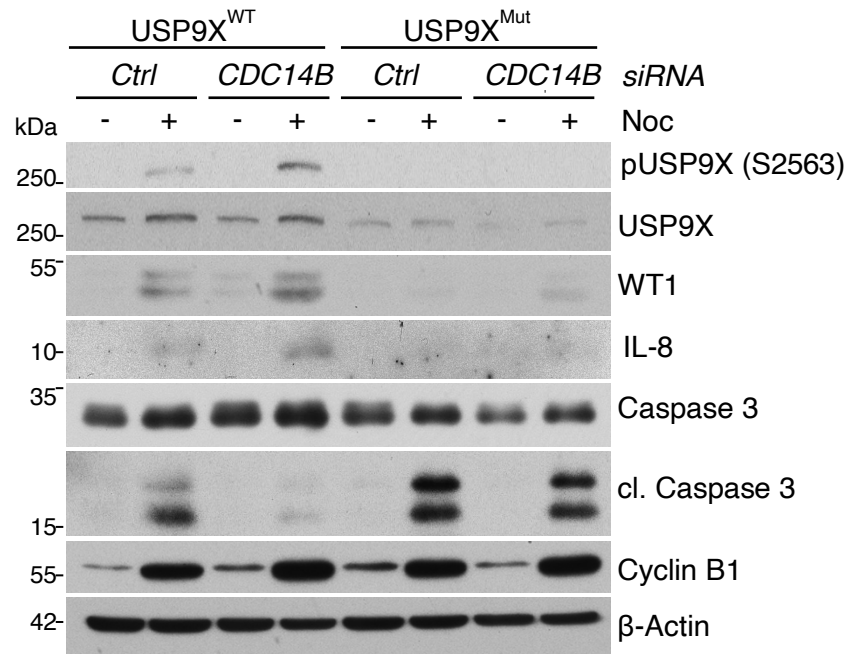


Figure 38 CDC14B regulates mitotic survival via USP9X phosphorylation in U2-OS cells Immunoblot analysis showing decreased apoptosis in mitosis under CDC14B knockdown in USP9X^{WT} but not in USP9X^{Mut} U2-OS cells. Cells were treated with *control* (Ctrl) or *CDC14B* siRNA, arrested in mitosis using nocodazole for 14h and collected for analysis by Western Blot. Afterwards, immunoblot analysis was performed with the indicated antibodies. Cl. Caspase 3= cleaved Caspase 3. (kDa: kilo Dalton).

4. Discussion

To orchestrate the exceptionally complex cell cycle phase mitosis highly specific regulation is necessary. Any disruption of correct mitosis can lead to chromosomal instability which further favors tumorigenesis (Levine and Holland 2018). Therefore, cell cycle aberrations and loss of cell cycle control are described to be hallmarks of cancer (Hanahan 2022).

Cdc14 is a highly conserved phosphatase which regulates exit from mitosis in budding yeast after cells have passed the spindle assembly checkpoint by antagonizing Cdk1 function (Wurzenberger and Gerlich 2011). Recent publications could show that one human ortholog of Cdc14, called CDC14B, plays a critical role in G2 DNA damage checkpoint response (Bassermann, Frescas et al. 2008). Beside this, recent work could shed more light on mitotic function of CDC14B as it was demonstrated that CDC14B regulates passage through mitosis by influencing function of CDC25 and CDK1-Cyclin B (Tumurbaatar, Cizmecioglu et al. 2011). Furthermore, CDC14B seems to stabilize and bundle microtubules in mitosis and to induce exit from mitosis by dephosphorylation of SIRT 2 (Dryden, Nahhas et al. 2003, Cho, Liu et al. 2005). If there are further signaling pathways which influence mitotic progression and mitotic survival and in which CDC14B is involved is poorly understood.

In this study, a so far unknown mode of mitotic survival and therefore mitotic regulation was identified. The initial event of this axis comprises the phosphorylation of USP9X on serine 2563. This phosphorylation is highly regulated and occurs specific in mitosis. CDK1 was identified to be the relevant mitotic kinase, CDC14B to be the phosphatase reversing mitotic phosphorylation of USP9X on serine 2563. The phosphorylation as posttranslational modification of USP9X on serine 2563 was found to regulate its enzymatic activity. Furthermore, phosphorylated USP9X deubiquitinates WT1 in mitosis and therefore regulates mitosis specific transcription of the gene CXCL8. Active transcription of CXCL8 with the consequence of high IL-8 expression and secretion increases mitotic survival in an autocrine manner.

This signaling pathways provides different aspects of DUB activity control by posttranslational modification, cell cycle specific apoptosis and mitotic transcription.

4.1 CDC14B and CDK1 regulate mitotic phosphorylation of USP9X on serine 2563 and regulate activity of USP9X

First of all, the phosphatase CDC14B was identified to bind to the deubiquitinase USP9X in mitosis by a mass spectrometry-based interaction screen. This could be verified by binding experiments performing an immunoprecipitation and Western Blot analysis. The interaction of CDC14B and USP9X was enhanced in mitosis compared to unsynchronized cells. In a next step, phosphorylation site of USP9X was assessed by a SILAC-based phospho-proteomic screen which yielded serine 2563 to be phosphorylated in mitosis and to be phosphorylated to a lower extent under the overexpression of CDC14B. Knockdown

experiments of CDC14B in U2-OS cells and overexpression of CDC14B in HeLa cells could identify CDC14B as the phosphatase of USP9X. Western Blots and immunoblotting experiments were performed using a custom-made phosphorylation specific antibody against USP9X serine 2563 phosphorylation.

In cell cycle experiments using thymidine or nocodazole to synchronize cells in G1/S-phase and mitosis it could be demonstrated that serine 2563 phosphorylation of USP9X is highly regulated and phosphorylation is restricted to mitosis. Interestingly, cell cycle regulated expression of USP9X does not seem to be one of the main regulatory means of USP9X as its total protein abundance is quite stable throughout different cell cycle phases. CDK1 and CD14B have been found as counteracting pair in regulation of mitotic phosphorylation of KIBRA (Ji, Yang et al. 2012). CDK1 is one of the main kinases in mitosis influencing a wide range of cellular mitotic processes (Malumbres 2014). The initial assumption that the mitotic kinase CDK1-Cyclin B phosphorylates USP9X on serine 2563 could be supported by CDK1 consensus motif matching. USP9X serine 2563 proceeds the amino acid proline which comprises the consensus motif of CDK1 (Errico, Deshmukh et al. 2010). To verify that CDK1 is the kinase of USP9X, an in vitro kinase assay was conducted. Therefore, USP9X C-terminal fragments were purified from bacteria and subjected to in vitro kinase assay using CDK1-Cyclin B and radioactively labeled ATP. C-terminal fragment of USP9X^{WT} was phosphorylated in vitro by CDK1-Cyclin B. In contrast, C-terminal fragment of USP9X which harbored a serine to alanine mutation in position 2563 depicted significantly lower phosphorylation suggesting that CDK1-Cyclin B phosphorylates USP9X on serine 2563 in vitro. Additionally, inhibition of CDK1-Cyclin B in mitotic cells using the inhibitor RO-3306 prevented USP9X from phosphorylation on serine 2563.

In general, deubiquitinases (DUBs) are highly regulated to prevent unspecific substrate cleavage and to avoid uncontrolled deubiquitylation activity (Reyes-Turcu, Ventii et al. 2009). This is accomplished by means of posttranslational modification like phosphorylation or ubiquitylation of DUBs (Wada and Kamitani 2006, Matsuoka, Ballif et al. 2007). The understanding of USP9X posttranslational modification in the context of different cellular processes is growing (Yoon, Parnell et al. 2020). More specifically, USP9X was characterized to be posttranslational modified as it is phosphorylated on serine 1600 to deubiquitinate the protein ZAP70 in lymphocytes (Naik and Dixit 2016). In line with recent findings that phosphorylation influences activity of USP9X, USP9X phosphorylation on serine 2563 regulates its deubiquitylation activity. In a DUB activity assay using HA-Ubiquitin-VS it could be demonstrated that purified FLAG-USP9X^{WT} exerts higher deubiquitinating activity in mitosis than a FLAG-USP9X mutant which cannot be phosphorylated on serine 2563 (USP9X^{S2563A}). Supporting the idea of cell cycle specific regulation, FLAG-USP9X^{WT} shows no difference in activity to FLAG-USP9X^{S2563A} in G1/S-phase cells. In this cell cycle phase, no phosphorylation of USP9X on serine 2563 is found and expected. Furthermore, FLAG-USP9X^{WT} and FLAG-USP9X^{S2563A} which were purified from mitotic HEK 293T were shown to have different enzyme kinetics. The substrate Ubiquitin-AMC was used in a serial dilution to assess V_{max} by fluorescence measurement of AMC liberation. This yielded a V_{max} value for USP9X^{WT} of about 36 μ M/min and for USP9X^{S2563A} of about 31 μ M/min.

Bringing these finding in a clinical context, inhibition of kinases seems to be an attractive concept of cancer treatment, more specific in combination with spindle poisons to inhibit

phosphorylation and therefore oncogenic activities of USP9X in mitotically arrested cells (Zhang, Zhang et al. 2021).

To which extend USP9X phosphorylation on position 1226 which was identified in the SILAC-based phospho-proteomic screen takes influence on deubiquitination activity of USP9X, binding to substrates or cellular localization needs to be further investigated. If there are other posttranslational modifications than phosphorylation of USP9X like SUMOylation, hydroxylation or ubiquitylation that take influence on USP9X function has not been found yet.

4.2 USP9X deubiquitinates WT1 in mitosis in a phosphorylation dependent manner

For a better understanding of USP9X function in mitotic cells mass spectrometry based ubiquitome analysis under loss of USP9X was conducted. This screen yielded the protein Wilms' tumor protein 1 (WT1) as a potential mitotic substrate of USP9X. WT1 seemed to be a promising hit as it was found to be a transcription factor which exerts an oncogenic function in regulating angiogenesis, tumor invasion, cell proliferation and inhibition of apoptosis (Tuna, Chavez-Reyes et al. 2005) (Wu, Zhu et al. 2013, Katuri, Gerber et al. 2014). Beside this, WT1 was shown to be ubiquitylated and degraded by the proteasome (Bansal, Bansal et al. 2010). Recently, the E3 ligase CMIP was identified to ubiquitinate WT1 but until now, the corresponding deubiquitinase has not been found yet (Zhang, Fan et al. 2021). Furthermore, comparing ubiquitome analysis results under USP9X knockdown in asynchronous and mitotic cells, WT1 scored higher in nocodazole arrested cells suggesting a cell cycle specific deubiquitination event. Additionally, ubiquitome analysis yielded the protein catenin beta-1 to be more ubiquitinated and purified under loss of USP9X which is in line with recent publications and validated the ubiquitome screen (Murray, Jolly et al. 2004, Yang, Zhang et al. 2016). In immunoprecipitation assays of WT1 and USP9X interaction of these two proteins was found to be enhanced in mitotic cells compared to asynchronous cells. Interestingly, increased phosphorylation of USP9X on serine 2563 reflected increased binding of WT1 to USP9X. In addition, overexpression of USP9X leads to higher abundance of WT1 protein.

Taking the results above into account, phosphorylation dependent binding of USP9X to WT1 could be demonstrated. USP9X serine 2563 regulates binding of WT1 to USP9X. This effect is restricted to mitosis as in asynchronous cells, only little phosphorylation of USP9X serine 2563 is expected. This introduces a new level of DUB-substrate interaction of USP9X which has been already described for other DUBs (Elliott, Nielsen et al. 2014, Esposito, Akman et al. 2020). USP9X was shown to deubiquitinate WT1 in mitosis and in accordance with the binding and activity assay, this is dependent on serine 2563 phosphorylation of USP9X. Further, ubiquitylated mitotic WT1 is targeted for proteasomal degradation which can be rescued by bortezomib (Figure 39).

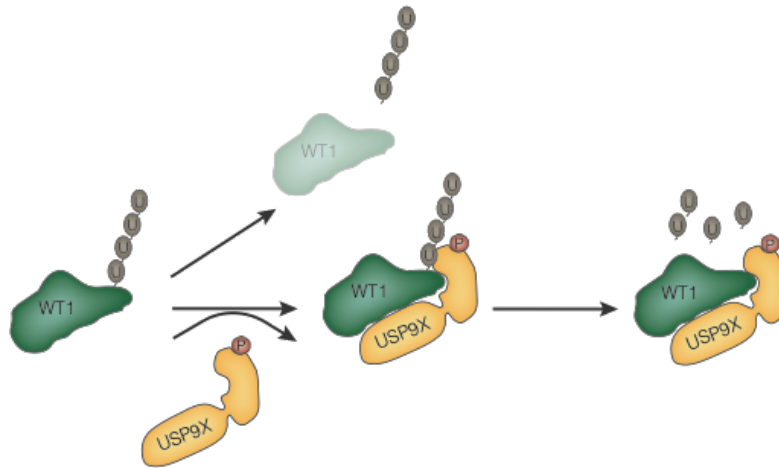


Figure 39 Model of USP9X deubiquitylation activity towards WT1 in mitosis The protein WT1 is polyubiquitylated in mitotic cells which targets WT1 for proteasomal degradation and reduces protein levels of WT1 in mitosis (left side, in green). Competing degradation of polyubiquitylated WT1, USP9X (in yellow) is phosphorylated on serine 2563 in mitosis (depicted as “P” in brown). This phosphorylation is regulated by the kinase CDK1 and phosphatase CDC14B (not depicted in model). Phosphorylation of USP9X on serine 2563 leads to enzymatic activation of USP9X and to enhanced interaction of USP9X and WT1. Binding of the deubiquitinase to its substrate reverses WT1 ubiquitylation and rescues it from degradation.

Supplementary, performing confocal microscopy experiments USP9X could be demonstrated to colocalize with WT1 in mitotic cells.

Further, it could be shown that inhibition of USP9X with the unspecific deubiquitinase inhibitor WP1130 decreases protein levels of WT1. Intriguingly, WT1 was recently found to induce self-renewal in murine leukemia cells and this function could be blocked by treating cells with WP1130 (Zhou, Jin et al. 2020). WT1 and USP9X expression is upregulated in certain tumor entities like osteogenic sarcoma, Ewing sarcoma and lymphoma (Srivastava, Fuchs et al. 2006, Yang, Han et al. 2007, Schwickart, Huang et al. 2010, Katuri, Gerber et al. 2014). Therefore, downregulation of USP9X activity using a specific inhibitor could be a potential therapeutic option in treatment of these tumor entities.

Given the number of substrates which have already been described for USP9X, it would be interesting if USP9X binding to other substrates than WT1 is also regulated by serine 2563 phosphorylation or if this regulatory means is restricted to WT1 (Schwickart, Huang et al. 2010, Naik and Dixit 2016, Yang, Zhang et al. 2016).

Concerning posttranslational modifications of WT1 beside ubiquitylation, phosphorylation of WT1 changes its transcriptional activity (Ye, Raychaudhuri et al. 1996). To which extend phosphorylation or other posttranslational modifications of WT1 influence its binding to USP9X with the consequence of modifying WT1 ubiquitylation needs to be further assessed.

4.3 Active transcription and secretion of IL-8 in mitosis is regulated by WT1 and USP9X

The concept of transcription and its understanding has changed within the last few years. Until 2017, transcription was thought to be silenced during mitosis. Though, it has been demonstrated before that transcription factors are bound to condensed DNA during mitosis to ensure rapid reactivation of transcription of a subset of genes upon the daughter cell has passed through mitosis which is termed mitotic bookmarking (Lodhi, Ji et al. 2016). In 2017, active low-level transcription of specific genes was found to be retained during mitosis (Palozola, Donahue et al. 2017).

WT1 is a transcription factor harboring zinc fingers in the C-terminal part for DNA-interaction, whereas the N-terminal part with a proline-glutamine rich sequence is responsible for RNA and protein interaction (Yang, Han et al. 2007). Among others, transcriptional targets of WT1 are P21, Bcl-2 or c-Myc (Englert, Maheswaran et al. 1997, Mayo, Wang et al. 1999, Han, San-Marina et al. 2004).

In order to find a so far undescribed gene which expression is regulated by WT1 in mitosis, RNA sequencing analysis under WT1 knockdown condition and in U2-OS cells harboring a non-phosphorylatable USP9X mutant was performed. This screen yielded the gene CXCL8 to be transcriptionally downregulated under loss of WT1 and in an USP9X phosphorylation dependent manner in mitotic cells.

Increasing evidence is suggesting that the cytokine IL-8 which is encoded by the gene CXCL8, plays a pivotal role in cell proliferation, apoptosis and response to anticancer drugs (Gales, Clark et al. 2013, Guo, Zang et al. 2017). Comparing the WT1 consensus binding motif according to the Homo sapiens COmprehensive MOdel Collection (HOCOMOCO) web tool (<http://hocomoco11.autosome.ru>) and CXCL8 genomic sequence using position weight matrix supported the assumption of WT1 being the transcription factor of CXCL8.

In experiments verifying the result of RNA sequencing, mRNA levels of IL-8 are lowered under loss of WT1 in mitosis. Supporting the model that WT1 is the downstream target of USP9X, the same effect was seen under knockdown of USP9X and in a non-phosphorylatable USP9X serine 2563 cell line.

Furthermore, extracellular levels of IL-8 are decreased under WT1 and USP9X knockdown and in a non-phosphorylatable USP9X serine 2563 cell line. Of notion and as seen in the quantitative mRNA experiments, double knockdown of WT1 and USP9X does not exceed loss of IL-8 compared to single knockdown experiments. This can be interpreted that USP9X and WT1 act in the same pathway with transcription of CXCL8 to be the downstream event.

In a recent publication by Palozola et al., mitotic cells were treated with the transcriptional inhibitor alpha-amanitin to investigate newly synthesized RNA (Palozola, Donahue et al. 2017). In a similar approach and using the RNA-polymerase inhibitor Actinomycin D, it could be demonstrated that IL-8 is actively transcribed in mitosis in a WT1 dependent manner. Furthermore, chromatin immunoprecipitation indicates that WT1 is binding to CXCL8 promoter in mitosis. This idea is supported by activation of the CXCL8 promoter in mitotic cells under overexpression of WT1 using a luciferase assay.

As mentioned above, WT1 deubiquitylation and stability is regulated by USP9X. Beside ubiquitylation, how WT1 activity in mitotic transcription is regulated remains elusive. It is

tempting to speculate that WT1 binding to DNA is influenced by phosphorylation not only in untreated cells but also in mitotic cells (Ye, Raychaudhuri et al. 1996). Additionally, further investigation of other possible mitotic WT1 target genes beside CXCL8 which were identified in RNA sequencing could bring more clearness in the upcoming field of mitotic transcription. For example, the gene KRT17 coding for the protein KRT17 was found to be transcriptionally upregulated by WT1 in mitosis. KRT17 is overexpressed in pancreatic cancer stimulating proliferation and migration (Li, Ni et al. 2020). In mitosis, a cell cycle phase with high dynamics in cellular shape, it would be interesting to further investigate the role of KRT17. WT1 could also be part of a new regulatory means of KRT17 by active mitotic transcription.

Mitotic bookmarking comprises histone modifications like H3K4 or H3K79 occur during mitosis and are responsible for chromatin accessibility and transcriptional start after mitosis (Kouskouti and Talianidis 2005). A further and main aspect of mitotic bookmarking is the incorporation of specific histones into the mitotic nucleosomes (Lodhi, Ji et al. 2016). For instance, histone H3.3 promotes transcription of the gene MyoD as soon as cells have passed mitosis and enter G1-phase (Ng and Gurdon 2008). With more focus on mitotic histone modification or histone exchange, it would be interesting to shed more light on this regulatory means in active mitotic transcription.

4.4 CDK1 and CDC14B mediated phosphorylation of USP9X on serine 2563 regulates survival in mitosis via WT1 and IL-8

Uncontrolled cell survival and avoidance of cell death are characteristics which are frequently found in tumor cells and which are counted to the hallmarks of cancer (Hanahan 2022). Cell cycle checkpoints, in case of mitosis the spindle assembly checkpoint, are established to control and detect any defects in DNA integrity or segregation and which further induce cellular signaling for cell fate decision (Dominguez-Brauer, Thu et al. 2015). Exceeding activation for example of the spindle assembly checkpoint by improper attachment of microtubule to chromatids can end in the activation of cellular apoptosis via a caspase activating cascade including caspase 3 (Ruan, Lim et al. 2019). Any dysfunction of the spindle assembly checkpoint or dysregulation of downstream protein networks can therefore induce chromosomal instability, aneuploidy and tumor development. Any newly identified cellular pathway regulating apoptosis under activation of the spindle assembly checkpoint can improve the understanding of cancer biology.

Taxanes and vinca alkaloids are a main pillar in modern cancer therapy targeting mitosis and the spindle assembly checkpoint (Janssen and Medema 2011). Drug resistance under treatment with microtubule-active drugs therefore limits the selection of antitumor therapy and represents a significant obstacle in tumor therapy (Jordan and Wilson 2004). Identifying regulators of cell survival in mitosis can help to dissect possible resistance mechanisms which are relevant under microtubule-active drug treatment.

Recent work could show that USP9X and WT1 expression is upregulated in a variety of tumor entities (Yang, Han et al. 2007, Schwickart, Huang et al. 2010, Katuri, Gerber et al. 2014, Fu, Xie et al. 2017, Ruan, Lim et al. 2019). In contrast, CDC14B protein is downregulated in tumor cells suggesting a tumor suppressive role (Kim, Choi et al. 2014).

To elucidate a new mitotic signaling pathway regulating mitotic survival knockdown experiments of IL-8 were performed. The protein IL-8 is involved in mitotic cell survival as loss of IL-8 induces caspase dependent apoptosis.

IL-8 as chemokine is actively secreted by tumor cells and binds to the CXCR1/2 receptor and therefore promotes tumorigenesis (Russo, Garcia et al. 2014). Blockage of CXCR1/2 receptor using the small molecular inhibitor reparixin in cell culture increases apoptosis activating the caspase dependent cellular program (Figure 40). A similar oncogenic effect in mitosis was found for WT1 and experiments in this study suggest that WT1 prosurvival function is mainly exerted via IL-8. Additionally, USP9X phosphorylation on serine 2563 regulates mitotic survival in a WT1 dependent manner. Interestingly, loss of CDC14B in a USP9X serine 2563 non-phosphorylatable U2-OS cell line has no detectable effect on mitotic cell survival while reduced activity of CDC14B in mitotic cells with USP9X wildtype protein improves cell survival.

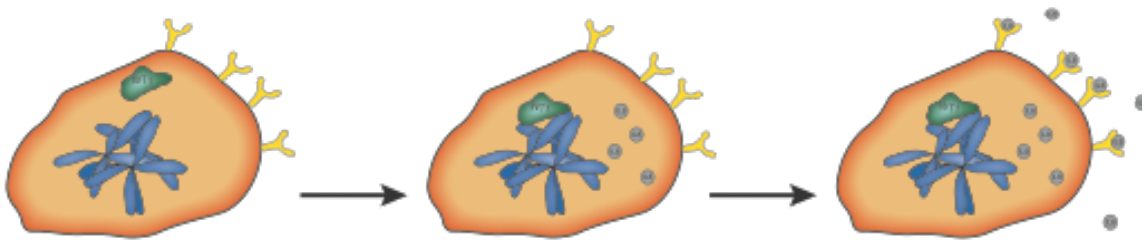


Figure 40 Model of WT1 regulated mitotic transcription of IL-8 During mitosis chromatids are accessible to binding of transcription factor which is termed mitotic bookmarking. In mitotic cells, the transcription factor WT1 (green) binds to the promoter of CXCL8. Condensed DNA is depicted in blue. In mitotic cells, this initiates WT1-dependent active transcription of the gene CXCL8 which codes for the protein IL-8 (middle part). The chemokine IL-8 is secreted and attaches to the receptor CXCR1 or CXCR2 (yellow) in an autocrine manner. Downstream signaling of the CXCR1/2 receptor activates a cellular survival program in mitosis.

In summary, USP9X is a central player in mitotic survival and is responsible for cell fate decision via regulating abundance via WT1 and IL-8. Upstream regulators of USP9X are CDK1 and CDC14B which phosphorylate and dephosphorylate USP9X on serine 2563. Blockage of CXCR1/2 receptor using reparixin is an upcoming aspect in tumor therapy. In metastasized breast cancer, reparixin is used in combination with paclitaxel in a phase Ib pilot study and phase II study (Schott, Goldstein et al. 2017). Final results of the latter clinical trial have not been published yet. This underpins the potential of targeting the described mitotic survival pathway.

In ovarian cancer patients under platinum-based chemotherapeutic treatment, high levels of serum IL-8 are associated with shorter survival time (Zhang, Liu et al. 2019). The molecular mechanism has not been described yet, but the model of this study could improve understanding and interpretation of these results.

One interesting aspect would be to correlate IL-8 levels in serum of ovarian cancer patients with phosphorylation of USP9X on serine 2563 in histopathological specimens. Alternatively, whole cellular levels of USP9X can be assessed. High phosphorylation of USP9X on serine 2563 as the upstream event of the newly found mitotic survival hub is expected to lead to high expression of IL-8 according to the results shown here. If a

positive correlation is found, investigation of other cancer type specimens, for example of lung cancer patients, can be a plausible approach (Zhu, Webster et al. 2004). If promising results can be gained, a further step could be investigation of reparixin cancer treatment and response depending on the phosphorylation of USP9X on serine 2563 in tumor specimens.

5. Materials

5.1 Instruments

Amaya® Cell Line Nucleofector®, Lonza
Analytical balance ABJ 220, Kern & Sohn GmbH
Aqualine water bath, Lauda-Brinkmann
Bioraptor, Diagenode
Centrifuge Multifuge 3SR+, Thermo Scientific™
Concentrator plus, Eppendorf AG
Cool-Centrifuge 5417R, Eppendorf AG
Digital Sonifier® 250D, Branson-Emerson
E-Box VX2 Imager, VILBER
FACSCalibur™, BD Biosciences
FACSAria™ II, BD Biosciences
FluoView FV10i, Olympus
Fridges and lab freezers, Liebherr
HERAcell® 150i CO2-Incubator, Thermo Scientific™
HERAfreeze™, Thermo Scientific™
Hypercassettes™, Amersham / GE Healthcare
Innova® 40 shaker for bacteria, New Brunswick™ / Eppendorf AG
Invitrogen Chamber for Ready Gels, Invitrogen™
Leica SP8 Confocal Laser Scanning Microscope
Light cycler® 480 system, Roche Diagnostics GmbH
LS4800 liquid nitrogen tank, Taylor-Wharton Lab Systems
Magnetic thermo stirrer RCT basic IKA®, Laboratory Equipment
Microscope Axiovert 40 CFL, Carl Zeiss AG
MidiMACS™ Separator, Miltenyi Biotec
Mini-Sub® Cell GT system for agarose electrophoresis, Bio-Rad Laboratories
Mithras LB 940 Reader, Berthold Technologies
Multifuge 3SR+, Thermo Scientific™
NanoPhotometer®, Implen GmbH
Novex® Mini cell system for precast NuPAGE gels, Thermo Scientific™
Nucleofector™ 2b Device
peqSTAR2x gradient thermocycler, Peqlab Life Science
pH-meter pH720, InoLab WTW GmbH
Pipetman neo (P10N, P20N, P100N, P200N, P1000N), Gilson®
Polymax 1040 platform shaker, Heidolph Instruments
PowerPac™ Basic power supply, Bio-Rad Laboratories
PowerPac™ HC power supply, Bio-Rad Laboratories
Precision balance 572 -37, Kern & Sohn GmbH
Promega GloMax® Discover Microplate Reader
Rotating Wheel 3000, Fröbel Labortechnik
Safety cabinet HERAsafe® KS, Thermo Scientific

Scanner V750, Pro Epson®
SDS-gel Electrophoresis chamber Mini-Protean, Bio-Rad Laboratories
Sorvall® RC-5B centrifuge (rotors SS-24 & GS-3), Du Pont Instruments
SRX-101A developer, Konica-Minolta
Superose 6 PC 3.2/30 analytical column, GE Healthcare
Tabletop centrifuge 5424, Eppendorf AG
Thermo block MBT 250, Kleinfeld Labortechnik
Thermomixer compact, Eppendorf AG
Trans Blot Cell Blotting chamber, Bio-Rad Laboratories
Tumbling roller mixer RM5, Neolab

5.2 Reagents and chemical compounds

Actinomycin D, Sigma-Aldrich™
Amaxa® Cell Line Nucleofector® Kit V
[alpha-P32]ATP, Hartmann Analytics
β-Mercaptoethanol, Sigma-Aldrich™
3x FLAG® Peptide, Sigma-Aldrich™
Acetic acid, Carl Roth GmbH
Adefodur developer solution, Adefo Chemie GmbH
Adefofix fixer solution, Adefo Chemie GmbH
Adenosintriphosphate (ATP), Sigma-Aldrich™
Agarose NEEO, Carl Roth GmbH
Albumin fraction V (BSA), Carl Roth GmbH
Ammoniumbicarbonate, Sigma-Aldrich™
Ammonium persulfate (APS), Carl Roth GmbH
Ampicillin, Carl Roth GmbH
ANTI-FLAG® M2 Affinity Gel, Sigma-Aldrich™
ANTI-HA Agarose, Sigma-Aldrich™
Aprotinin from bovine lung, Sigma-Aldrich™
Aqua, sterile B., Braun Melsungen AG
BES buffered saline, pH 7.1, Sigma-Aldrich™
Bio-Rad DC protein assay (Lowry assay)
Bortezomib 3.25 μM (pharmacy MRI, TUM)
Bromphenol blue, Sigma-Aldrich™
Buffer G, New England Biolabs®
Calcium chloride (CaCl₂), Sigma-Aldrich™
Chelex resin, Bio-Rad Laboratories
Coomassie Brilliant Blue, Carl Roth GmbH
Cycloheximide (CHX), Sigma-Aldrich™
Deoxynucleotide triphosphate (dNTP) mix (10mM), Thermo Scientific™
Dimethyl sulfoxide (DMSO), Carl Roth GmbH
DNA Loading Dye (6x), Thermo Scientific™
Ethanol, Merck Millipore

Ethidium bromide Carl Roth GmbH
Ethylenediaminetetraacetic acid (EDTA), Sigma-Aldrich™
FACS Flow, BD Biosciences
FLAG peptide, Sigma-Aldrich™
Gluthatione Sepharose™ 4B, GE Healthcare
Glycine, Carl Roth GmbH
Glycerol, Sigma-Aldrich™
Glycerol 2-phosphate disodium salt hydrate (G2P), Sigma-Aldrich™
HA-Ubiquitin-Vinyl Sulfone, Boston Biochem
HEPES, SERVA Electrophoresis GmbH
Hexanucleotide Mix (10x), Roche Diagnostics GmbH
Hoechst 33342 Thermo Scientific™
IL-8 Protein, PeproTech
Imidazole, Sigma-Aldrich™
Isopropanol, Carl Roth GmbH
Isopropyl β-D-1-thiogalactopyranoside (IPTG), Sigma-Aldrich™
L-Glutathione, Sigma-Aldrich™
Leupeptin, Sigma-Aldrich™
Lipofectamine™ 2000 Reagent, Thermo Scientific™
Lithium chloride, Sigma-Aldrich™
Lysozyme from chicken egg white, Sigma-Aldrich™
Magnesium chloride (MgCl₂), Sigma-Aldrich™
Methanol, J.T.Baker® Avantor™ Performance Materials
Nocodazole, Sigma-Aldrich™
NuPAGE® MES SDS Running Buffer, Invitrogen™
Ni-NTA-Agarose, QIAGEN
Okadaic acid, Sigma-Aldrich™
Paraformaldehyde (PFA), Sigma-Aldrich™
PBS Dulbecco powder, Biochrom Merck Millipore
Phenylmethylsulfonyl fluoride (PMSF), Sigma-Aldrich™
poly-D-lysine hydrobromide, Sigma-Aldrich™
Ponceau S solution, Sigma-Aldrich™
ProLong® GOLD antifade reagent with DAPI, Thermo Scientific™
Propidium iodide (PI), Sigma-Aldrich™
Protein A Sepharose CL-4B, GE Healthcare
Protein G Sepharose, Fast Flow, GE Healthcare
Protein Kinase Buffer, New England Biolabs®
Puromycin, Sigma-Aldrich™
RO-3306, Sigma-Aldrich™
Reparixin, Sigma-Aldrich™
Skim milk powder Sigma-Aldrich™
SlowFade Diamond Antifade Mountant, Thermo Scientific™
SOC medium, New England Biolabs®
Sodium acetate, Merck Millipore
Sodium azide (NaN₃), Merck Millipore
Sodium chloride (NaCl), Carl Roth GmbH
Sodium citrate, Sigma-Aldrich™
Sodium deoxycholate, Sigma-Aldrich™

Sodium dihydrogenphosphat, Merck Millipore
Sodium dodecylsulfate (SDS), SERVA Electrophoresis GmbH
Sodium fluoride (NaF), Sigma-Aldrich™
Sodium hydroxid (NaOH), Carl Roth GmbH
Sodium orthovanadate (Na₃VO₄), Sigma-Aldrich™
Soybean trypsin inhibitor, Sigma-Aldrich™
Strep-Tactin® Superflow 50%, IBA Life Sciences
Strep-tag® elution buffer (10x) with D-Desthiobiotin, IBA Life Sciences
Sucrose, Thermo Scientific™
SuperSignal® Stable Peroxide Solution, Thermo Scientific™
SuperSignal® Luminol/Enhancer Solution, Thermo Scientific™
Tetramethylethylenediamine (TEMED), Sigma-Aldrich™
Thymidine, Sigma-Aldrich™
Tosyl-L-lysyl-chloromethyl ketone hydrochloride (TLCK), Sigma-Aldrich™
Tosyl-phenylalanyl-chloromethyl ketone (TPCK), Sigma-Aldrich™
Trichloroacetic acid (TCA), Sigma-Aldrich™
Tris(hydroxymethyl)aminomethane (TRIS), Carl Roth GmbH
Tris buffered saline (TBS) (10X), Sigma-Aldrich™
Triton™ X-100, Sigma-Aldrich™
Trypan blue 0,4% solution, Gibco™
Trypsin inhibitor from soybean, Sigma-Aldrich™
Tween 20, Sigma-Aldrich™
Tween 80, Sigma-Aldrich™
Ubiquitin-AMC, Boston Biochem
Urea, Sigma-Aldrich™
WP1130, Sigma-Aldrich™
Z-VAD-FMK, Selleckchem

5.3 Consumables

3mm CHR paper Whatman TM, GE Healthcare
Cell Scraper, SARSTEDT AG
CELLSTAR® serological pipettes (5ml, 10ml, 25ml), Greiner Bio-One GmbH
CELLSTAR® sterile PP tube (15ml, 50ml), Greiner Bio-One GmbH
CL-XPosure™ Films, Thermo Scientific™
CryoPure Tubes with 1,6ml, SARSTEDT AG
CULTUBE™ sterile culture tube T406-2A, Simport®
Flexi-PCR-Tubes with 0,2ml, Kisker Biotech GmbH
LS Columns, Miltenyi Biotec
Pipette tips (10 µl, 200 µl, 1000µl), SARSTEDT AG
PVDF membrane (Immobilon® -P), Merck Millipore
Micro-fine insulin syringe, BD Medical
SafeSeal micro tubes (1,5ml, 2,0ml), SARSTEDT AG
Sterican® disposable needle (26Gx1“), B. Braun Melsungen AG

Syringe Injekt® (10ml), B. Braun Melsungen AG
Syringe filter 0,45 µm, TPP Techno Plastic Products
Tissue culture dish (100mm x 20mm), CORNING
Tissue culture dish (150mm x 20mm; 6-well), TPP Techno Plastic Products
UVette® cuvette (50-2000µl), Eppendorf AG
Vasofix® safety catheter, B. Braun Melsungen AG

5.4 Enzymes

Agel, Thermo Scientific™
BamHI, Thermo Scientific™
BbsI, Thermo Scientific™
Benzonase® Nuclease, Sigma-Aldrich™
CDK1-Cyclin B, Enzo Life Sciences AG
DNase I, Sigma-Aldrich™
DpnI, Thermo Scientific™
EcoRI, Thermo Scientific™
KpnI, Thermo Scientific™
NheI, Thermo Scientific™
NotI, Thermo Scientific™
Ribonuclease A, Sigma-Aldrich™
Pfu Ultra II DNA Polymerase, Agilent Technologies
Proteinase K, Thermo Scientific™
Q5 Polymerase, Thermo Scientific™
RNase A, Thermo Scientific™
Sall, Thermo Scientific™
SuperScript III Reverse Transcriptase, Invitrogen™ (Thermo Scientific™)
T4 DNA Ligase, Roche Diagnostics GmbH
XbaI, Thermo Scientific™
XhoI, Thermo Scientific™

5.5 Cell culture media and supplements

Bovine Serum (BS), Biochrom Merck Millipore
DMEM (Dulbecco's Modified Eagle's Medium), Gibco® Life Technologies™
Fetal Bovine Serum (FBS), Gold Biochrom Merck Millipore
GlutaMAX™ Supplement for McCoy's medium, Gibco® Life Technologies™
McCoy's (modified) Medium 5A, Gibco® Life Technologies™
Opti-MEM™ I reduced serum media, Invitrogen™
Phosphate buffered saline (PBS) used in 1:10 dilution sterile, Gibco® Life Technologies™

Penicillin/ Streptomycin used in 1:100 dilution, Gibco® Life Technologies™
Trypan Blue Stain (0,4%), Gibco® Life Technologies™
Trypsin-EDTA (10X) solution, Biochrom Merck Millipore

For SILAC experiments:

„heavy medium“: Arg-10 0.8 mM and Lys-8 0.4 mM

„medium medium“: Arg-6 and Lys-4

Medium SILANTES: 282986444 and 282946423

Proline 2 mM, Sigma-Aldrich™

5.6 Primary antibodies (dilution and company)

β -actin (1:5000, mouse, Sigma™ #A2228)

Caspase 3 (1:1000, rabbit, Cell Signaling® #9665)

Cleaved caspase 3 (1:500, rabbit, Cell Signaling® #9664)

CUL1 (1:500, mouse, Invitrogen® #32-2400)

Cyclin B1 (1:1000, mouse, Cell Signaling® #4138)

Cyclin E (1:1000, mouse, gift of M. Pagano)

FLAG (1:1000, rabbit, Sigma™ #F7425)

FLAG M2 (1:1000, mouse, Sigma™ #F3165)

HA-16B12 (1:1000, mouse, BioLegend® #901501)

pHH3 (serine 10; 1:500, rabbit, Cell Signaling® #9701)

IgG (2.5 μ g for ChIP, rabbit, Cell Signaling®, #2729)

PLK1 (1:500, rabbit, Invitrogen® #33-1700)

USP9X (for WB: 1:1000, rabbit, Bethyl Laboratorys® #A301-351A)

USP9X (for WB of U2-OS^{WT} or USP9X^{MUT} U2-OS cells: 1:1000, rabbit, Novus Biologicals® #NBP1-48321)

USP9X (for IF: 1:500, rabbit, Proteintech® #55054-1-AP)

WT1 (for WB: 1:1000, rabbit, Abcam #89901; for endogenous IP: rabbit, Cell Signaling® #83535; and for ChIP: 90 μ l per IP, rabbit, kind gift of Dr. Stefan Roberts)

PARP1 (1:1000, rabbit, Diagenode® #C15410245)

IL-8 (1:1000, mouse, R&D Systems® #MAB208)

5.7 Primary antibodies costume-made

USP9X phosphorylation on serine 2563 (1:1000, rabbit, custom-made by Innovagen®)

5.8 Secondary antibodies

anti-mouse IgG Alexa Fluor 488, Life Technologies
anti-mouse IgG Alexa Fluor 594, Life Technologies
anti-rabbit IgG Alexa Fluor 488, Life Technologies
anti-rabbit IgG Alexa Fluor 594, Life Technologies
anti-goat IgG, HRP-linked (#sc-2020), Santa Cruz Biotechnology ®

5.9 Kits

DNeasy Blood & Tissue Kits, Qiagen
DualGlo Luciferase Assay System, Promega
GeneJET™ Gel Extraction Kit, Thermo Scientific™
GeneJET™ PCR Purification Kit, Thermo Scientific™
Human IL-8 ELISA Kit, Proteintech
peqGOLD Plasmid Miniprep Kit, Peqlab Life Science
Plasmid Maxi Kit, Qiagen
Rapid DNA Dephos & Ligation Kit, Roche Diagnostics GmbH
RNeasy Mini Kit, Qiagen
Calibration Kit MWGF200, Sigma-Aldrich™
LightCycler 480 SYBR Green I Master, Roche Diagnostics GmbH

5.10 Primers

5.10.1 Primers used for quantitative RT-PCR

CDC14B forward 5'-GTGCCATTGCAGTACATT-3'

CDC14B reverse 5'-AGCAGGCTATCAGAGTG-3'

CXCL8 forward 5'-ATG ACT TCC AAG CTG GCC GTG GCT-3'

CXCL8 reverse 5'-TCT CAG CCC TCT TCA AAA ACT TCT-3'

RPLP0 forward 5'-GCACTGGAAGTCCAACACTTC-3'

RPLP0 reverse 5'-TGAGGTCCTCCTTGGTGAACAC-3'

HNRNPK forward 5'-AGCACTGCAGACGCCATTAT-3'

HNRNPK reverse 5'-AAACGGGCACACCAATCAGT-3'

5.10.2 Primers used for ChIP

CXCL8 prom forward 5'-AAGTGTGATGACTCAGGTTTGCC-3'

CXCL8 prom reverse 5'-GAGTGCTCCGGTGGCTTTTTA-3'

5.10.3 Primers used for luciferase reporter assay

CXCL8 forward 5'-CTGAGCCTCGAGAAATTATTTTAAAGATCAAAGAAAAC-3'

CXCL8 reverse 5'-GCTCAGAAGCTTTGTGCCTTATGGAGTGCTC-3'

5.10.4 Primers used for cloning of CDC14B

CDC14B forward 5'-CCGCTCGAGAAGCGGAAAAGCGAGCGGC-3'

CDC14B reverse 5'-CCGGGGCCCTTAACGCAAGACTGTTTTAGTCC-3'

5.10.5 Primers used for GST-USP9X constructs

USP9X forward 5'-GCCGGATCCGAAGTTTCAGAGCATGGGCGTCATTTAC-3'

USP9X_WT reverse 5'-GCCGTCGACCCTTGATCCTTGGTTTGAGGTG-3'

5.10.6 Primers used for USP9X S2563A mutagenesis PCR

USP9X mutagenesis forward

5'-GAAGGCAGTGAAGAAGTAGCCCCACCTCAAACCAAGGATC-3'

USP9X mutagenesis reverse

5'-GATCCTTGGTTTGAGGTGGGGCTACTTCTTCACTGCCTTC-3'

5.10.7 Primers used for cloning WT1 constructs

WT1 forward 5'-GCCGGTACCTCTGCAGGACCCGGCTTCCACGTGTG-3'

WT1 reverse 5'-GCCGCGGCCGCTCAAAGCGCCAGCTGGAGTTTGG-3'

5.10.8 Primers used for cloning 6xHis-Ubiquitin construct

Ubiquitin forward

5'-GCCACCGGTGCCACCATGCATCATCACCATCACACATGCAGA

TCTTCGTGAAAACCCTTACC-3'

Ubiquitin reverse 5'-GCCTCTAGACTAACCACCTCTCAGACGCAGG-3'

5.10.9 Primers for short hairpin RNA (shRNA)

USP9X shRNA 5'-GATGAGGAACCTGCATTTCCA-3'

5.10.10 Primers used as single guide RNA (sgRNA)

USP9X forward 5'-CACCGAGTATCCCCACCTCAAACCA-3'

USP9X reverse 5'-AAACTTGGTTTGAGGTGGGGATACTC-3'

5.10.11 Primers used for amplification of genomic DNA after genome editing

USP9X_Crispr_PCR_forward

5'-GGCCCATGTGCATGGACAGCCATATACAGGCC-3'

USP9X_Crispr_PCR_reverse

5'-GGCGATAAGACAGTGAATAAACTCTCCACTCCATGTTG-3'

5.11 Short interfering RNA

CDC14B (cat. no. L-003470-00), Thermo Scientific Dharmacon®

USP9X (cat. no. L-006099-00), Thermo Scientific Dharmacon®

WT1 (cat. no. L-009101-00; and cat. no. J-009101-08), Thermo Scientific Dharmacon®

CXCL8 (cat. no. L-004756-00), Thermo Scientific Dharmacon®

5.12 Plasmids

C-SF-TAP-pcDNA3.0, Prof. Dr. M.Ueffing (Gloeckner et al., 2007)

N-SF-TAP-pcDNA3.0 Prof. Dr. M.Ueffing (Gloeckner et al., 2007)

C-SF-TAP-pcDNA3.0-CDC14B, cloned by V. Fernandez-Saiz

pcDNA3.1-FLAG, Prof. Dr. F. Bassermann

pcDNA3.1-HA, Prof. Dr. F. Bassermann

pcDNA3.1-FLAG-USP9X^{WT}, cloned by K. Clemm von Hohenberg

pcDNA3.1-FLAG-USP9X^{S2563A}, cloned by K. Clemm von Hohenberg

pcDNA3.1-FLAG-WT1, cloned by M. Dietachmayr

pcDNA3.1-HA-WT1, cloned by M. Dietachmayr

pcDNA3.1-2xStrep-WT1, cloned by M. Dietachmayr

pSpCas9(BB)-2A-Puro (PX459) kind gift from F. Zhang

NanoLuc vector (pNL1.1) Promega (#N1001)

pGEX4T2-USP9X^{WT}-C-terminal fragment

pGEX4T2-USP9X^{S2563A}-C-terminal fragment

plenti puro 6xHis-Ubiquitin

5.13 Bacteria

BL21(DE3) Competent *E. coli*, New England Biolabs

NEB®-alpha Competent *E. coli*, New England Biolabs

5.14 Cell lines

HEK 293T human embryonic kidney cell line, ATCC (American Type Culture Collection) (CRL-3216)

U-2 OS, ATCC (American Type Culture Collection) HTB-96TM

A549, ATCC (American Type Culture Collection) CRM-CCL-185™

HeLa human cervix carcinoma cell line, ATCC (CCL-2)

5.15 Solutions and Buffer

Cell lysis buffer

Tris/HCl pH 7.5 50 mM
NaCl 250 mM
Ethylenediaminetetraacetic acid (EDTA) 1 mM
Triton X-100 0,1%
NaF 50 mM
Aprotinin 1 µg/ml
Leupeptin 1 µg/ml
Tosyl phenylalanyl chloromethyl ketone 10 µg/ml
Tosyl-L-lysyl-chloromethane hydrochloride 5 µg/m
Sodium orthovanadate 0.1 mM
DTT 1 mM
Glycerol-bisphosphate 10 mM
phenylmethylsulfonyl fluoride (PMSF) 0.1 mM

Cell lysis buffer for immunoprecipitation experiments

Tris/HCl pH 7.5 50 mM
NaCl 150 mM
EDTA 1 mM
NP40 0,1%
MgCl₂ 5 mM
Glycerol 5%
Aprotinin 1 µg/ml
Leupeptin 1 µg/ml
Tosyl phenylalanyl chloromethyl ketone 10 µg/ml
Tosyl-L-lysyl-chloromethane hydrochloride 5 µg/m
Sodium orthovanadate 0.1 mM
DTT 1 mM
Glycerol-bisphosphate 10 mM
Phenylmethylsulfonyl fluoride (PMSF) 0.1 mM

Cell lysis buffer for CHIP

HEPES pH 7.5 25 mM
NaCl 150 mM
EDTA 20 mM
NP40 0.5% (v/v)
1% Triton X-100
Aprotinin 1 µg/ml

Leupeptin 1 µg/ml
Tosyl phenylalanyl chloromethyl ketone 10 µg/ml
Tosyl-L-lysyl-chloromethane hydrochloride 5 µg/m
Sodium orthovanadate 0.1 mM
DTT 1 mM
Glycerol-bisphosphate 10 mM
Phenylmethylsulfonyl fluoride (PMSF) 0.1 mM

Cell lysis buffer for nuclei

HEPES pH 8.0 50 mM
NaCl 150 mM
EDTA 20 mM
NP40 1% (v/v)
Na deoxycholate 5% (w/v)

Lysis buffer for mass spectrometry

Tris/HCl pH 7.5 50 mM
NaCl 150mM
EDTA 1mM
NP40 0.1%
MgCl₂ 5 mM
Glycerol 5%
Aprotinin 1 µg/ml
Leupeptin 1 µg/ml
Tosyl phenylalanyl chloromethyl ketone 10 µg/ml
Tosyl-L-lysyl-chloromethane hydrochloride 5 µg/m
Sodium orthovanadate 0.1 mM
DTT 1 mM
Glycerol-bisphosphate 10 mM
Phenylmethylsulfonyl fluoride (PMSF) 0.1 mM

Protein kinase buffer

895µl aqua dest.
ATP 10mM 5µl
Protein Kinase Buffer (10X) 100µl

Urea cell lysis buffer

Urea 8 M
NaCl 300 mM
NP40 0.5%
Na₂HPO₄ 50 mM
Tris pH 8.0 50 mM
Imidazole 20 mM

Urea washing buffer A

Urea 8M
NaCl 300 mM
NP40 0,5%
Na₂HPO₄ 50 mM
Tris pH 6.3 50 mM

Urea washing buffer B

Urea 8 M
NaCl 300 mM
NP40 0.5%
Na₂HPO₄ 50 mM
Tris pH 6.3 50 mM
Imidazole 10 mM)

Cell lysis for in vivo ubiquitylation assay

Tris/HCl pH 7.5 50 mM
NaCl 250 mM
EDTA 1 mM
Triton X-100 0.1%
NaF 50 mM
Aprotinin 1 µg/ml
Leupeptin 1 µg/ml
Tosyl phenylalanyl chloromethyl ketone 10 µg/ml
Tosyl-L-lysyl-chloromethane hydrochloride 5 µg/m
Sodium orthovanadate 0.1 mM
DTT 1 mM
Glycerol-bisphosphate 10 mM
Phenylmethylsulfonyl fluoride (PMSF) 0.1 mM

Coomassie destaining buffer

45% methanol
10% acetic acid
50% aqua dest.

Coomassie staining

45% methanol
10% acetic acid
0.25% Coomassie brilliant blue

DUB buffer for DUB activity assay with Ubiquitin-AMC

Hepes 50mM
NaCl 100mM
EDTA 1mM

DTT 5mM
Tween 20 0,05%
MgCl₂ 5mM

DUB buffer for DUB activity assay with HA-Ubiquitin-VS

Tris/HCl pH 7.4 50 mM
MgCl₂ 5 mM
Sucrose 250 mM
DTT 1 mM
ATP 2 mM

Immunofluorescence buffer

PBS (1×)
0.5% Tween 20

Laemmli buffer

Tris/HCl pH 6.8 300 mM
50% glycerol
10% SDS
5% β-mercaptoethanol
0.05% bromphenolblue

GST-lysis buffer

Tris/HCl pH 8.0 20 mM
NaCl 100 mM
NP40 0.5%
EDTA 1 mM
PMSF 2 mM
Aprotinin 1 µg/ml
Leupeptin 1 µg/ml
Tosyl phenylalanyl chloromethyl ketone 10 µg/ml
Tosyl-L-lysyl-chloromethane hydrochloride 5 µg/m
Sodium orthovanadate 0.1 mM
DTT 1 mM
Glycerol-bisphosphate 10 mM 0.1 mM

Luria-Bertani (LB) medium

1% Bacto Tryptone
0.5% Bacto Yeast Extract
170 mM NaCl

Luria-Bertani (LB)-agar plates

LB medium
1.5% Bacto Aga

SDS separating gel buffer
1.5 M Tris pH 8.8

SDS stacking gel buffer
0.5 M Tris pH 6.8

SDS transfer buffer
48 mM Tris pH 7.5
39 mM glycine
20% methanol

Blocking buffer for Western Blot
PBS (1×)
0.1% Tween 20
5% skim milk powder

Washing buffer for Western Blot membranes
PBS (1×)
0.1% Tween 20

Stripping buffer for Western Blot membranes
62.5 mM Tris pH 6.8
0.867% β -Mercaptoethanol
2% SDS

6. Methods

6.1 Molecular biology

6.1.1 Polymerase chain reaction

Polymerase chain reaction (PCR) is a biochemical technique to amplify specific DNA fragments. The technique is based on oligonucleotides which anneal to a certain DNA fragment and which are further needed for amplification of this certain DNA by a thermostable DNA-polymerase.

For PCR reaction a reaction mix was prepared which contained 200 ng of template DNA, 10 pmol each of forward and reverse primers, 1 μ l dNTPs (10mM each), 1 μ l Pfu Ultra II DNA Polymerase and 5 μ l of the according 10 \times reaction buffer. The volume to 50 μ l was filled up with aqua disilled. The settings for the reaction were a denaturation temperature of 95 $^{\circ}$ C, annealing temperature depending on the sequence of the primers between 52-65 $^{\circ}$ C (meaning 5 $^{\circ}$ C lower than the melting temperature) and an amplification temperature of 72 $^{\circ}$ C for 30sec per 1000bp of DNA-fragment to be amplified.

6.1.2 Mutagenesis PCR

To generate a mutated version of a double-stranded DNA the technique of site-directed mutagenesis was applied. This technique is based on amplification of DNA in a polymerase chain reaction. The primers which are used are designed in a way to harbor a mutation of the gene of interest leading to a point mutation. Beside this, it would also be possible to generation insertions or deletion in a double-stranded DNA. The complementary primers which were used had a length of about 35-40 bp length. The primers were designed that the mutated base pair was flanked by about 15-20 compatible base pairs to the 5' and 3' ending of DNA.

For the PCR a reaction mix was prepared which contained 50ng of template cDNA. The rest of the mixture and the settings of the PCR was like above. Except the annealing temperature which was chosen about 10 $^{\circ}$ C lower than the melting temperature of the oligonucleotides. Afterwards, the PCR products were digested with 1 μ l DpnI which cleaves methylated DNA. In a next step, PCR products were run in a gel electrophoresis (6.1.11). PCR product of interest with expected size was cut out of gel and purified with the GeneJet Gel Extraction Kit (Thermo Scientific) according to the manual. Further, purified DNA was transformed into bacteria (6.1.9). Next, bacteria were plated on LB agar plates and incubated overnight. Growing clones were further picked for incubation, DNA was extracted and cDNA was sent for sequencing (6.1.10).

6.1.3 RNA extraction

For measuring mRNA amounts to evaluate gene expression of specific genes RNA needs to be extracted from eucaryotic cells. This was done with the RNeasy Mini Kit (Qiagen) following the manual.

6.1.4 Reverse transcription of mRNA into DNA

Reverse transcription is a method to produce cDNA out of mRNA depending on the reverse transcription activity of a transcriptase. The resulting cDNA can further be quantified by the technique of quantitative RT-PCR (6.1.5).

To product cDNA, 1µg extracted RNA (6.1.3) was incubated with oligo-dT primers at 42°C for 5min. Afterwards, polyA-tails, dNTPs and SuperScript III Reverse Transcriptase were added and incubated for 60min at 72°C for producing cDNA. The SuperScript III enzyme was deactivated by boiling reaction mix at 95°C for 10min.

6.1.5 Quantitative RT-PCR

Quantitative Real-time PCR (RT-PCR), is a PCR-based method to quantify DNA which was for example generated from mRNA. The technique is based on amplification of DNA by PCR using oligonucleotides of interest, a DNA Polymerase and a dye for double-stranded-DNA. In this case the LightCycler® 480 SYBR Green I Master containing SYBR Green was used which specifically binds to double-stranded amplicons. Fluorescence signal can be detected and correlates with the amount of synthesized DNA, therefore correlates with the initial DNA amount. The quantitative RT-PCR machine which was used for this experiment was a LightCycler 480 by Roche following the manufacturer's instructions. Each condition was performed in technical triplicates in a 96-well plate. The DNA which was used was a reverse transcribed cDNA from cells of the corresponding experiment.

Primers of target genes are listed in 5.10 and were either designed according to the internal laboratory standard or sequences used as in former publications. To normalized the input of total cDNA the reference genes RPLP0 and HNRNPK were amplified and measured.

6.1.6 Cloning

Cloning is a molecular method to generate recombinant DNA plasmids. First, DNA fragments (for example PCR-products) and the plasmid which should carry the new fragment are incubated with restriction enzymes, ligated and transformed into bacteria. Afterwards, bacteria can be grown and the plasmid of interest can be isolated from those bacteria.

6.1.7 Digestion of DNA

For cloning DNA, for example PCR products which were amplified before, into plasmid restriction enzymes were used. Those enzymes recognized and cut certain sequences in DNA. The result of cutting with restriction enzymes is a DNA fragment with one of two strands overhanging.

First of all, PCR product and 1µg of plasmid were incubated separately with specific restriction enzymes for 1h at 37°C. The reaction was incubated in a specific buffer fitting the corresponding enzyme.

6.1.8 Ligation

DNA ligation was performed using the Rapid DNA Dephos & Ligation Kit (Roche) according to the manufacturer's instructions. In brief, ligation was done with insert and vector at a ratio of 4:1 in weight. About 200ng of DNA insert and about 50-100ng of vector were used. The reaction mixture containing T4 ligase was filled up to 20µl and incubated for 5min at room temperature.

6.1.9 Transformation of DNA into bacteria and selection

Ligated DNA insert and vector were transformed into NEB® 5-alpha competent E. coli. To this end, 2µl of the ligation reaction mixture were used (6.1.8) and incubated it with 25µl of competent bacteria for 30min on ice. Afterwards, a heat shock was performed for 30 seconds at 42°C to increase the membrane permeability of bacteria to enhance uptake of the ligated vector and insert. Further, 200µl of SOC media were added to the bacteria for recovering for 1h at 37°C. Then, bacteria were plated on LB agar plates containing the antibiotic ampicillin and incubated at 37°C overnight. The plasmid which was transformed -beside the insert- encoded for a resistance gene against ampicillin. Therefore, it could be expected that only bacteria containing the plasmid can grow on the LB agar plates.

6.1.10 DNA isolation und test digestion

To identify a bacterial clone harboring the plasmid of interest several clones were picked and grown on the LB agar plate to culture them separately in 5ml LB liquid media overnight at 37°C shaking at 250rpm. DNA was extracted from those bacterial clones with the PeqGOLD Plasmid Miniprep Kit (Peqlab Life Science) following the manual. Afterwards, DNA was test-digested with restriction enzymes with the result of specific DNA fragments which were only obtained if our DNA of interest was inserted into the plasmid in the ligation process. DNA fragments were run in a gel electrophoresis as described below (6.1.11). If the DNA fragments were correct in the expected size, they were sent for sequencing with the respective primers.

6.1.11 Gel electrophoresis and gel purification

Agarose gel electrophoresis is a method to separate DNA in an electric field depending on the size of each DNA fragment or plasmid.

First of all, specific DNA was mixed with a 6x loading DNA dye. Further, DNA was loaded on a 1% agarose gel (1% agarose in 1xTBS buffer and supplemented with ethidium bromide) and an electric field was applied for separation using a Mini-Sub® Cell GT system for agarose electrophoresis. Afterwards, UV-light can be used to visualize ethidium bromide which has been added to the gel before and which interacts with the loaded DNA. The DNA size can be measured with a DNA ladder which was also initially loaded on the agarose gel.

6.2 Biochemical methods

6.2.1 Cell lysis

For cell lysis to extract cellular proteins and to obtain a whole cell lysate, cells were resuspended in 20-100µl cell lysis buffer supplemented with inhibitors (see 5.15). The amount of cell lysis buffer used depends on the number of cells used. After 20 min incubation on ice, samples were centrifuged for 20 min at 20,800 × g at 4 °C with a Cool-Centrifuge 5417R. Finally, supernatants were transferred into a new Eppendorf tube and protein concentrations of supernatants were measured with the colorimetric Bio-Rad DC protein assay based on the Lowry method (Lowry, Rosebrough et al. 1951). Afterwards, samples were mixed with 5x Laemmli and boiled for 5min at 95°C using a Thermo block MBT 250 before loading on an SDS-Gel in equal amounts for electrophoresis.

6.2.2 Cell lysis and co-Immunoprecipitation experiments

Immunoprecipitation (IP) is a biochemical method where specific cellular proteins are bound by a specific antibody after cell lysis. After further purification steps, interactions of immunoprecipitated proteins with co-immunoprecipitated proteins can be measured.

Proteins of interest can either be overexpressed in eukaryotic cells via transfecting cells with cDNA. If the protein is attached to a tag, this tag can be used depending on its amino acids for purification in immunoprecipitation experiments with the corresponding antibodies. These antibodies are mostly conjugated to agarose or sepharose beads. For immunoprecipitating endogenous proteins antibodies for the corresponding proteins can be applied and further bound by protein A or G antibodies which are conjugated to agarose or sepharose beads.

For cell lysis of immunoprecipitation experiments, cells were resuspended in 500- 1000µl of cell lysis buffer of immunoprecipitation experiments containing inhibitors. Samples were incubated on ice for 20 min and centrifuged for 20 min at 20,800 × g at 4 °C with a Cool-Centrifuge 5417R, supernatant was divided into samples for whole cell extract and for immunoprecipitation. The latter were incubated with 10µl corresponding beads for

1.5 hours at 4 °C rotating on a Rotating Wheel 3000. Before using the beads they were washed twice with PBS and 1 time with lysis buffer.

For immunoprecipitation of endogenous proteins, 1-3µg of the respective antibody were added to the cell lysate and rotated the sample for 1.5h at 4°C rotating on a Rotating Wheel 3000. Thereafter, 10 µl of protein A or G agarose or sepharose beads which were blocked with 5% BSA in PBS and washed 2 times with PBS were added.

Further, beads with the immunoprecipitated proteins were centrifuged for 2 min at 200 × g with a Cool-Centrifuge 5417R. Supernatant was removed and 1ml of cell lysis buffer as mentioned above was added to the beads. The tube was inverted several times and centrifuged for 2 min at 200 × g with a Cool-Centrifuge 5417R. These steps were repeated three times. Before loading samples on SDS gel for electrophoresis protein concentration of whole cell extracts were measured as described above (6.2.1) and mixed with 5x Laemmli Buffer. Beads with immunoprecipitated proteins were mixed with 50µl of 1x Laemmli Buffer. Finally, whole cell extracts and immunoprecipitates were incubated for 10min and 5 min at 95°C using a Thermo block MBT 250, respectively.

For SILAC-based ubiquitin purification a protocol for ubiquitin purification under denaturing conditions (Maine, Li et al. 2010) was slightly modified. First, cells were lysed in 7ml urea cell lysis buffer, resuspended 10 times and sonicated with the sonicator Digital Sonifier® 250D for 1 sec with an amplitude of 51% for 13 times with a pause of 1,5 seconds. Lysis was enhanced by aspiration lysates with a syringe. Next, samples were centrifuged for 20 min at 20,800 × g at 4 °C with a Cool-Centrifuge 5417R. Immediately after lysis, an aliquot of each sample was taken as whole cell extract and protein concentrations were measured. Afterward, the control knockdown and the USP9X knockdown of asynchronous and mitotic samples were combined using 22,5mg each to purify ubiquitinated proteins with 670µl Ni-NTA-Agarose (Qiagen). After rotating at 4 °C for 1.5 h on Rotating Wheel 3000, Ni-NTA-Agarose was centrifuged for 2 min at 200 × g with a Cool-Centrifuge 5417R, supernatant was removed, and 10ml lysis buffer was added. Ni-NTA-Agarose was then rotated at room temperature for 5 min in lysis buffer on a Tumbling roller mixer RM5, centrifuged for 2 min at 200 × g, and supernatant was again removed. These washing steps were repeated twice with urea washing buffer A and twice with urea washing buffer B adding 10ml each step. Finally, Ni-NTA beads were washed once with ammoniumbicarbonate 50 mM solution as described above prior to on-bead proteolysis and liquid chromatography–mass spectrometry (LC-MS)/MS analysis done by Christian Johannes Gloeckner.

6.2.3 In vivo ubiquitylation assay

For in vivo ubiquitylation cells were transfected with cDNA to express proteins with a double Strep-tag. After harvesting, cells were directly lysed without freezing in 200-500µl lysis buffer depending on the number of cells. Samples were resuspended several times, incubated for 10 min on ice and then centrifuged for 10 min at 20,800 × g at 4 °C using a Cool-Centrifuge 5417R. Subsequently supernatant was divided for precipitation experiment and for whole cell lysates. To 100µl of sample sodium dodecyl sulfate (SDS) and EDTA were added to a final concentrations of 1% and 5 mM, respectively. For denaturation, samples were boiled at 95 °C for 5 min using a Thermo block MBT 250. Afterwards, for quenching 900µl of lysis buffer containing 10 % of Triton X were added.

Hence, for affinity-based purification Strep-Tactin® Superflow® was washed twice in PBS and once in lysis buffer. Further, 10µl of Strep-Tactin® Superflow® were added to quenched proteins. Next, samples were incubated for 1.5 h rotating at 4 °C on a Rotating Wheel 3000. In a further step, purified proteins were centrifuged for 2 min at 200 × *g* with a Cool-Centrifuge 5417R. Supernatant was removed and 500-1000µl lysis buffer were added and the tube inverted. Afterwards, samples were centrifuged again like mentioned above and washing steps were repeated for 4 times. Finally, supernatant was removed, 30µl of 1x Laemmli were added and samples boiled at 95°C for 5 min.

6.2.4 SDS polyacrylamide gel electrophoresis (SDS-PAGE)

SDS polyacrylamide gel electrophoresis is a technique of biochemistry to separate proteins depending on their molecular weight. This can be established via loading proteins on a polyacrylamide gel containing SDS which coats proteins resulting in a negative charge of the proteins. When this gel is subjected to an electric field, proteins migrate depending on their weight, not their electric loading.

Separating gel with different concentrations of polyacrylamide were prepared depending on the proteins which were further analyzed for Western Blot. For a 10% separating gel, 4.8 ml of H₂O, 2.5 ml of 1,5 M Tris (pH 8.8), 2.5 ml of 40% acrylamide, 100 µl of 10% APS, 100 µl of 10% SDS and 4 µl TEMED were mixed. Further, gels were poured in specific chambers and allowed to polymerize in a gel caster. The stacking gel mixture was independent of further Western Blot analysis and consisted of 3 ml H₂O, 1.25 ml of 0.5 M Tris (pH 6.8), 550 µl acrylamide, 50 µl of 10% SDS and 10% APS and 5 µl TEMED. The gel was poured on top of the separating gel and polymerized. When separating and stacking gels were polymerized, proteins samples were loaded onto SDS-polyacrylamide gels. For measuring protein weight a molecular weight marker was also loaded. For whole cell lysates 15–25 µg protein per sample and slot were loaded, for immune- and affinity-based experiments between 10 and 30 µl of 1x Laemmli mixed with beads were loaded. Afterwards, for gel electrophoresis in running buffer a voltage of 80–120 V was applied using a PowerPac™ Basic power supply and a SDS gel electrophoresis chamber Mini-Protean. Following gel electrophoresis, proteins were transferred to a polyvinylidene difluoride (PVDF) membrane for further immunoblotting.

6.2.5 Western Blot or Immunoblot analysis

Western Blot analysis is a technique to detected proteins via a specific antibody-protein binding. First of all, proteins are separated by polyacrylamide gel electrophoresis as described above (6.2.4). In the next step, proteins are transferred from the polyacrylamide gel to a polyvinylidene difluoride (PVDF) membrane. This is established by applying an electric field of 30V overnight at 4°C in blotting buffer using a PowerPac™ Basic power supply and a Trans Blot Cell Blotting chamber. Next, to ensure proper transferring of proteins the whole membrane was dyed with Ponceau S. The following steps were destaining with washing buffer (WB) for 10 min and blocking unspecific antibody-binding to the membrane by incubating the membrane for 15min in blocking buffer, each done on a Polymax 1040 platform shaker. Afterwards, membranes were incubated with antibodies which specifically bind to proteins of interest diluted in 5% milk (dilutions described in 5.6)

for 1,5 hours at room temperature or overnight at 4°C on Tumbling roller mixer RM5. Then, membranes were washed 3 times with washing buffer on a Polymax 1040 platform shaker to remove any residual, non-binding first antibodies. Hence, membranes were incubated with antibodies coupled to HRP (horse radish peroxidase in a dilution of 1:5000 in 5% milk. Those HRP-coupled antibodies can bind the first antibodies in a specific way, depending on the species in which the first antibody was produced. Membranes were incubated for 30 min at room temperature on a Polymax 1040 platform shaker following washing of the membranes for 4 times 10 min each step with washing buffer. Developing was done by using enhanced chemiluminescence. We incubated membranes with HRP coupled antibodies with chemiluminescence substrates. HRP uses a chemical substrate to generate a luminescent signal that can be measured with photosensitive films. In a next step, luminescence can be measured by photosensitive films. Therefore, in a Hypercassettes™ films were brought in contact with luminescence emitting membranes and films were developed using the SRX-101A developer. For developing and fixing of films Adefodur developer solution and Adefofix fixer solution were used. The films were exposed to membranes depending on the luminescence signal to get a non-saturated signal. Quantification and normalization of Western Blot signal were done with the software ImageJ (image analysis software).

6.2.6 Reincubation of Western Blot membranes

For reincubation of Western Blot membranes with different antibodies previously bound antibodies had to be removed from the PVDF membrane. First, membranes were activated with methanol, incubated with distilled water for 1 min and further with stripping buffer at 65°C for 45min. Afterwards, membranes were washed 4 times 15min at room temperature on a Polymax 1040 platform shaker and blocked in 5% milk for 10min and incubated with a first antibody as described in 6.2.5.

6.2.7 Induction and purification of GST-tagged proteins

For in vitro assays with purified proteins the technique of GST-tagged protein purification was applied.

Initially two variants of cDNA coding for C-terminal truncated USP9X with the amino acids 2165 to 2570 were cloned into the vector pGEX-4T2 as described in 6.1.6. One variant encodes for truncated USP9X wildtype, the other one harbors alanine instead of serine on position 2563. This allowed to express a GST-tagged truncated version of USP9X in bacteria after transformation in *E. coli* BL21. The advantage of the vector pGEX-4T2 is that the gene of interest is under a LAC promoter, which is blocked by a Lac repressor molecule. Adding isopropyl β -D-1-thiogalactopyranoside (IPTG) can inhibit the repressor meaning expression of the coded protein.

To express GST-fused USP9X variants *E. coli* BL21 were transformed with the pGEX-4T2 vector coding for the USP9X variants. To this end, *E. coli* BL21 were thawed on ice, then 20 μ l of bacteria were mixed with 0,34 μ l β -mercaptoethanol and incubated for 10min on ice. Next, 50ng of plasmid were added and bacteria were slightly mixed. After 30min on ice, bacteria were heated shocked at 42°C for 45sec and again kept on ice for 2 minutes. Afterwards, 900 μ l of 42°C SOC medium were added followed by shaking 30min

at 37°C. Further, transformed bacteria were transferred into 5ml liquid LB media overnight at 37°C with 200rpm. This was called preculturing. Then the bacteria of preculture were diluted in 200ml LB liquid media in Erlenmeyer flasks without ampicillin and bacteria were grown until an optical density of 0,8 (OD₆₀₀). The OD₆₀₀ was measured with the NanoPhotometer®. When OD₆₀₀ of 0,8 was reached, IPTG was added to a final concentration of 1,5mM which induced protein expression in E. coli BL21 for 16 hours at 16°C at 200 rpm. Afterwards, bacteria were pelleted by centrifugation for 20 min at 4°C and pellets were frozen at -80°C.

For lysis of bacteria and following purification of the truncated GST-tagged USP9X protein the bacteria pellets were resuspended in NETN buffer. Afterwards, bacteria were incubated with lysozyme at a concentration of 100µg/ml and incubated for 40min at 4°C. Then, sonification with the sonicator Digital Sonifier® 250D followed with an amplitude of 51% for 1,1 seconds with a pause of 0,5 second. This step was repeated for 11 times. Next, lysates were centrifuged for 20min with 15300xg at 4°C. Then, for purification GST-tagged USP9X supernatants were incubated with Glutathione Sepharose 4B for 1,5 hours at 4 °C after Glutathione Sepharose 4B had been washed 3 times with NETN buffer. Finally, Glutathione Sepharose were centrifuged for 2min with 253xg and washed four times with GST lysis buffer as described above.

6.2.8 In vitro phosphorylation of USP9X by CDK1-Cyclin B

Freshly purified either GST-tagged C-terminal USP9X^{WT} (GST-USP9X_WT), USP9X^{S2563A} mutant (GST-USP9X_Mut) or control GST-protein (GST empty) were stored at 4°C in a 1:1 mixture of Glutathione Sepharose and NETN-Buffer. First, 100µl of purified proteins on Glutathione Sepharose were washed 2 times with PBS and once with Protein kinase buffer. Afterwards, 100µl of GST empty, GST-USP9X_WT or GST-USP9X_Mut were either incubated with 10 units of active CDK1-Cyclin B in 100µl protein kinase buffer or empty buffer. Next, samples were supplemented with 3 µCi [alpha-P32] ATP and incubated for 10 min at 30 °C. Reaction was stopped by adding 5x laemmli and heating samples to 95°C for 10 min. Afterwards, proteins were separated by SDS-PAGE in a 10% polyacrylamide SDS gel with 10mm thickness as described in 6.2.4. Hence, the polyacrylamide SDS gel was stained with Coomassie for 5min to visualize absolute protein amounts of GST-USP9X_WT and GST-USP9X_Mut followed by destaining for 5 min. Next, polyacrylamide gel was dried for 2h with a Gel dryer. Then polyacrylamide gels containing radioactive proteins were exposed to films for five days at -80 °C.

6.2.9 In vitro DUB activity assay using Ubiquitin-AMC

To measure in vitro activity of purified USP9X^{WT} and USP9X^{S2563A} we used the known and commercially available DUB substrate Ubiquitin-AMC. Enzymatic activity of a DUB, in our case of USP9X, leads to liberation of fluorogenic AMC. The fluorescence signal can be measured and therefore indicates indirectly the in vitro activity of a DUB (Dang, Melandri et al. 1998).

First of all, HEK 293T cells which expressed FLAG-tagged USP9X^{WT} or FLAG-tagged USP9X^{S2563A} were lysed in 500µl cell lysis buffer and incubated for 20min on ice. In this case, cell lysis buffer was supplemented with okadaic acid which is a phosphatase

inhibitor and which preserve USP9X^{WT} phosphorylation on serine 2563. Next, samples were centrifuged for 20 min at 20,800 × g at 4 °C with a Cool-Centrifuge 5417R. Further, supernatants were incubated with 10µl ANTI-FLAG® M2 for 1,5 hours at 4 °C rotating on a Rotating Wheel 3000. Afterwards, ANTI-FLAG® M2 were centrifuged for 2 min at 200 × g with a Cool-Centrifuge 5417R, supernatant was removed and 1ml of cell lysis buffer was added to remove any unspecifically bound proteins. Further, beads were centrifuged again like above and this washing step was repeated 4 times.

The next steps aimed to elute immunoprecipitated FLAG-tagged USP9X^{WT} and FLAG-tagged USP9X^{S2563A} from ANTI-FLAG® M2. Generally, in the process of elution FLAG peptide can be added to ANTI-FLAG® M2 which competes for binding to ANTI-FLAG® M2 with FLAG-tagged proteins to detached proteins of interest from the beads. In our case we added commercially available FLAG peptide to DUB Buffer (DB) in a concentration of 1mg/ml. Then 100µl of DB+ FLAG peptide were added to ANTI-FLAG® M2 and incubated for 10min on a Rotating Wheel 3000 at room temperature. Then, beads were centrifuged for 2 min at 200 × g with a tabletop centrifuge and supernatant containing eluted FLAG-tagged USP9X^{WT} and FLAG-tagged USP9X^{S2563A} protein was carefully transferred into a fresh tube. This step elution step was repeated once.

10µl of eluates of FLAG-tagged USP9X^{WT} and FLAG-tagged USP9X^{S2563A} proteins were boiled after adding 5x laemmli, SDS-PAGE was performed followed by Coomassie staining to obtain the exact protein amounts by quantification using the ImageJ software. For the final in vitro activity assay eluates of FLAG-tagged USP9X^{WT} and FLAG-tagged USP9X^{S2563A} proteins were diluted 1:10. Next, equal amounts of DUBs were plated on a flat bottom 96-well plate in technical triplicates and Ubiquitin-AMC was added in concentrations of 3µM, 1,5µM, 0,75µM, 0,365µM and 0,1825µM in order to calculate K_m and V_{max} . Per well we filled up reaction mixture to 30µl with DUB buffer. Fluorescence signal was measured every 5 min using the Promega GloMax® Discover Multimode Microplate Reader with an emission filter of 415-445 nm and an excitation filter of 365nm.

6.2.10 In vitro deubiquitination activity assay with HA-Ubiquitin-vinyl sulfone

HA-Ubiquitin-vinyl sulfone is a modified ubiquitin derivate to measure deubiquitination activity of a subset of DUBs. It is based on the detection of active DUBs by Western Blot that are irreversibly captured as soon as they act on the recombinant substrate HA(Hemagglutinin)-Ubiquitin-vinyl sulfone in vitro (Borodovsky, Kessler et al. 2001).

For assessment of USP9X activity HEK 293T cells were transfected with plasmid coding for FLAG-tagged USP9X^{WT} or FLAG-tagged USP9X^{S2563A} as described in 6.3.1 and the cells synchronized in S phase or mitosis as described in 6.3.3. After cells were harvested, samples were directly lysed in DUB buffer for activity assay with HA-Ubiquitin-VS for 20 min on ice, followed by centrifugation at 20,800 × g at 4 °C. Subsequently, supernatants were transferred into a fresh Eppendorf tube and protein concentrations of supernatants were measured. Further, equal amounts of total protein of each sample were transferred into an Eppendorf tube and either incubated with solvent or with human recombinant HA-Ubiquitin-vinyl sulfone (Boston Biochem) at a concentration of 5 µM at 37 °C for 45 min. After every 10 min incubation, reaction tubes were inverted several times and centrifuged for a few seconds. Thereafter, SDS was added to a final concentration of 1% followed by boiling samples at 95 °C for 5 min. Afterwards, samples were incubated at room temperature for 5 min. In the next step, 10µl of monoclonal Anti-HA Agarose were added

to each sample which had been washed 3x with PBS before. This led to immunoprecipitation of HA-Ubiquitin and indirectly precipitation of irreversibly bound FLAG-tagged USP9X^{WT} or FLAG-tagged USP9X^{S2563A} depending on its enzymatic activity. After 2h incubation at 4 °C on a Rotating Wheel 3000, beads were centrifuged for 2 min at 200 × g with a tabletop centrifuge and supernatant was discarded. Afterwards, 1ml of cell lysis buffer was added, the tube inverted several times and centrifuged for 2 min at 200 × g. This step was repeated 3 times and finally 50µl of 1x laemmli were added followed by boiling for 5min at 95°C.

6.3 Cell culture

HEK 293T, HeLa, and A549 cells were cultured in Dulbecco's modified Eagle's medium (DMEM), U2-OS cells were cultured in McCoy's medium which was supplemented with GlutaMAXTM. Both media were supplemented with either 10% bovine (HEK 293T) or 10% fetal bovine serum (HeLa, A549, and U2-OS), and 1% penicillin/streptomycin. Cell lines which are listed were tested negative for mycoplasma contamination. For incubation cells were cultured at 37°C with 5% CO₂ in a humidified incubator.

For cell counting in cell culture a Neubauer hemocytometer was used after 20µl of resuspended cells were diluted in 20µl of trypan blue.

6.3.1 Transfection of eukaryotic cells

In general, transfection is a method to transfer DNA or RNA, into a eukaryotic cell. Therefore, reagents or chemical are used which increase permeability of the cell membrane transiently to induced proper uptake of genomic material into a cell. In the experiments listed here advantage of two different techniques of transfection were taken.

First transfection method is based on the chemical calcium phosphate and was first described by Graham and van der Eb. Here, DNA precipitates with calcium phosphate which results in a suspension that enhances adsorption of DNA (Graham and van der Eb 1973). In detail plasmids to be transfected were added to 450µl of water in different amounts (3-20 µg). Afterwards, 50µl of CaCl₂ were added and resuspended several times and incubated for 5 min. Next, 500µl of BES [N,N-Bis-(2-hydroxyethyl)-2-aminoethanesulfonic acid) buffered in NaCl and Na₂HPO₄ to pH 7.1] were added during vortexing. After 20min at room temperature, DNA calcium phosphate precipitates were added to cells which were cultured on a 10cm cell culture dish in 10ml media.

The second method of transfection used is called lipofection. The principle of this technique was first described by Felgner et al. in 1987. Lipofection is based on a lipid-based reagent that interacts with DNA forming unilamellar liposomes which fuse with cellular membrane to ensure uptake of DNA (Felgner, Gadek et al. 1987).

In this case, the reagent LipofectamineTM 2000 was used. For transfection of cells on a 10cm cell culture dish with plasmid DNA 40µl of LipofectamineTM 2000 were mixed with 1ml Opti-MEMTM and incubated the mixture for 5min. In parallel 1ml Opti-MEMTM was supplemented with plasmid to be transfected. Depending on the experiment 10-20µg of

DNA were used. Afterwards, the Opti-MEM™ containing DNA and Opti-MEM™ containing Lipofectamine™ 2000 were mixed. After changing media of cells which should be transfected to penicillin/streptomycin-free medium and 20min incubation at room temperature the mixture was added to the cells. After 3 hours incubation medium was changed again to penicillin/streptomycin-free medium.

In general, cells were transfected as described in the corresponding experiment.

6.3.2 Transfection of eukaryotic cells with short interfering RNA (siRNA)

For siRNA experiments U2-OS or A549 cells were used. On day 0 about 5×10^5 cells were plated on a 10cm cell culture dish. On day 1 cell culture media was aspirated and cells were washed 2 times with DPBS to reduce transfection associated toxicity followed by adding 7ml of penicillin/streptomycin-free medium. Transfected siRNA was used in a final concentration of $2 \mu\text{M}$ and stored at -20°C . The mixture for transfection was prepared as described above (6.3.1). For single knockdown experiments of CDC14B and USP9X $62,5 \mu\text{l}$ of siRNA were used per 10cm cell culture dish. For double knockdown experiments of USP9X and WT1 $50 \mu\text{l}$ of USP9X siRNA and $6 \mu\text{l}$ of WT1 siRNA were used. For double knockdown experiments of WT1 and IL-8 amounts of siRNA were optimized to generate comparable proteins loss. For WT1 knockdown $40 \mu\text{l}$ of WT1 siRNA and for IL-8 knockdown $30 \mu\text{l}$ of IL-8 siRNA were used.

6.3.3 Cell cycle synchronization and drug treatment

To synchronize cells at the indicated cell cycle phases different chemicals were used.

First, the advantage of high thymidine concentration to block cells in S-phase was taken (Xeros 1962).

Second, the reversible microtubule inhibitor nocodazole was used to inhibit microtubule organization and depolymerization which further leads to arrest of cells in mitosis (Zieve, Turnbull et al. 1980).

For synchronization of U2-OS cells in mitosis cells were treated with thymidine at a final concentration of 2mM to inhibit cell cycle at the stage S-phase. For experiments with USP9X or CDC14B knockdown thymidine was added 24 h after small interfering RNA (siRNA) transfection, for experiments with WT1 or IL-8 knockdown thymidine was 16h before transfection. Twenty-four hours after adding thymidine medium was removed and 5-10ml of DPBS depending on dish size was added to cells which were incubated for 5-10 minutes. This step was repeated once again with DPBS and once with medium. Following washing steps medium supplemented with nocodazole at a final concentration of 400ng/ml was added for the indicated time as described in the corresponding experiment. If not otherwise specified, cells were treated with nocodazole for 14h.

Cells of experiments which were conducted with the IL-8 inhibitor reparixin at a concentration of $200 \mu\text{M}$ or IL-8 knockdown were synchronized differently. Cell were exposed either to nocodazole only for the indicated time or released from a thymidine blockage at G1/S-phase and collected by mitotic shake-off 13 hours later. Mitotic shake-off uses the advantage that mitotic cells lose proper attachment to cell culture dishes. Hence, mitotic cells can be shaken-off by application of vertical shear forces without mobilization of attached cells. To finally harvest mitotic cells medium containing mitotic

cells was centrifuged for 4 min with 288xg in a 15ml or 50ml Falcon, cells were resuspended in 1ml DPBS and transferred into a 1,5ml Eppendorf tube. Next, cells were pelleted for 1min at 20 000xg and supernatant was removed before cells were frozen at -80°C.

For harvesting non-mitotic HEK 293T cells, cells were mobilized by washing them off the cell culture dish in cell culture medium followed by the steps above. For adherent U2-OS cells a cell scraper was used.

For examination of USP9X phosphorylation on serine 2563 after double thymidine block U2-OS cells were plated on a 15cm diameter cell culture dish at a confluency of 25-30%. Next, medium which was supplemented with thymidine was added and cells grown for 24 hours. Then, medium was aspirated and to release cells from the thymidine block cells were washed once with medium and twice with DPBS as described above. Afterwards, cells were kept in usual cell culture medium for 12 hours before thymidine was added again for 24 hours. In the next step, cells were release as described above and collected at the indicated time points.

For analyzation of cells exiting mitosis, mitotic cells were shaken off as described above and carefully centrifuged for 3 min at 300 × g using a Multifuge 3SR+. Following centrifugation supernatant was aspirated, cells were resuspended in cell culture medium and incubated for 5 min. Then, cells were again centrifuged for 3 min at 300 × g and the steps before were repeated twice. To ensure proper exit of cells out of mitosis cells were finally grown on a 10cm cell culture dish in nocodazole-free medium. Harvesting using a cell scraper was done at the indicated time points.

To harvest mitotic cells that were further treated with different reagents in mitosis mitotic shake-off was done as described above and off-shaken cells were either directly harvested for time point “0” or further kept in cell culture medium which was supplemented with different drugs. For stability assays of WT1 in mitosis cells were treated with cycloheximide at a final concentration of 100 µg/ml. Cycloheximide can be used as an inhibitor of protein synthesis (Baliga, Pronczuk et al. 1969). Beside cycloheximide the proteasome inhibitor bortezomib was used to rescue WT1 from proteasomal degradation. Bortezomib is a reversible inhibitor of the 20S core subunit of the 26S proteasome (Lü and Wang 2013). For analyzing WT1 stability and to avoid cleavage of WT1 by caspase 3 the commercially available pan-caspase inhibitor Z-VAD-FMK was added at a concentration of 10µM were indicated (Ruan, Gao et al. 2018).

For experiments to investigate in vivo ubiquitylation of WT1 Z-VAD-FMK was added together with bortezomib at indicated concentrations 14 hours before collection of cells. This was performed to inhibit caspase dependent degradation of WT1 and for valid examination of proteasome-dependent WT1 degradation.

To inhibit the intracellular signaling pathway of IL-8 in cell culture the small molecular inhibitor repertaxin also called reparixin was used (Bertini, Allegretti et al. 2004). Therefore, on day 0 16×10^5 U2-OS cells were plated on a 15cm diameter cell culture dish and either DMSO or reparixin was added at a final concentration of 200µM. On day 2 nocodazole was added and mitotic shake-off was performed after 8 hours incubation for harvesting as described above.

For experiments to inhibit active transcription of IL-8 mRNA in mitotic cells actinomycin D was used which intercalates into DNA and further stalls RNA polymerase activation (Goldberg, Rabinowitz et al. 1962).

First, U2-OS cells were transfected with *control* or *WT1* siRNA as described above. On day 2 after transfection treatment of cells with nocodazole was performed for 17h hours. Afterwards, mitotic shake-off was done, cells were replated on a cell culture dish and grown in 3ml of medium. Next, cells were either treated with DMSO or with actinomycin D at a concentration of 7,5µM for 3 hours followed by harvesting of cells as described above.

To examine phosphorylation of USP9X on serine 2563 by CDK1 cells were treated with RO-3306 in cell culture. RO-3306 is a selective inhibitor of CDK1 (Vassilev, Tovar et al. 2006). In these experiments U2-OS cells were synchronized with thymidine as described in above. For detaching mitotic cells for further analysis we performed a mitotic shake-off as described above and kept cells in nocodazole supplemented medium. In a next step we added either DMSO or RO-3306 for specific CDK1 inhibition for 30 min before harvesting cells. The final concentration of RO-3306 was 9µM.

Treatment of cells with the DUB inhibitor WP1130 to analyzed WT1 stability was done the following way. First, cells were synchronized in mitosis with a sequential thymidine and nocodazole treatment as described in above. Then, mitotic shake-off was performed and cells were either harvested or treated either with DMSO or WP1130 for 3 hours before harvesting as described above.

6.3.4 Viral transduction of eukaryotic cells

Viral transduction is a powerful technique to express proteins in eukaryotic cells. Therefore, viral vectors are used to achieve integration of cDNA of interest into a eukaryotic genome which can lead to stable expression o specific proteins.

In our case, cDNA of interest was encoded by a lentiviral vector with the backbone pLenti carrying a gene for puromycin resistance. Vector pLenti puro was co-transfected with two further plasmids to ensure proper assembly of the virus. Those plasmids are called psPAX which encodes for the protein Gag-HIV and which is therefore needed for packaging and pMD2-G which encodes for VSV-G and which is therefore necessary for the envelope.

6.3.5 Generating HEK 293T cells stably expressing 6xHis-Ubiquitin

First, coding sequence of ubiquitin was cloned into the vector for lentiviral transduction pLenti using the enzymes Agel and XbaI as described in 6.1.6. The primers which were used for tagging the ubiquitin protein with a 6x His tag are listed in 5.10.

Second, lentivirus was produced by transfection of HEK 293T grown on a 10cm cell culture dish with 20µg of lentiviral plasmid, 15µg of plasmid psPAX and 5µg of plasmid pMD2-G. Therefore, the method of calcium phosphate was used as described in 6.3.1. After 4 hours of incubation, medium was changed and after further 48 hours medium containing the produced virus was filtered with a 0,45µm filter and frozen at -80°C.

To prepare cells for transduction HEK 293T cells were plated on a 10cm cell culture dish on day 0 at a confluency of 30%. After one day of passaging, the virus-containing medium

was thawed and supplemented with hexadimethrine bromide to a final concentration of 8µg/ml. Then, medium was added to cells which was counted as day 1. Hexadimethrine bromide is a chemical which is widely used to transduce cells with virus as it increases infection rate of cells by enhancing cell-virus interaction (Davis, Morgan et al. 2002). After 24 hours incubation, virus containing medium was aspirated and fresh medium was added (day 2). On day 3 medium which contained puromycin at a concentration of 1µg/ml was added. Puromycin is an inhibitor of protein synthesis and can be used to select for cells which carry a gene which induces puromycin resistance (Vara, Portela et al. 1986). In this case the vector pLenti is encoding for puromycin resistance. Cells were expanded and on day 7 puromycin was removed.

6.3.6 Preparation of cells for mass spectrometry in mitotic and asynchronous HEK 293T cells

For our mass spectrometric approach advantage of “SILAC” as metabolic labeling was taken (Ong and Mann 2007). This means that cell culture medium is supplemented with different isotopes of L-Lysine and L-Arginine. These amino acids are used for protein synthesis and can be further measured in mass spectrometry.

First, HEK 293T cells were kept in DMEM medium with differently labeled isotopes. Either cells were culture in DMEM which was supplemented with L-Lysine D₄ 0,4mM and L-Arginine ¹³C 0,8mM (DMEM “medium”) or in DMEM with L-Lysine ¹³C ¹⁵N 0,4mM and L-Arginine ¹³C ¹⁵N 0,8mM (DMEM “heavy”). Further, the amino acid proline was added to a final concentration of 2mM. Cells were kept in medium for 5 days until transfection. Then, cells were plated on a 15cm diameter cell culture dish and transfected with plasmids encoding for short hairpin against USP9X (shUSP9X) or control (shcontrol). Per plate 20µg of plasmids, 60µl of Lipofectamine™ 2000 and 3ml Opti-MEM™ was added and incubated for 4 hours. HEK 293T cells in DMEM “medium” were transfected with control short hairpin and HEK 293T cells culture in DMEM “heavy” were transfected with short hairpin against USP9X. On day 2 after transfection, to one half of shcontrol and shUSP9X nocodazole was added to synchronize cells as described in 6.3.3. The other half was kept asynchronous. After incubation for 11 hours, bortezomib was added in a final concentration of 65nM. Following 3,5 hours bortezomib treatment cells were harvested in ice cold PBS, centrifuged and frozen at -80°C.

6.3.7 Overexpression of FLAG-USP9X^{WT} or FLAG-USP9X^{S2563A} in HEK 293T cells for DUB activity assay using Ubiquitin-AMC or HA-Ubiquitin-vinyl sulfone

First, HEK 293T cells were plated on a 15cm diameter cell culture dish. On day 1 cells were transfected with 20µg plasmid encoding for FLAG-tagged USP9X^{WT} or FLAG-tagged USP9X^{S2563A} using 20µl Lipofectamine™ 2000 in 12ml penicillin/streptomycin free medium. On day 2 nocodazole was added in standard concentration and after 14 hours cells were harvested and directly processed.

6.3.8 Flow cytometry

Flow cytometry is a powerful method for a wide range of cell analyses on a single-cell level. The technique is based on measuring cell characteristics and properties by scattering of laser light by a single cell or measuring fluorescence signal emitted by antibodies or by cells expressing fluorescence emitting proteins.

In the experiments described flow cytometry for cell viability measurement was applied. Therefore, cells were stained in cell culture with the DNA intercalating reagent propidium iodide (PI). The method is based on the fact that PI is a membrane impermeant reagent and can only pass a cellular membrane if membrane becomes permeable for example in the process of apoptosis which can be further measure with flow cytometry (Nicoletti, Migliorati et al. 1991).

For flow cytometry cells were treated as described for the corresponding experiment. Further, mitotic shake-off was performed to collect mitotically arrested cells. Collected cells were centrifuged in a Multifuge 3SR+ and supernatant was removed. Afterwards, cells were slightly resuspended in 2ml DPBS for washing and centrifuged again. This step was repeated once. Then, 1ml of DPBS was added to cell pellet which were again resuspended followed by adding PI to a final concentration of 1µg/ml. Finally, cells were subjected flow cytometry using a CyAn ADP LxP8 cytometer to distinguish between PI-positive and PI-negative cells.

For analysis of raw data the software FlowJo was used. First, cell counts were depicting in a graph with the sideward scatter (SSC) for cell granularity on the x-axis. On the y-axis the forward scatter (FSC) is shown which represents cell size. Hence, cell debris could be excluded by proper gating for further analysis ("intact cells"). In a next step, absolute cell counts were blotted against the PI-signal which was measured in the FL3 channel of the cytometer.

6.3.9 Generation of USP9X mutated U2-OS cells (USP9X^{Mut}) using CRISPR/Cas9

The CRISPR/Cas9 system is a new and powerful method for genome editing. The microbial nuclease Cas9 can be expressed in mammalian cells and targeted to a specific genomic DNA sequence by transfecting a single guide RNA (sgRNA) consisting of a 20 nucleotides guide sequence. In consequence, Cas9 induces DNA double strand breaks that are repaired by non-homologous end joining (Ran, Hsu et al. 2013).

In the case of USP9X the aim was to disrupt the consensus motif for CDK1 phosphorylation in the protein USP9X.

First of all, sgRNA sequence was cloned into the Cas9-carrying vector pSpCas9(BB)-2A-Puro with a gene for puromycin resistance (PX459). Therefore, primers for sgRNA were annealed by mixing 1µl of each primer, adding 5µl of Buffer G and 43µl of water. Then, mixture was incubated at 95°C for 5min followed by 10min at 80°C and cooling down in a water bath which was initially heated to 80°C and kept at room temperature. In parallel, 1,5µg of plasmid were linearized by cutting with the enzyme BbsI at 37°C for 1 hour. The cut vector was run in a gel electrophoresis as described in 6.1.11. To extract the linear plasmid it was cut out of the gel and purified it with the GeneJET™ Gel Extraction Kit. 1µl of purified plasmid and 4µl of annealed oligonucleotides were ligated as described in 6.1.8 and further procedure of cloning was done as described in 6.1.9-10.

For expression of the plasmid encoding for Cas9 and the sgRNA nucleofection was conducted using in the Amaxa® cell line Nucleofector® Kit V. First, freshly thawed U2-OS

cells were detached from cell culture dishes for counting. This was achieved by aspirating the medium, washing the cells with 10ml DPBS and adding 1ml of 37°C warm trypsin. Cells are dissociated from the Petri dish after 5 min and were washed off the cell culture dish with 9ml medium. In the next step, cells were counted, 6×10^5 cells per transfection were centrifuged at 200xg for 5 min and supernatant was removed. Afterwards, solution V was mixed with the supplement of the Amaxa® cell line Nucleofector® Kit V and cell pellet was resuspended with 35µl of solution V with supplement. Then, cells were transferred into a Nucleovette chamber, nucleofected with 1,5µg vector using the program X-001 and replated in 1,5ml Penicillin/Streptomycin-free medium. On day 1 after transfection medium was removed and cells were incubated in medium which had been supplemented with puromycin in a concentration of 1µg/ml. Cells were grown under puromycin selection for 3 days. To ensure single cell expansion after genome editing and to avoid a polyclonal cell-cohort cell populations were expanded beginning with a single cell. Therefore, selected cells were trypsinated as described above, counted and diluted to a concentration of 0,5 cells/100µl medium. Next, 100µl of the respective medium was filled into each well of a 96-well plate to minimize risk of plating two cells per well. Afterwards, cells were grown for several passages and for validation of genome editing with disruption of CDK1 consensus site in the USP9X gene an aliquot of each cell population was harvested and genomic DNA using the DNeasy Blood & Tissue Kits was extracted following the manufacturer's instructions. Genomic DNA was subjected to polymerase chain reaction as described in 6.1.1 with specific oligonucleotides to amplify the genomic locus encoding for the CDK1 consensus motif. The amplicons of several clones were sent for sequencing to verify genome editing and the positive cellular clone was used for further experiments (USP9X^{Mut}). Genomic sequence of USP9X^{WT} and USP9X^{Mut} are depicted in Figure 41.

CDK1 consensus site

USP9X protein (C terminus)	WT: 2557 G S E E V S P P Q T K D Q Stop
	Mut: 2557 G S E E G S M K C T Stop

Figure 41 Generation of USP9X mutated U2-OS cells (USP9X^{Mut}) using CRISPR/Cas9 CRISPR/Cas9-mediated homozygous disruption of the CDK1 recognition site in USP9X generates U2-OS cells harboring a mutated USP9X gene encoding for a USP9X^{Mut} protein (bottom line). For comparison, the C-terminus of the wildtype USP9X protein (USP9X^{WT}) is depicted.

6.4 Biological assays

6.4.1 Enzyme-linked immunosorbent assay (ELISA) of IL-8 in cell culture supernatant

An enzyme-linked immunosorbent assay (ELISA) is a technique to measure the amount of soluble proteins and antigens based on antibodies. There are different variants of ELISA and the most common is the so-called sandwich ELISA. This variant of ELISA is characterized by antibodies which are immobilized on a respective plate and which can bind the protein of interest. Incubation with a second antibody results in binding to the

protein of interest on another epitope. In a next step, an enzyme-linked antibody can be added which recognizes and binds to the second antibody. Incubating the enzyme-linked antibody with an enzymatic substrate produces a detectable signal depending on the concentration of protein of interest. In our case, we used an ELISA measuring the concentration of IL-8 in cell culture supernatants.

Cells were treated as described in 6.3.3. After supernatants were collected, supernatants were frozen at -80°C until further analysis.

For analysis supernatants were thawed at room temperature and diluted 1:16, 1:50 and 1:100. Of each sample a total volume of 100 μl was analyzed as technical duplicate. The procedure was performed following the manufacturer's protocol. For final measurement absorbance at wave length at 450nm with a reference filter at a wave length of 600nm was measured. For absolute amounts of IL8 protein a standard curve was calculated followed by a linear regression.

6.4.2 Immunofluorescence

Immunofluorescence is a technique which has the potential to visualize cellular proteins in a widely structurally intact cell. It is based on binding of fluorochrome-coupled antibodies to specific proteins followed by fluorescence microscope.

In this case to ensure proper attachment of mitotic U2-OS cells to the cell culture chamber, cell culture chambers were coated with poly-D-lysine hydrobromide for 5 min followed by washing the chamber with distilled water. Afterwards cells were treated as described in 6.3.1.

In a first step cells were fixed by aspiration cell culture medium and adding 1,5ml methanol for 20 min at -20°C . Afterwards, methanol was aspirated and cells were carefully washed once with PBS and twice with IF buffer. Next, samples were incubated with primary antibodies that were diluted in IF buffer +1% FBS and incubated for 1.5 hours at room temperature shaking on a Polymax 1040 platform shaker. Final concentration of primary antibodies against USP9X or FLAG can be found in 5.6. In a next step antibodies were aspirated and samples were washed three times with 700 μl of IF buffer for about 5 minutes each step. Following, samples were incubated with secondary antibodies Alexa Fluor488 rabbit and Alexa Fluor594 goat at a dilution of 1:1000 for 1 hour on a Polymax 1040 platform shaker under protection of light. Antibodies were diluted in IF buffer +1% FBS. Then, antibodies were again aspirated and samples were washed twice with IF buffer and once with PBS. Further, DNA was stained using Hoechst 33342 in a concentration of 1 $\mu\text{g/ml}$ diluted in PBS and incubated for 15 min. After removing Hoechst 33342 cells were washed once with PBS, once with water and cells were mounted with SlowFade Diamond Antifade Mountant. Finally, samples were stored at 4°C under light protection. Images were taken using a Leica SP8 Confocal Laser Scanning Microscope.

To quantify colocalization of endogenous USP9X and FLAG-WT1 Fiji software was used calculating the Pearson's coefficient and the Manders' coefficients (tM1 and tM2) (Manders, Stap et al. 1992) (Pearson and Henrici 1896). The signal of USP9X or FLAG-WT1 was measured in different channels meaning channel 1 and 2. The value for tM1 is the intensity of all measured pixels from channel 1, in which the intensity for channel 2 is above unspecific background, divided by the total intensity from channel 1. The value for tM2 is the intensity of all measured pixels from channel 2, in which the intensity for channel

1 is above background, divided by the total intensity from channel 2. For channels 1 and 2 an automatically calculated threshold was applied.

6.4.3 Normalization of protein levels in Western Blot and statistical analysis

When not otherwise specified all experiments were performed in triplicates.

To visualize differences in protein levels or protein phosphorylation corresponding protein levels were normalized to a so called loading control. Those are proteins which levels are typically not regulated in response to cell cycle progression, are very stable independent of cell stimuli (for example CUL1 and β -actin) and which can be easily subjected to Western Blot followed by immunoblot analysis.

Immunoblot films were scanned using a Scanner V750 Pro and signal intensity of non-saturated protein bands were quantified using the software ImageJ. Afterwards values of quantified protein of interest were normalized to the associated loading control.

Protein quantification, mRNA levels or extracellular IL-8 were subjected to statistical analysis as mentioned in the corresponding experiment.

For statistical analysis the software GraphPad Prism was used. When two independent mean values were compared and statistically analyzed the one sample t-test or ratio paired t-test was applied. Having more than two mean values for statistical analysis one-way ANOVA was applied.

The bars shown in the graphs depict the calculated mean with standard deviation when not otherwise specified.

7. Literature

Afonso, O., C. M. Castellani, L. P. Cheeseman, J. G. Ferreira, B. Orr, L. T. Ferreira, J. J. Chambers, E. Morais-de-Sá, T. J. Maresca and H. Maiato (2019). "Spatiotemporal control of mitotic exit during anaphase by an aurora B-Cdk1 crosstalk." *eLife* **8**: e47646.

Agrawal, P., Y.-T. Chen, B. Schilling, B. W. Gibson and R. E. Hughes (2012). "Ubiquitin-specific Peptidase 9, X-linked (USP9X) Modulates Activity of Mammalian Target of Rapamycin (mTOR) *." *Journal of Biological Chemistry* **287**(25): 21164-21175.

Aguilera, M., M. Oliveros, M. Martínez-Padrón, J. A. Barbas and A. Ferrús (2000). "Ariadne-1: A Vital Drosophila Gene Is Required in Development and Defines a New Conserved Family of RING-Finger Proteins." *Genetics* **155**(3): 1231-1244.

Ahuja, S. K. and P. M. Murphy (1996). "The CX₂C Chemokines Growth-regulated Oncogene (GRO)₁, GRO₂, GRO₃, Neutrophil-activating Peptide-2, and Epithelial Cell-derived Neutrophil-activating Peptide-78 Are Potent Agonists for the Type B, but Not the Type A, Human Interleukin-8 Receptor *." *Journal of Biological Chemistry* **271**(34): 20545-20550.

Allan, L. A. and P. R. Clarke (2007). "Phosphorylation of caspase-9 by CDK1/cyclin B1 protects mitotic cells against apoptosis." *Mol Cell* **26**(2): 301-310.

Anger, M., W. A. Kues, J. Klima, M. Mielenz, M. Kubelka, J. Motlik, M. Esner, P. Dvorak, J. W. Carnwath and H. Niemann (2003). "Cell cycle dependent expression of Plk1 in synchronized porcine fetal fibroblasts." *Mol Reprod Dev* **65**(3): 245-253.

Azenshtein, E., T. Meshel, S. Shina, N. Barak, I. Keydar and A. Ben-Baruch (2005). "The angiogenic factors CXCL8 and VEGF in breast cancer: regulation by an array of pro-malignancy factors." *Cancer Letters* **217**(1): 73-86.

Azzam, R., S. L. Chen, W. Shou, A. S. Mah, G. Alexandru, K. Nasmyth, R. S. Annan, S. A. Carr and R. J. Deshaies (2004). "Phosphorylation by Cyclin B-Cdk Underlies Release of Mitotic Exit Activator Cdc14 from the Nucleolus." *Science* **305**(5683): 516-519.

Baliga, B. S., A. W. Pronczuk and H. N. Munro (1969). "Mechanism of cycloheximide inhibition of protein synthesis in a cell-free system prepared from rat liver." *J Biol Chem* **244**(16): 4480-4489.

Bansal, H., S. Bansal, M. Rao, K. P. Foley, J. Sang, D. A. Proia, R. K. Blackman, W. Ying, J. Barsoum, M. R. Baer, K. Kelly, R. Swords, G. E. Tomlinson, M. Battiwalla, F. J. Giles, K. P. Lee and S. Padmanabhan (2010). "Heat shock protein 90 regulates the expression of Wilms tumor 1 protein in myeloid leukemias." *Blood* **116**(22): 4591-4599.

Bansal, H., S. Bansal, M. Rao, K. P. Foley, J. Sang, D. A. Proia, R. K. Blackman, W. Ying, J. Barsoum, M. R. Baer, K. Kelly, R. Swords, G. E. Tomlinson, M. Battiwalla, F. J. Giles, K. P. Lee and S. Padmanabhan (2010). "Heat shock protein 90 regulates the expression of Wilms tumor 1 protein in myeloid leukemias." *Blood* **116**(22): 4591-4599.

Bardin, A. J. and A. Amon (2001). "Men and sin: what's the difference?" *Nat Rev Mol Cell Biol* **2**(11): 815-826.

Bassermann, F., D. Frescas, D. Guardavaccaro, L. Busino, A. Peschiaroli and M. Pagano (2008). "The Cdc14B-Cdh1-Plk1 Axis Controls the G2 DNA-Damage-Response Checkpoint." Cell **134**(2): 256-267.

Bassermann, F., D. Frescas, D. Guardavaccaro, L. Busino, A. Peschiaroli and M. Pagano (2008). "The Cdc14B-Cdh1-Plk1 axis controls the G2 DNA-damage-response checkpoint." Cell **134**(2): 256-267.

Berdougo, E., M. V. Nachury, P. K. Jackson and P. V. Jallepalli (2008). "The nucleolar phosphatase Cdc14B is dispensable for chromosome segregation and mitotic exit in human cells." Cell Cycle **7**(9): 1184-1190.

Bertini, R., M. Allegretti, C. Bizzarri, A. Moriconi, M. Locati, G. Zampella, M. N. Cervellera, V. Di Cioccio, M. C. Cesta, E. Galliera, F. O. Martinez, R. Di Bitondo, G. Troiani, V. Sabbatini, G. D'Anniballe, R. Anacardio, J. C. Cutrin, B. Cavalieri, F. Mainiero, R. Strippoli, P. Villa, M. Di Girolamo, F. Martin, M. Gentile, A. Santoni, D. Corda, G. Poli, A. Mantovani, P. Ghezzi and F. Colotta (2004). "Noncompetitive allosteric inhibitors of the inflammatory chemokine receptors CXCR1 and CXCR2: Prevention of reperfusion injury." Proceedings of the National Academy of Sciences of the United States of America **101**(32): 11791-11796.

Bohrer, L. R. and K. L. Schwertfeger (2012). "Macrophages Promote Fibroblast Growth Factor Receptor-Driven Tumor Cell Migration and Invasion in a Cxcr2-Dependent Manner." Molecular Cancer Research **10**(10): 1294-1305.

Borodovsky, A., B. M. Kessler, R. Casagrande, H. S. Overkleeft, K. D. Wilkinson and H. L. Ploegh (2001). "A novel active site-directed probe specific for deubiquitylating enzymes reveals proteasome association of USP14." The EMBO Journal **20**(18): 5187-5196.

Brat, D. J., A. C. Bellail and E. G. Van Meir (2005). "The role of interleukin-8 and its receptors in gliomagenesis and tumoral angiogenesis." Neuro-Oncology **7**(2): 122-133.

Brew, R., J. S. Erikson, D. C. West, A. R. Kinsella, J. Slavin and S. E. Christmas (2000). "INTERLEUKIN-8 AS AN AUTOCRINE GROWTH FACTOR FOR HUMAN COLON CARCINOMA CELLS IN VITRO." Cytokine **12**(1): 78-85.

Burke, L. J., R. Zhang, M. Bartkuhn, V. K. Tiwari, G. Tavoosidana, S. Kurukuti, C. Weth, J. Leers, N. Galjart, R. Ohlsson and R. Renkawitz (2005). "CTCF binding and higher order chromatin structure of the H19 locus are maintained in mitotic chromatin." The EMBO Journal **24**(18): 3291-3300.

Call, K. M., T. Glaser, C. Y. Ito, A. J. Buckler, J. Pelletier, D. A. Haber, E. A. Rose, A. Kral, H. Yeger, W. H. Lewis, C. Jones and D. E. Housman (1990). "Isolation and characterization of a zinc finger polypeptide gene at the human chromosome 11 Wilms' tumor locus." Cell **60**(3): 509-520.

Castedo, M., J.-L. Perfettini, T. Roumier, K. Andreau, R. Medema and G. Kroemer (2004). "Cell death by mitotic catastrophe: a molecular definition." Oncogene **23**(16): 2825-2837.

Cho, H. P., Y. Liu, M. Gomez, J. Dunlap, M. Tyers and Y. Wang (2005). "The dual-specificity phosphatase CDC14B bundles and stabilizes microtubules." Mol Cell Biol **25**(11): 4541-4551.

Curtis, N. L., G. F. Ruda, P. Brennan and V. M. Bolanos-Garcia (2020). "Deregulation of Chromosome Segregation and Cancer." Annual Review of Cancer Biology **4**(1): 257-278.

- Dang, L. C., F. D. Melandri and R. L. Stein (1998). "Kinetic and mechanistic studies on the hydrolysis of ubiquitin C-terminal 7-amido-4-methylcoumarin by deubiquitinating enzymes." Biochemistry **37**(7): 1868-1879.
- Davis, H. E., J. R. Morgan and M. L. Yarmush (2002). "Polybrene increases retrovirus gene transfer efficiency by enhancing receptor-independent virus adsorption on target cell membranes." Biophys Chem **97**(2-3): 159-172.
- De Larco, J. E., B. R. K. Wuertz, K. A. Rosner, S. A. Erickson, D. E. Gamache, J. C. Manivel and L. T. Furcht (2001). "A Potential Role for Interleukin-8 in the Metastatic Phenotype of Breast Carcinoma Cells." The American Journal of Pathology **158**(2): 639-646.
- Delcuve, G. P., S. He and J. R. Davie (2008). "Mitotic partitioning of transcription factors." J Cell Biochem **105**(1): 1-8.
- Deshaies, R. J. and C. A. P. Joazeiro (2009). "RING Domain E3 Ubiquitin Ligases." Annual Review of Biochemistry **78**(1): 399-434.
- Dey, A., A. Nishiyama, T. Karpova, J. McNally and K. Ozato (2009). "Brd4 marks select genes on mitotic chromatin and directs postmitotic transcription." Mol Biol Cell **20**(23): 4899-4909.
- Dominguez-Brauer, C., Kelsie L. Thu, Jacqueline M. Mason, H. Blaser, Mark R. Bray and Tak W. Mak (2015). "Targeting Mitosis in Cancer: Emerging Strategies." Molecular Cell **60**(4): 524-536.
- Dovat, S., T. Ronni, D. Russell, R. Ferrini, B. S. Cobb and S. T. Smale (2002). "A common mechanism for mitotic inactivation of C2H2 zinc finger DNA-binding domains." Genes Dev **16**(23): 2985-2990.
- Dryden, S. C., F. A. Nahhas, J. E. Nowak, A. S. Goustin and M. A. Tainsky (2003). "Role for human SIRT2 NAD-dependent deacetylase activity in control of mitotic exit in the cell cycle." Mol Cell Biol **23**(9): 3173-3185.
- Egli, D., G. Birkhoff and K. Eggan (2008). "Mediators of reprogramming: transcription factors and transitions through mitosis." Nature Reviews Molecular Cell Biology **9**(7): 505-516.
- Elliott, Paul R., Sofie V. Nielsen, P. Marco-Casanova, Berthe K. Fiil, K. Keusekotten, N. Mailand, Stefan M. V. Freund, M. Gyrd-Hansen and D. Komander (2014). "Molecular Basis and Regulation of OTULIN-LUBAC Interaction." Molecular Cell **54**(3): 335-348.
- Engel, K., M. Rudelius, J. Slawska, L. Jacobs, B. Ahangarian Abhari, B. Altmann, J. Kurutz, A. Rathakrishnan, V. Fernández-Sáiz, A. Brunner, B.-S. Targosz, F. Loewecke, C. J. Gloeckner, M. Ueffing, S. Fulda, M. Pfreundschuh, L. Trümper, W. Klapper, U. Keller, P. J. Jost, A. Rosenwald, C. Peschel and F. Bassermann (2016). "USP9X stabilizes XIAP to regulate mitotic cell death and chemoresistance in aggressive B-cell lymphoma." EMBO molecular medicine **8**(8): 851-862.
- Englert, C., S. Maheswaran, A. J. Garvin, J. Kreidberg and D. A. Haber (1997). "Induction of p21 by the Wilms' Tumor Suppressor Gene WT11." Cancer Research **57**(8): 1429-1434.
- Errico, A., K. Deshmukh, Y. Tanaka, A. Pozniakovsky and T. Hunt (2010). "Identification of substrates for cyclin dependent kinases." Adv Enzyme Regul **50**(1): 375-399.
- Espert, A., P. Uluocak, R. N. Bastos, D. Mangat, P. Graab and U. Gruneberg (2014). "PP2A-B56 opposes Mps1 phosphorylation of Knl1 and thereby promotes spindle assembly checkpoint silencing." Journal of Cell Biology **206**(7): 833-842.

Esposito, M., H. B. Akman, P. Giron, M. A. Ceregido, R. Schepers, L. C. Ramos Paez, E. La Monaca, J. De Greve, O. Coux, C. De Trez, C. Lindon and G. J. Gutierrez (2020). "USP13 controls the stability of Aurora B impacting progression through the cell cycle." Oncogene **39**(37): 6009-6023.

Felgner, P. L., T. R. Gadek, M. Holm, R. Roman, H. W. Chan, M. Wenz, J. P. Northrop, G. M. Ringold and M. Danielsen (1987). "Lipofection: a highly efficient, lipid-mediated DNA-transfection procedure." Proceedings of the National Academy of Sciences **84**(21): 7413-7417.

Fraile, J. M., V. Quesada, D. Rodríguez, J. M. P. Freije and C. López-Otín (2012). "Deubiquitinases in cancer: new functions and therapeutic options." Oncogene **31**(19): 2373-2388.

Freund, A., C. Chauveau, J.-P. Brouillet, A. Lucas, M. Lacroix, A. Licznar, F. Vignon and G. Lazennec (2003). "IL-8 expression and its possible relationship with estrogen-receptor-negative status of breast cancer cells." Oncogene **22**(2): 256-265.

Fu, X., W. Xie, X. Song, K. Wu, L. Xiao, Y. Liu and L. Zhang (2017). "Aberrant expression of deubiquitylating enzyme USP9X predicts poor prognosis in gastric cancer." Clinics and Research in Hepatology and Gastroenterology **41**(6): 687-692.

Galeano, F., C. Rossetti, S. Tomaselli, L. Cifaldi, M. Lezzerini, M. Pezzullo, R. Boldrini, L. Massimi, C. M. Di Rocco, F. Locatelli and A. Gallo (2013). "ADAR2-editing activity inhibits glioblastoma growth through the modulation of the CDC14B/Skp2/p21/p27 axis." Oncogene **32**(8): 998-1009.

Gales, D., C. Clark, U. Manne and T. Samuel (2013). "The Chemokine CXCL8 in Carcinogenesis and Drug Response." ISRN Oncol **2013**: 859154.

Gascoigne, K. E. and S. S. Taylor (2008). "Cancer Cells Display Profound Intra- and Interline Variation following Prolonged Exposure to Antimitotic Drugs." Cancer Cell **14**(2): 111-122.

Gessler, M., A. Poustka, W. Cavenee, R. L. Neve, S. H. Orkin and G. A. P. Bruns (1990). "Homozygous deletion in Wilms tumours of a zinc-finger gene identified by chromosome jumping." Nature **343**(6260): 774-778.

Gimbrone, M. A., M. S. Obin, A. F. Brock, E. A. Luis, P. E. Hass, C. A. Hébert, Y. K. Yip, D. W. Leung, D. G. Lowe, W. J. Kohr, W. C. Darbonne, K. B. Bechtol and J. B. Baker (1989). "Endothelial Interleukin-8: A Novel Inhibitor of Leukocyte-Endothelial Interactions." Science **246**(4937): 1601-1603.

Goldberg, I. H., M. Rabinowitz and E. Reich (1962). "Basis of actinomycin action. I. DNA binding and inhibition of RNA-polymerase synthetic reactions by actinomycin." Proceedings of the National Academy of Sciences of the United States of America **48**(12): 2094-2101.

Goto, H., Y. Tomono, K. Ajiro, H. Kosako, M. Fujita, M. Sakurai, K. Okawa, A. Iwamatsu, T. Okigaki, T. Takahashi and M. Inagaki (1999). "Identification of a novel phosphorylation site on histone H3 coupled with mitotic chromosome condensation." J Biol Chem **274**(36): 25543-25549.

Graham, F. L. and A. J. van der Eb (1973). "A new technique for the assay of infectivity of human adenovirus 5 DNA." Virology **52**(2): 456-467.

Guo, Y., Y. Zang, L. Lv, F. Cai, T. Qian, G. Zhang and Q. Feng (2017). "IL-8 promotes proliferation and inhibition of apoptosis via STAT3/AKT/NF- κ B pathway in prostate cancer Corrigendum in /10.3892/mmr.2019.9942." Mol Med Rep **16**(6): 9035-9042.

Hagting , A., N. den Elzen , H. C. Vodermaier , I. C. Waizenegger , J.-M. Peters and J. Pines (2002). "Human securin proteolysis is controlled by the spindle checkpoint and reveals when the APC/C switches from activation by Cdc20 to Cdh1." Journal of Cell Biology **157**(7): 1125-1137.

Hammes, A., J.-K. Guo, G. Lutsch, J.-R. Leheste, D. Landrock, U. Ziegler, M.-C. Gubler and A. Schedl (2001). "Two Splice Variants of the Wilms' Tumor 1 Gene Have Distinct Functions during Sex Determination and Nephron Formation." Cell **106**(3): 319-329.

Han, Y., S. San-Marina, J. Liu and M. D. Minden (2004). "Transcriptional activation of c-myc proto-oncogene by WT1 protein." Oncogene **23**(41): 6933-6941.

Hanahan, D. (2022). "Hallmarks of Cancer: New Dimensions." Cancer Discovery **12**(1): 31-46.

Harada, A., N. Sekido, T. Akahoshi, T. Wada, N. Mukaida and K. Matsushima (1994). "Essential involvement of interleukin-8 (IL-8) in acute inflammation." Journal of Leukocyte Biology **56**(5): 559-564.

Harrigan, J. A., X. Jacq, N. M. Martin and S. P. Jackson (2018). "Deubiquitylating enzymes and drug discovery: emerging opportunities." Nature Reviews Drug Discovery **17**(1): 57-78.

Hartmann, A., S. Hunot, P. P. Michel, M. P. Muriel, S. Vyas, B. A. Faucheux, A. Mouatt-Prigent, H. Turmel, A. Srinivasan, M. Ruberg, G. I. Evan, Y. Agid and E. C. Hirsch (2000). "Caspase-3: A vulnerability factor and final effector in apoptotic death of dopaminergic neurons in Parkinson's disease." Proc Natl Acad Sci U S A **97**(6): 2875-2880.

Hartwig, S., J. Ho, P. Pandey, K. MacIsaac, M. Taglienti, M. Xiang, G. Alterovitz, M. Ramoni, E. Fraenkel and J. A. Kreidberg (2010). "Genomic characterization of Wilms' tumor suppressor 1 targets in nephron progenitor cells during kidney development." Development **137**(7): 1189-1203.

Hastie, N. D. (2017). "Wilms' tumour 1 (WT1) in development, homeostasis and disease." Development **144**(16): 2862-2872.

Hayward, D., T. Alfonso-Pérez, M. J. Cundell, M. Hopkins, J. Holder, J. Bancroft, L. H. Hutter, B. Novak, F. A. Barr and U. Gruneberg (2019). "CDK1-CCNB1 creates a spindle checkpoint–permissive state by enabling MPS1 kinetochore localization." Journal of Cell Biology **218**(4): 1182-1199.

Heinemeyer, W., M. Fischer, T. Krimmer, U. Stachon and D. H. Wolf (1997). "The Active Sites of the Eukaryotic 20 S Proteasome and Their Involvement in Subunit Precursor Processing *." Journal of Biological Chemistry **272**(40): 25200-25209.

Henzel, M. J., Y. Wei, M. A. Mancini, A. Van Hooser, T. Ranalli, B. R. Brinkley, D. P. Bazett-Jones and C. D. Allis (1997). "Mitosis-specific phosphorylation of histone H3 initiates primarily within pericentromeric heterochromatin during G2 and spreads in an ordered fashion coincident with mitotic chromosome condensation." Chromosoma **106**(6): 348-360.

Hoffmann, E., O. Dittrich-Breiholz, H. Holtmann and M. Kracht (2002). "Multiple control of interleukin-8 gene expression." Journal of Leukocyte Biology **72**(5): 847-855.

Hornig, N. C., P. P. Knowles, N. Q. McDonald and F. Uhlmann (2002). "The dual mechanism of separase regulation by securin." Curr Biol **12**(12): 973-982.

Hu, M., P. Li, M. Li, W. Li, T. Yao, J.-W. Wu, W. Gu, R. E. Cohen and Y. Shi (2002). "Crystal Structure of a UBP-Family Deubiquitinating Enzyme in Isolation and in Complex with Ubiquitin Aldehyde." Cell **111**(7): 1041-1054.

- Huibregtse, J. M., M. Scheffner, S. Beaudenon and P. M. Howley (1995). "A family of proteins structurally and functionally related to the E6-AP ubiquitin-protein ligase." Proceedings of the National Academy of Sciences **92**(7): 2563-2567.
- Husnjak, K. and I. Dikic (2012). "Ubiquitin-Binding Proteins: Decoders of Ubiquitin-Mediated Cellular Functions." Annual Review of Biochemistry **81**(1): 291-322.
- Inoue, K., J. W. Slaton, S. J. Kim, P. Perrotte, B. Y. Eve, M. Bar-Eli, R. Radinsky and C. P. N. Dinney (2000). "Interleukin 8 Expression Regulates Tumorigenicity and Metastasis in Human Bladder Cancer1." Cancer Research **60**(8): 2290-2299.
- Janssen, A. and R. H. Medema (2011). "Mitosis as an anti-cancer target." Oncogene **30**(25): 2799-2809.
- Jaspersen, S. L., J. F. Charles and D. O. Morgan (1999). "Inhibitory phosphorylation of the APC regulator Hct1 is controlled by the kinase Cdc28 and the phosphatase Cdc14." Current Biology **9**(5): 227-236.
- Ji, M., S. Yang, Y. Chen, L. Xiao, L. Zhang and J. Dong (2012). "Phospho-regulation of KIBRA by CDK1 and CDC14 phosphatase controls cell-cycle progression." Biochem J **447**(1): 93-102.
- Jordan, M. A. and L. Wilson (2004). "Microtubules as a target for anticancer drugs." Nature Reviews Cancer **4**(4): 253-265.
- Kadauke, S. and G. A. Blobel (2013). "Mitotic bookmarking by transcription factors." Epigenetics & Chromatin **6**(1): 6.
- Kasahara, T., N. Mukaida, K. Yamashita, H. Yagisawa, T. Akahoshi and K. Matsushima (1991). "IL-1 and TNF-alpha induction of IL-8 and monocyte chemotactic and activating factor (MCAF) mRNA expression in a human astrocytoma cell line." Immunology **74**(1): 60-67.
- Katuri, V., S. Gerber, X. Qiu, G. McCarty, S. D. Goldstein, H. Hammers, E. Montgomery, A. R. Chen and D. M. Loeb (2014). "WT1 regulates angiogenesis in Ewing Sarcoma." Oncotarget **5**(9): 2436-2449.
- Kim, Y., J.-W. Choi, J.-H. Lee and Y.-S. Kim (2014). "Loss of CDC14B Expression in Clear Cell Renal Cell Carcinoma: Meta-Analysis of Microarray Data Sets." American Journal of Clinical Pathology **141**(4): 551-558.
- Knudson, A. G., Jr. and L. C. Strons (1972). "Mutation and Cancer: A Model for Wilms' Tumor of the Kidney2." JNCI: Journal of the National Cancer Institute **48**(2): 313-324.
- Komander, D. (2009). "The emerging complexity of protein ubiquitination." Biochemical Society Transactions **37**(5): 937-953.
- Komander, D., M. J. Clague and S. Urbé (2009). "Breaking the chains: structure and function of the deubiquitinases." Nature Reviews Molecular Cell Biology **10**(8): 550-563.
- Kouskouti, A. and I. Talianidis (2005). "Histone modifications defining active genes persist after transcriptional and mitotic inactivation." The EMBO Journal **24**(2): 347-357.
- Kreidberg, J. A., H. Sariola, J. M. Loring, M. Maeda, J. Pelletier, D. Housman and R. Jaenisch (1993). "WT-1 is required for early kidney development." Cell **74**(4): 679-691.
- Lee, K. Y., Y. J. Jeon, H. G. Kim, J. Ryu, D. Y. Lim, S. K. Jung, D. H. Yu, H. Chen, A. M. Bode and Z. Dong (2017). "The CUG-translated WT1, not AUG-WT1, is an oncogene." Carcinogenesis **38**(12): 1228-1240.

- Lee, S., K.-S. Lee, S. Huh, S. Liu, D.-Y. Lee, Seung H. Hong, K. Yu and B. Lu (2016). "Polo Kinase Phosphorylates Miro to Control ER-Mitochondria Contact Sites and Mitochondrial Ca²⁺ Homeostasis in Neural Stem Cell Development." Developmental Cell **37**(2): 174-189.
- Lee, S. B., K. Huang, R. Palmer, V. B. Truong, D. Herzlinger, K. A. Kolquist, J. Wong, C. Paulding, S. K. Yoon, W. Gerald, J. D. Oliner and D. A. Haber (1999). "The Wilms Tumor Suppressor WT1 Encodes a Transcriptional Activator of amphiregulin." Cell **98**(5): 663-673.
- Levine, M. S. and A. J. Holland (2018). "The impact of mitotic errors on cell proliferation and tumorigenesis." Genes & development **32**(9-10): 620-638.
- Li, D., X.-F. Ni, H. Tang, J. Zhang, C. Zheng, J. Lin, C. Wang, L. Sun and B. Chen (2020). "KRT17 Functions as a Tumor Promoter and Regulates Proliferation, Migration and Invasion in Pancreatic Cancer via mTOR/S6k1 Pathway." Cancer management and research **12**: 2087-2095.
- Liakopoulos, D., J. Kusch, S. Grava, J. Vogel and Y. Barral (2003). "Asymmetric loading of Kar9 onto spindle poles and microtubules ensures proper spindle alignment." Cell **112**(4): 561-574.
- Liu, S., C. Ginestier, S. J. Ou, S. G. Clouthier, S. H. Patel, F. Monville, H. Korkaya, A. Heath, J. Dutcher, C. G. Kleer, Y. Jung, G. Dontu, R. Taichman and M. S. Wicha (2011). "Breast Cancer Stem Cells Are Regulated by Mesenchymal Stem Cells through Cytokine Networks." Cancer Research **71**(2): 614-624.
- Lodhi, N., Y. Ji and A. Tulin (2016). "Mitotic bookmarking: maintaining post-mitotic reprogramming of transcription reactivation." Curr Mol Biol Rep **2**(1): 10-16.
- Lodhi, N., Y. Ji and A. Tulin (2016). "Mitotic Bookmarking: Maintaining Post-Mitotic Reprogramming of Transcription Reactivation." Current Molecular Biology Reports **2**(1): 10-15.
- Lopez, J. and S. W. G. Tait (2015). "Mitochondrial apoptosis: killing cancer using the enemy within." British Journal of Cancer **112**(6): 957-962.
- Lowry, O. H., N. J. Rosebrough, A. L. Farr and R. J. Randall (1951). "Protein measurement with the Folin phenol reagent." J Biol Chem **193**(1): 265-275.
- Lü, S. and J. Wang (2013). "The resistance mechanisms of proteasome inhibitor bortezomib." Biomarker Research **1**(1): 13.
- Luise, C., M. Capra, M. Donzelli, G. Mazzarol, M. G. Jodice, P. Nuciforo, G. Viale, P. P. Di Fiore and S. Confalonieri (2011). "An Atlas of Altered Expression of Deubiquitinating Enzymes in Human Cancer." PLOS ONE **6**(1): e15891.
- Maine, G. N., H. Li, I. W. Zaidi, V. Basrur, K. S. J. Elenitoba-Johnson and E. Burstein (2010). "A bimolecular affinity purification method under denaturing conditions for rapid isolation of a ubiquitinated protein for mass spectrometry analysis." Nature Protocols **5**(8): 1447-1459.
- Malumbres, M. (2014). "Cyclin-dependent kinases." Genome Biology **15**(6): 122.
- Manders, E. M., J. Stap, G. J. Brakenhoff, R. van Driel and J. A. Aten (1992). "Dynamics of three-dimensional replication patterns during the S-phase, analysed by double labelling of DNA and confocal microscopy." Journal of Cell Science **103**(3): 857-862.
- Manic, G., F. Corradi, A. Sistigu, S. Siteni and I. Vitale (2017). Chapter Four - Molecular Regulation of the Spindle Assembly Checkpoint by Kinases and Phosphatases. International Review of Cell and Molecular Biology. L. Galluzzi, Academic Press. **328**: 105-161.

- Marshall, R. S. and R. D. Vierstra (2019). "Dynamic Regulation of the 26S Proteasome: From Synthesis to Degradation." Frontiers in Molecular Biosciences **6**.
- Martínez-Balbás, M. A., A. Dey, S. K. Rabindran, K. Ozato and C. Wu (1995). "Displacement of sequence-specific transcription factors from mitotic chromatin." Cell **83**(1): 29-38.
- Martínez-Estrada, O. M., L. A. Lettice, A. Essafi, J. A. Guadix, J. Slight, V. Velecela, E. Hall, J. Reichmann, P. S. Devenney, P. Hohenstein, N. Hosen, R. E. Hill, R. Muñoz-Chapuli and N. D. Hastie (2010). "Wt1 is required for cardiovascular progenitor cell formation through transcriptional control of Snail and E-cadherin." Nature Genetics **42**(1): 89-93.
- Matsuoka, S., B. A. Ballif, A. Smogorzewska, E. R. McDonald, 3rd, K. E. Hurov, J. Luo, C. E. Bakalarski, Z. Zhao, N. Solimini, Y. Lerenthal, Y. Shiloh, S. P. Gygi and S. J. Elledge (2007). "ATM and ATR substrate analysis reveals extensive protein networks responsive to DNA damage." Science **316**(5828): 1160-1166.
- Mattiroli, F. and T. K. Sixma (2014). "Lysine-targeting specificity in ubiquitin and ubiquitin-like modification pathways." Nature Structural & Molecular Biology **21**(4): 308-316.
- Mayo, M. W., C.-Y. Wang, S. S. Drouin, L. V. Madrid, A. F. Marshall, J. C. Reed, B. E. Weissman and A. S. Baldwin (1999). "WT1 modulates apoptosis by transcriptionally upregulating the bcl-2 proto-oncogene." The EMBO Journal **18**(14): 3990-4003.
- Menke, A. L., A. J. van der Eb and A. G. Jochemsen (1998). The Wilms' Tumor 1 Gene: Oncogene or Tumor Suppressor Gene? International Review of Cytology. K. W. Jeon, Academic Press. **181**: 151-212.
- Middleton, A. J. and C. L. Day (2015). "The molecular basis of lysine 48 ubiquitin chain synthesis by Ube2K." Scientific Reports **5**(1): 16793.
- Miller, L. J., S. H. Kurtzman, Y. Wang, K. H. Anderson, R. R. Lindquist and D. L. Kreutzer (1998). "Expression of interleukin-8 receptors on tumor cells and vascular endothelial cells in human breast cancer tissue." Anticancer research **18**(1A): 77-81.
- Miller, M. D. and M. S. Krangel (1992). "Biology and biochemistry of the chemokines: a family of chemotactic and inflammatory cytokines." Critical reviews in immunology **12**(1-2): 17-46.
- Modi, W. S., M. Dean, H. N. Seuanez, N. Mukaida, K. Matsushima and S. J. O'Brien (1990). "Monocyte-derived neutrophil chemotactic factor (MDNCF/IL-8) resides in a gene cluster along with several other members of the platelet factor 4 gene superfamily." Human Genetics **84**(2): 185-187.
- Morgan, D. O. (1995). "Principles of CDK regulation." Nature **374**(6518): 131-134.
- Morris, J. R. and E. Solomon (2004). "BRCA1 : BARD1 induces the formation of conjugated ubiquitin structures, dependent on K6 of ubiquitin, in cells during DNA replication and repair." Human Molecular Genetics **13**(8): 807-817.
- Mouchantaf, R., B. A. Azakir, P. S. McPherson, S. M. Millard, S. A. Wood and A. Angers (2006). "The Ubiquitin Ligase Itch Is Auto-ubiquitylated *in Vivo* and *in Vitro* but Is Protected from Degradation by Interacting with the Deubiquitylating Enzyme FAM/USP9X *." Journal of Biological Chemistry **281**(50): 38738-38747.
- Moura, M., M. Osswald, N. Leça, J. Barbosa, A. J. Pereira, H. Maiato, C. E. Sunkel and C. Conde (2017). "Protein Phosphatase 1 inactivates Mps1 to ensure efficient Spindle Assembly Checkpoint silencing." eLife **6**: e25366.

- Murray, A. W. (2004). "Recycling the Cell Cycle: Cyclins Revisited." Cell **116**(2): 221-234.
- Murray, R. Z., L. A. Jolly and S. A. Wood (2004). "The FAM deubiquitylating enzyme localizes to multiple points of protein trafficking in epithelia, where it associates with E-cadherin and beta-catenin." Mol Biol Cell **15**(4): 1591-1599.
- Murray, R. Z., L. A. Jolly and S. A. Wood (2004). "The FAM Deubiquitylating Enzyme Localizes to Multiple Points of Protein Trafficking in Epithelia, where It Associates with E-cadherin and β -catenin." Molecular Biology of the Cell **15**(4): 1591-1599.
- Murtaza, M., L. A. Jolly, J. Gecz and S. A. Wood (2015). "La FAM fatale: USP9X in development and disease." Cellular and molecular life sciences : CMLS **72**(11): 2075-2089.
- Musacchio, A. (2011). "Spindle assembly checkpoint: the third decade." Philosophical Transactions of the Royal Society B: Biological Sciences **366**(1584): 3595-3604.
- Musacchio, A. (2015). "The Molecular Biology of Spindle Assembly Checkpoint Signaling Dynamics." Current Biology **25**(20): R1002-R1018.
- Nagai, H., T. Noguchi, K. Homma, K. Katagiri, K. Takeda, A. Matsuzawa and H. Ichijo (2009). "Ubiquitin-like Sequence in ASK1 Plays Critical Roles in the Recognition and Stabilization by USP9X and Oxidative Stress-Induced Cell Death." Molecular Cell **36**(5): 805-818.
- Naik, E. and V. M. Dixit (2016). "Usp9X Is Required for Lymphocyte Activation and Homeostasis through Its Control of ZAP70 Ubiquitination and PKC β Kinase Activity." J Immunol **196**(8): 3438-3451.
- Nakagama, H., G. Heinrich, J. Pelletier and D. E. Housman (1995). "Sequence and structural requirements for high-affinity DNA binding by the WT1 gene product." Molecular and Cellular Biology **15**(3): 1489-1498.
- Ng, R. K. and J. B. Gurdon (2008). "Epigenetic memory of an active gene state depends on histone H3.3 incorporation into chromatin in the absence of transcription." Nature Cell Biology **10**(1): 102-109.
- Nicoletti, I., G. Migliorati, M. C. Pagliacci, F. Grignani and C. Riccardi (1991). "A rapid and simple method for measuring thymocyte apoptosis by propidium iodide staining and flow cytometry." Journal of Immunological Methods **139**(2): 271-279.
- Nigg, E. A. (1991). "The substrates of the cdc2 kinase." Semin Cell Biol **2**(4): 261-270.
- Nijman, S. M. B., M. P. A. Luna-Vargas, A. Velds, T. R. Brummelkamp, A. M. G. Dirac, T. K. Sixma and R. Bernards (2005). "A Genomic and Functional Inventory of Deubiquitinating Enzymes." Cell **123**(5): 773-786.
- Nurse, P. (1990). "Universal control mechanism regulating onset of M-phase." Nature **344**(6266): 503-508.
- Ohtake, F., H. Tsuchiya, Y. Saeki and K. Tanaka (2018). "K63 ubiquitylation triggers proteasomal degradation by seeding branched ubiquitin chains." Proceedings of the National Academy of Sciences **115**(7): E1401-E1408.
- Ong, S. E. and M. Mann (2007). "Stable isotope labeling by amino acids in cell culture for quantitative proteomics." Methods Mol Biol **359**: 37-52.

- Palozola, K. C., G. Donahue, H. Liu, G. R. Grant, J. S. Becker, A. Cote, H. Yu, A. Raj and K. S. Zaret (2017). "Mitotic transcription and waves of gene reactivation during mitotic exit." Science **358**(6359): 119-122.
- Pearson, K. and O. M. F. E. Henrici (1896). "VII. Mathematical contributions to the theory of evolution.—III. Regression, heredity, and panmixia." Philosophical Transactions of the Royal Society of London. Series A, Containing Papers of a Mathematical or Physical Character **187**: 253-318.
- Petrone, A., M. E. Adamo, C. Cheng and A. N. Kettenbach (2016). "Identification of Candidate Cyclin-dependent kinase 1 (Cdk1) Substrates in Mitosis by Quantitative Phosphoproteomics." Molecular & cellular proteomics : MCP **15**(7): 2448-2461.
- Preisinger, C., R. Körner, M. Wind, W. D. Lehmann, R. Kopajtich and F. A. Barr (2005). "Plk1 docking to GRASP65 phosphorylated by Cdk1 suggests a mechanism for Golgi checkpoint signalling." Embo j **24**(4): 753-765.
- Prescott, D. M. and M. A. Bender (1962). "Synthesis of RNA and protein during mitosis in mammalian tissue culture cells." Experimental Cell Research **26**(2): 260-268.
- Primorac, I., J. R. Weir, E. Chirolì, F. Gross, I. Hoffmann, S. van Gerwen, A. Ciliberto and A. Musacchio (2013). "Bub3 reads phosphorylated MELT repeats to promote spindle assembly checkpoint signaling." eLife **2**: e01030.
- Quesada, V. c., A. Díaz-Perales, A. Gutiérrez-Fernández, C. Garabaya, S. Cal and C. López-Otín (2004). "Cloning and enzymatic analysis of 22 novel human ubiquitin-specific proteases." Biochemical and Biophysical Research Communications **314**(1): 54-62.
- Raman, D., T. Sobolik-Delmaire and A. Richmond (2011). "Chemokines in health and disease." Experimental Cell Research **317**(5): 575-589.
- Ran, F. A., P. D. Hsu, J. Wright, V. Agarwala, D. A. Scott and F. Zhang (2013). "Genome engineering using the CRISPR-Cas9 system." Nature Protocols **8**(11): 2281-2308.
- Reyes-Turcu, F. E., K. H. Ventii and K. D. Wilkinson (2009). "Regulation and cellular roles of ubiquitin-specific deubiquitinating enzymes." Annual review of biochemistry **78**: 363-397.
- Rhind, N. and P. Russell (2012). "Signaling pathways that regulate cell division." Cold Spring Harbor perspectives in biology **4**(10): a005942.
- Rossi, D. and A. Zlotnik (2000). "The Biology of Chemokines and their Receptors." Annual Review of Immunology **18**(1): 217-242.
- Rosso, L., A. C. Marques, M. Weier, N. Lambert, M.-A. Lambot, P. Vanderhaeghen and H. Kaessmann (2008). "Birth and Rapid Subcellular Adaptation of a Hominoid-Specific CDC14 Protein." PLOS Biology **6**(6): e140.
- Ruan, J., S. Gao, J. Yang, H. Li, H. Huang and X. Zheng (2018). "WT1 protein is cleaved by caspase-3 in apoptotic leukemic cells." Leuk Lymphoma **59**(1): 162-170.
- Ruan, J., S. Gao, J. Yang, H. Li, H. Huang and X. Zheng (2018). "WT1 protein is cleaved by caspase-3 in apoptotic leukemic cells." Leukemia & Lymphoma **59**(1): 162-170.
- Ruan, W., H. H. Lim and U. Surana (2019). "Mapping Mitotic Death: Functional Integration of Mitochondria, Spindle Assembly Checkpoint and Apoptosis." Frontiers in cell and developmental biology **6**: 177-177.

- Russo, R. C., C. C. Garcia, M. M. Teixeira and F. A. Amaral (2014). "The CXCL8/IL-8 chemokine family and its receptors in inflammatory diseases." Expert Rev Clin Immunol **10**(5): 593-619.
- Ryu, M. Y., S. K. Cho, Y. Hong, J. Kim, J. H. Kim, G. M. Kim, Y.-J. Chen, E. Knoch, B. L. Møller, W. T. Kim, M. F. Lyngkjær and S. W. Yang (2019). "Classification of barley U-box E3 ligases and their expression patterns in response to drought and pathogen stresses." BMC Genomics **20**(1): 326.
- Sarvaiya, P. J., D. Guo, I. Ulasov, P. Gabikian and M. S. Lesniak (2013). "Chemokines in tumor progression and metastasis." Oncotarget **4**(12): 2171-2185.
- Schott, A. F., L. J. Goldstein, M. Cristofanilli, P. A. Ruffini, S. McCanna, J. M. Reuben, R. P. Perez, G. Kato and M. Wicha (2017). "Phase Ib Pilot Study to Evaluate Reparixin in Combination with Weekly Paclitaxel in Patients with HER-2-Negative Metastatic Breast Cancer." Clin Cancer Res **23**(18): 5358-5365.
- Schraufstatter, I. U., J. Chung and M. Burger (2001). "IL-8 activates endothelial cell CXCR1 and CXCR2 through Rho and Rac signaling pathways." American Journal of Physiology-Lung Cellular and Molecular Physiology **280**(6): L1094-L1103.
- Schröder, J. M., M. Sticherling, H. H. Henneicke, W. C. Preissner and E. Christophers (1990). "IL-1 alpha or tumor necrosis factor-alpha stimulate release of three NAP-1/IL-8-related neutrophil chemotactic proteins in human dermal fibroblasts." J Immunol **144**(6): 2223-2232.
- Schwickart, M., X. Huang, J. R. Lill, J. Liu, R. Ferrando, D. M. French, H. Maecker, K. O'Rourke, F. Bazan, J. Eastham-Anderson, P. Yue, D. Dornan, D. C. S. Huang and V. M. Dixit (2010). "Deubiquitinase USP9X stabilizes MCL1 and promotes tumour cell survival." Nature **463**(7277): 103-107.
- Seaton, A., P. Scullin, P. J. Maxwell, C. Wilson, J. Pettigrew, R. Gallagher, J. M. O'Sullivan, P. G. Johnston and D. J. J. Waugh (2008). "Interleukin-8 signaling promotes androgen-independent proliferation of prostate cancer cells via induction of androgen receptor expression and activation." Carcinogenesis **29**(6): 1148-1156.
- Sherr, C. J. and J. M. Roberts (1995). "Inhibitors of mammalian G1 cyclin-dependent kinases." Genes Dev **9**(10): 1149-1163.
- Singh, J. K., B. M. Simões, S. J. Howell, G. Farnie and R. B. Clarke (2013). "Recent advances reveal IL-8 signaling as a potential key to targeting breast cancer stem cells." Breast Cancer Research **15**(4): 210.
- Soldani, C. and A. I. Scovassi (2002). "Poly(ADP-ribose) polymerase-1 cleavage during apoptosis: An update." Apoptosis **7**(4): 321-328.
- Srivastava, A., B. Fuchs, K. Zhang, M. Ruan, C. Halder, E. Mahlum, K. Weber, M. E. Bolander and G. Sarkar (2006). "High WT1 Expression Is Associated with Very Poor Survival of Patients with Osteogenic Sarcoma Metastasis." Clinical Cancer Research **12**(14): 4237-4243.
- Stegeman, S., L. A. Jolly, S. Premarathne, J. Gecz, L. J. Richards, A. Mackay-Sim and S. A. Wood (2013). "Loss of Usp9x Disrupts Cortical Architecture, Hippocampal Development and TGFβ-Mediated Axonogenesis." PLOS ONE **8**(7): e68287.
- Sudakin, V., G. K. T. Chan and T. J. Yen (2001). "Checkpoint inhibition of the APC/C in HeLa cells is mediated by a complex of BUBR1, BUB3, CDC20, and MAD2." Journal of Cell Biology **154**(5): 925-936.

- Swatek, K. N. and D. Komander (2016). "Ubiquitin modifications." Cell Research **26**(4): 399-422.
- Tanenbaum, M. E., N. Stern-Ginossar, J. S. Weissman and R. D. Vale (2015). "Regulation of mRNA translation during mitosis." Elife **4**.
- Tanguay, P. L., G. Rodier and S. Meloche (2010). "C-terminal domain phosphorylation of ERK3 controlled by Cdk1 and Cdc14 regulates its stability in mitosis." Biochem J **428**(1): 103-111.
- Teichner, A., E. Eytan, D. Sitry-Shevah, S. Miniowitz-Shemtov, E. Dumin, J. Gromis and A. Hershko (2011). "p31^{comet} promotes disassembly of the mitotic checkpoint complex in an ATP-dependent process." Proceedings of the National Academy of Sciences **108**(8): 3187-3192.
- Terrano, D. T., M. Upreti and T. C. Chambers (2010). "Cyclin-Dependent Kinase 1-Mediated Bcl-x_L/Bcl-2 Phosphorylation Acts as a Functional Link Coupling Mitotic Arrest and Apoptosis." Molecular and Cellular Biology **30**(3): 640-656.
- Théard, D., F. Labarrade, M. Partisani, J. Milanini, H. Sakagami, E. A. Fon, S. A. Wood, M. Franco and F. Luton (2010). "USP9x-mediated deubiquitination of EFA6 regulates de novo tight junction assembly." The EMBO Journal **29**(9): 1499-1509.
- Trautmann, S. and D. McCollum (2002). "Cell Cycle: New Functions for Cdc14 Family Phosphatases." Current Biology **12**(21): R733-R735.
- Trinkle-Mulcahy, L., S. v. Boulon, Y. W. Lam, R. Urcia, F. o.-M. Boisvert, F. Vandermoere, N. A. Morrice, S. Swift, U. Rothbauer, H. Leonhardt and A. Lamond (2008). "Identifying specific protein interaction partners using quantitative mass spectrometry and bead proteomes." Journal of Cell Biology **183**(2): 223-239.
- Tumurbaatar, I., O. Cizmecioglu, I. Hoffmann, I. Grummt and R. Voit (2011). "Human Cdc14B promotes progression through mitosis by dephosphorylating Cdc25 and regulating Cdk1/cyclin B activity." PloS one **6**(2): e14711-e14711.
- Tuna, M., A. Chavez-Reyes and A. M. Tari (2005). "HER2/neu increases the expression of Wilms' Tumor 1 (WT1) protein to stimulate S-phase proliferation and inhibit apoptosis in breast cancer cells." Oncogene **24**(9): 1648-1652.
- Vara, J. A., A. Portela, J. Ortín and A. Jiménez (1986). "Expression in mammalian cells of a gene from *Streptomyces alboniger* conferring puromycin resistance." Nucleic Acids Res **14**(11): 4617-4624.
- Vassilev, L. T., C. Tovar, S. Chen, D. Knezevic, X. Zhao, H. Sun, D. C. Heimbrosk and L. Chen (2006). "Selective small-molecule inhibitor reveals critical mitotic functions of human CDK1." Proceedings of the National Academy of Sciences **103**(28): 10660-10665.
- Veleceta, V., L. A. Lettice, Y.-Y. Chau, J. Slight, R. L. Berry, A. Thornburn, Q. D. Gunst, M. van den Hoff, M. Reina, F. O. Martínez, N. D. Hastie and O. M. Martínez-Estrada (2013). "WT1 regulates the expression of inhibitory chemokines during heart development." Human Molecular Genetics **22**(25): 5083-5095.
- Venkatakrishnan, G., R. Salgia and J. E. Groopman (2000). "Chemokine Receptors CXCR-1/2 Activate Mitogen-activated Protein Kinase via the Epidermal Growth Factor Receptor in Ovarian Cancer Cells *." Journal of Biological Chemistry **275**(10): 6868-6875.
- Verma, R., R. Oania, J. Graumann and R. J. Deshaies (2004). "Multiubiquitin Chain Receptors Define a Layer of Substrate Selectivity in the Ubiquitin-Proteasome System." Cell **118**(1): 99-110.

Vij, N., M. O. Amoako, S. Mazur and P. L. Zeitlin (2008). "CHOP transcription factor mediates IL-8 signaling in cystic fibrosis bronchial epithelial cells." Am J Respir Cell Mol Biol **38**(2): 176-184.

Visintin, R., K. Craig, E. S. Hwang, S. Prinz, M. Tyers and A. Amon (1998). "The Phosphatase Cdc14 Triggers Mitotic Exit by Reversal of Cdk-Dependent Phosphorylation." Molecular Cell **2**(6): 709-718.

Wada, K. and T. Kamitani (2006). "UnpEL/Usp4 is ubiquitinated by Ro52 and deubiquitinated by itself." Biochemical and Biophysical Research Communications **342**(1): 253-258.

Wang, F. and J. M. G. Higgins (2013). "Histone modifications and mitosis: countermarks, landmarks, and bookmarks." Trends in Cell Biology **23**(4): 175-184.

Wang, K., B. Sturt-Gillespie, J. C. Hittle, D. Macdonald, G. K. Chan, T. J. Yen and S.-T. Liu (2014). "Thyroid Hormone Receptor Interacting Protein 13 (TRIP13) AAA-ATPase Is a Novel Mitotic Checkpoint-silencing Protein *." Journal of Biological Chemistry **289**(34): 23928-23937.

Watson, E. R., N. G. Brown, J.-M. Peters, H. Stark and B. A. Schulman (2019). "Posing the APC/C E3 Ubiquitin Ligase to Orchestrate Cell Division." Trends in Cell Biology **29**(2): 117-134.

Wei, Z., S. Peddibhotla, H. Lin, X. Fang, M. Li, J. M. Rosen and P. Zhang (2011). "Early-Onset Aging and Defective DNA Damage Response in *Cdc14b*-Deficient Mice." Molecular and Cellular Biology **31**(7): 1470-1477.

Wickliffe, K. E., A. Williamson, H.-J. Meyer, A. Kelly and M. Rape (2011). "K11-linked ubiquitin chains as novel regulators of cell division." Trends in Cell Biology **21**(11): 656-663.

Wong, M. M., J. S. Byun, M. Sacta, Q. Jin, S. Baek and K. Gardner (2014). "Promoter-bound p300 complexes facilitate post-mitotic transmission of transcriptional memory." PLoS One **9**(6): e99989.

Wu, C., W. Zhu, J. Qian, S. He, C. Wu, Y. Chen and Y. Shu (2013). "WT1 Promotes Invasion of NSCLC via Suppression of CDH1." Journal of Thoracic Oncology **8**(9): 1163-1169.

Wurzenberger, C. and D. W. Gerlich (2011). "Phosphatases: providing safe passage through mitotic exit." Nature Reviews Molecular Cell Biology **12**(8): 469-482.

Xeros, N. (1962). "Deoxyriboside Control and Synchronization of Mitosis." Nature **194**(4829): 682-683.

Xing, H., D. C. Wilkerson, C. N. Mayhew, E. J. Lubert, H. S. Skaggs, M. L. Goodson, Y. Hong, O. K. Park-Sarge and K. D. Sarge (2005). "Mechanism of hsp70i gene bookmarking." Science **307**(5708): 421-423.

Yang, B., S. Zhang, Z. Wang, C. Yang, W. Ouyang, F. Zhou, Y. Zhou and C. Xie (2016). "Deubiquitinase USP9X deubiquitinates β -catenin and promotes high grade glioma cell growth." Oncotarget **7**(48): 79515-79525.

Yang, L., Y. Han, F. Saurez Saiz and M. D. Minden (2007). "A tumor suppressor and oncogene: the WT1 story." Leukemia **21**(5): 868-876.

Yang, Q., J. Zhao, D. Chen and Y. Wang (2021). "E3 ubiquitin ligases: styles, structures and functions." Molecular biomedicine **2**(1): 23-23.

Ye, Y., B. Raychaudhuri, A. Gurney, C. E. Campbell and B. R. Williams (1996). "Regulation of WT1 by phosphorylation: inhibition of DNA binding, alteration of transcriptional activity and cellular translocation." The EMBO journal **15**(20): 5606-5615.

- Yellman, C. M. and G. S. Roeder (2015). "Cdc14 Early Anaphase Release, FEAR, Is Limited to the Nucleus and Dispensable for Efficient Mitotic Exit." PLOS ONE **10**(6): e0128604.
- Yoon, S., E. Parnell and P. Penzes (2020). "TGF- β -Induced Phosphorylation of Usp9X Stabilizes Ankyrin-G and Regulates Dendritic Spine Development and Maintenance." Cell Rep **31**(8): 107685.
- Young, D. W., M. Q. Hassan, J. Pratap, M. Galindo, S. K. Zaidi, S.-h. Lee, X. Yang, R. Xie, A. Javed, J. M. Underwood, P. Furcinitti, A. N. Imbalzano, S. Penman, J. A. Nickerson, M. A. Montecino, J. B. Lian, J. L. Stein, A. J. van Wijnen and G. S. Stein (2007). "Mitotic occupancy and lineage-specific transcriptional control of rRNA genes by Runx2." Nature **445**(7126): 442-446.
- Zaidi, S. K., J. B. Lian, A. van Wijnen, J. L. Stein and G. S. Stein (2017). "Mitotic Gene Bookmarking: An Epigenetic Mechanism for Coordination of Lineage Commitment, Cell Identity and Cell Growth." Advances in experimental medicine and biology **962**: 95-102.
- Zhang, L., W. Liu, X. Wang, X. Wang and H. Sun (2019). "Prognostic value of serum IL-8 and IL-10 in patients with ovarian cancer undergoing chemotherapy." Oncol Lett **17**(2): 2365-2369.
- Zhang, M., L. Zhang, R. Hei, X. Li, H. Cai, X. Wu, Q. Zheng and C. Cai (2021). "CDK inhibitors in cancer therapy, an overview of recent development." American journal of cancer research **11**(5): 1913-1935.
- Zhang, S. Y., Q. Fan, A. Moktefi, V. Ory, V. Audard, A. Pawlak, M. Ollero, D. Sahali and C. Henique (2021). "CMIP interacts with WT1 and targets it on the proteasome degradation pathway." Clin Transl Med **11**(7): e460.
- Zhang, X., Y. Ling, Y. Guo, Y. Bai, X. Shi, F. Gong, P. Tan, Y. Zhang, C. Wei, X. He, A. Ramirez, X. Liu, C. Cao, H. Zhong, Q. Xu and R. Z. Ma (2016). "Mps1 kinase regulates tumor cell viability via its novel role in mitochondria." Cell Death & Disease **7**(7): e2292-e2292.
- Zheng, N. and N. Shabek (2017). "Ubiquitin Ligases: Structure, Function, and Regulation." Annual Review of Biochemistry **86**(1): 129-157.
- Zhou, B., X. Jin, W. Jin, X. Huang, Y. Wu, H. Li, W. Zhu, X. Qin, H. Ye and S. Gao (2020). "WT1 facilitates the self-renewal of leukemia-initiating cells through the upregulation of BCL2L2: WT1-BCL2L2 axis as a new acute myeloid leukemia therapy target." Journal of Translational Medicine **18**(1): 254.
- Zhu, Y. M., S. J. Webster, D. Flower and P. J. Woll (2004). "Interleukin-8/CXCL8 is a growth factor for human lung cancer cells." British journal of cancer **91**(11): 1970-1976.
- Zieve, G. W., D. Turnbull, J. M. Mullins and J. R. McIntosh (1980). "Production of large numbers of mitotic mammalian cells by use of the reversible microtubule inhibitor nocodazole. Nocodazole accumulated mitotic cells." Exp Cell Res **126**(2): 397-405.

8. Acknowledgement

I want to thank Prof. Dr. Florian Bassermann, whose enthusiasm made me join the laboratory and whose contribution and supervision lead to publication of this project. Thank you for giving a medical student such an opportunity working in your laboratory. Especially I want to thank my supervisor of the project, Dr. Katharina Clemm von Hohenberg. You really inspired me in my scientific work and supervised this project in the best way I can imagine. You did not only find the right answers to scientific questions but you also found the right words when I began to lose my motivation and when frustration began to rise. The project would never have been finished if you had not done such a great supervision. Not only in science but also in clinical work you became an idol for me.

Special thanks to Abirami Rathakrishnan and Petra Schenk, two outstanding technicians who crucially contributed to this project. Also, many thanks to Oleksandra Karpiuk for conducting the ChIP and luciferase experiments.

Many thanks also go to Dr. Vanesa Fernández-Sáiz, who first started on this project together with Katharina Clemm von Hohenberg.

I also want to thank the collaborators for the uncomplicated cooperation. I especially want to thank Felix von Zweydorf and Christian Johannes Gloeckner for performing the mass spectrometry and Thomas Engleitner and Roland Rad for doing the RNA sequencing. Likewise, I want to thank Dr Ritu Mishra for great support in microscopy. Further, I would like to thank the program of translational medicine of the TUM and the German José Carreras Leukämie foundation for funding and fellowships.